SYNTHESIS AND CRYSTAL STRUCTURE OF 3,3,6,6-TETRAMETHYL-9-(2-HYDROXYPHENYL)-3,4,6,7,9,10-HEXAHYDROACRIDINE-1,8- DIONE

Imran Hussain, [a] Sumati Anthal, [a] M. B. Deshmukh, [b] and Rajni Kant[a]*

Keywords: Crystal structure; Acridine; Direct methods; Hydrogen bonds; Ring conformations.

The title compound 3,3,6,6-tetramethyl-9-(2-hydroxyphenyl)-3,4,6,7,9,10-hexahydroacridine-1,8-dione, crystallizes in the orthorhombic space group $Pna2_1$ with unit cell parameters: a = 13.669(5) Å, b = 14.753(5) Å, c = 10.043(5) Å, Z=8. The crystal structure is solved by Direct methods and refined by full matrix least squares procedure to a final R value of 0.0982 for 2602 observed reflections. The crystal structure is stabilized by N1–H1···O2, O3–H3···O1 and C13–H13···O3 hydrogen bonds.

*Corresponding Authors
Fax: +911912432051
E-Mail: rkant.ju@gmail.com
[a] X-ray Crystallography Laboratory, Department of Physics, University of Jammu, Jammu-Tawi, 180006.
[b] Department of Chemistry, Shivaji University, Kolhapur–416 004 (MS), India

Introduction

Acridine derivatives have occupied a unique position in medicinal chemistry due to their wide range of biological application[1]. The acridine derivatives containing two keto functional groups at its 2nd and 11th position give rise to acridinediones. Acridinediones and their derivatives possess a wide range of pharmaceutical activities, including antimicrobial[2], antimalarial[3], antitumor[4],anticancer[5], antibacterial[6],fungicidal[7], and DNA binding properties[8]. These derivatives have been used in chemotherapy for the treatment of cancer[9] and the treatment of cardiovascular diseases, such as angina pectoris and hypertension[10]. As a continuation of our research devoted to the development of acridine derivatives[11-13], we herein report the synthesis and the crystal structure of the title compound.

Experimental

Synthesis

The synthetic route for 3,3,6,6-tetramethyl-9-(2-hydroxyphenyl)-3,4,6,7,9,10-hexahydroacridine-1,8-dione (Figure 1) is presented in Scheme 1. A mixture of dimedone (2 mmol), 2-hydroxybenzaldehyde 2 (1 mmol) and ammonium acetate (1.2 mmol) in mixture of aqueous ethanol (5 ml) was stirred at RT for 5 min. To this [CMIM][HSO_4] (20 mol %) was added and the reaction mixture heated at 85 ^{0}C until completion of the reaction. The progress of the reaction was monitored by TLC. After completion of the reaction, the mixture was gradually cool to room temperature and poured on ice water under stirring, solid were precipitate out. Filter the product and dried. The crude product was recrystallized from ethanol.(M.p>300 ^{0}C, Yield: 81 %). The chemical structure of the title compound is given in Figure 1.

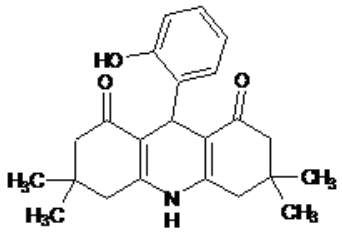

Figure 1. Chemical strcture of the 3,3,6,6-tetramethyl-9-(2-hydroxyphenyl)-3,4,6,7,9,10-hexahydroacridine-1,8-dione

Table 1. Crystal and experimental data for $C_{23}H_{27}NO_3$

CCDC Number	965867
Crystal description	Block
Crystal size	0.30 x 0.20 x 0.20 mm
Empirical formula	$C_{23}H_{27}NO_3$
Formula weight	365.46
Radiation, wavelength	MoK_α, 0.71073 Å
Unit cell dimensions	a= 13.669(5) Å
	b= 14.753(5) Å
	c=10.043(5) Å
Crystal system	Orthorhombic
Space group	$Pna2_1$
Unit cell volume	3328.7(5) Å^3
No. of molecules per unit cell, Z	8
Absorption coefficient	0.079 mm^{-1}
***F*(000)**	784
θ range for entire data collection	3.5986 < θ< 29.0363
Reflections collected / unique	7713 /3174
Reflections observed I > 2σ(I))	2602
Range of indices	h=-15 to 15,
	k=-16 to 16,
	l=-11 to 11
No. of parameters refined	249
Final *R*-factor	0.0982
w*R*(F_2)	0.2916
R_{int}	0.0373
R_{sigma}	0.0214
Goodness-of-fit	1.376
$(\Delta/\sigma)_{max}$	0.766
Final residual electron density	-0.308<Δρ>0.766 eÅ^{-3}

Table 2. Selected Bond Lengths and Bond angles

Bond lengths

Bond	Bond length, Å	Bond	Bond length, Å
C2-O1	1.209(7)	C11-O2	1.208(7)
C1- C2	1.476(7)	C7-C12	1.356(7)
C6- C5	1.503(8)	C19-O3	1.349(8)
C1- C6	1.350(7)	C13-C14	1.518(7)
N1-C6	1.363(7)	N1 - C7	1.373(7)
C12 -C7	1.356(7)	C12 - C11	1.450(7)
C12-C13	1.505(7)	C13-C14	1.518(7)
C18 - C17	1.344(12)	C19 - C18	1.430(9)
N1- H1	0.8600	O3- H3	0.8200

Bond Angles

Bond	Bond angle, °	Bond	Bond angle, °
C6-C1-C2	119.2(4)	C12-C13-C1	109.0(4)
C1-C6-C5	123.1(5)	N1-C7-C8	115.3(4)
O1-C2-C1	120.3(5)	C12-C7-C8	125.8(5)
O1-C2-C3	121.5(5	O2-C11-C12	121.5(5)
C1-C2-C3	118.1(5)	O2-C11-C10	121.4(6)
C5-C4-C3	113.6(6)	O3-C19-C14	122.8(5)
C23-C4-C3	114.4(6)	O3-C19-C18	117.4(6)
C1-C6-N1	120.7(4)	C14-C19-C18	119.8(6)
C12-C7-N1	118.9(5)	C15-C14-C13	122.3(5)
N1-C6-C5	116.2(5)	C19-C14- C13	121.1(5)
Torsion angles			
C1-C2-C3-C4	23.2(14)	O2-C11-C10-C9	160.6(12)
C5-C4-C3- C2	-38.1(15)	O3-C19-C18-C17	179.8(6)
C6-C1-C2-C3	-8.6(11)	C11-C12-C7-C8	-6.1(11)
C13-C1-C2-O1	-3.8(10)	C10-C9-C8-C7	-27.0(14)
C7-N1-C6-C1	14.1(11)	O1-C2-C3-C4	-159.1(8)
C7-C12-C7-N1	-3.9(9)	C21-C9-C8-C7	-172.5(9)
C21-C9-C10-C11	-73.1(12)	C23-C4-C3-C2	-173.6(9)
C23- C4- C5- C6	173.2(10)	C10-C9-C8-C7	-27.0(14)
C11-C12-C7-N1	176.8(7)	C11-C12-C7-C8	-6.1(11)
C11-C12-C13-C1	-161.5(6)	C11-C12-C13-C14	72.8(7)
C13-C12-C11-O2	5.1(11)	C13- C12 -C11- C10	-169.7(10)

Crystal structure determination and refinement

The crystallographic data are summarized in Table 1. A well-defined crystal of dimensions 0.30 x 0.20 x 0.20 mm^3 was used for data collection on *X'calibur CCD* area-detector diffractometer equipped with graphite monochromated MoK_α radiation (λ=0.71073 Å). X-ray intensity data of 24799 reflections were collected at 293(2) K and out of these reflections 3174 were found unique. The intensities were measured by ω scan mode for θ ranges 3.60° to 29.04°. 2602 reflections were treated as observed using (I>2σ(I)) as a criterion. Data were corrected for Lorentz-polarization and absorption factors. The structure was solved by direct methods using SHELXS97[14]. All non-hydrogen atoms of the molecule were located from the best E-map. All the hydrogen atoms were geometrically fixed and allowed to ride on the corresponding non-H atoms with O-H= 0.82 Å, N-H= 0.86 Å, C-H= 0.93-0.97Å and U_{iso}= 1.2 U_{eq}(C), except for the methyl groups where U_{iso}(H) = 1.5U_{eq}(C). The final refinement cycles converged to an R-factor of 0.0979 (wR(F^2)=0.2916) for the 2602 observed reflections. Residual electron densities range from -0.308 to 0.766 eÅ^{-3}. Atomic scattering factors were taken from International Tables for X-ray Crystallography. The geometry of the molecule was calculated using the WinGX[15], PARST[16]and PLATON[17]softwares.

Crystallographic information has been deposited with **CCDC-965867** to Cambridge Crystallographic Data Centre. This data can be obtained free of charge from Cambridge Crystallographic Data Centre via www.ccdc.cam.ac.uk/data_request/cif.

Results and discussion

The molecular structure containing atomic labeling is shown in Figure 2 (ORTEP)[18]. The molecule consists of four rings which are labeled as ring A, ring B, ring C and ring D Figure 1. The crystallographic and refinement data of the crystal is given in Table 1.

Table 3. Geometry of Intra and Inter molecular Hydrogen bonds

D–H…A	D–H(Å)	H…A(Å)	D…A(Å)	D–H…A(º)
N1-H1…O2^{i}	0.86	2.21	2.820(6)	128
O3-H3…O1	0.82	2.10	2.668(6)	126
C13-H13…O3	0.98	2.15	2.905(6)	104

Symmetry code: (i) -1/2+x, 1/2-y, z.

Some selected bond distances, bond angles and torsion angle values are given in Table 2. The structural parameters, including bond distances and bond angles, show a normal geometry[19] and agree with the values observed for some related structures.[11-13] The O3 atom attached with the carbon atom C19 is coplanar with the ring D, indicated by the torsion angles O3-C19-C18-C17 = 179.8(6)˚ and O3-C19-C18-C17 = 178.2(5)˚, this feature can also be seen in the related structures.[11-13] The double bonds C2=O1 [1.209(7) Å] and C11=O2 [1.208(7)Å] agree with the corresponding distances in structures containing similar systems.

The central ring B (N1/C6/C1/C13/C12/C7) of the acridinedione moiety adopts a *sofa* conformation with best mirror plane passing through atoms N1 and C13 [asymmetry parameter ΔCs(N1) = 0.46]. Ring A of the title compound (C1-C6) adopts a *sofa* conformation with best mirror plane passing through atoms C1 and C4 [asymmetry parameter Cs(C1)=1.50. Whereas ring C (C7-C12) adopt *half-chair* conformations with best two fold rotation axis bisecting the bond C9-C10 [asymmetry parameter (ΔC_2 (C9-C10) = 3.98].[20] In the title molecule, some carbon atoms are thermally disordered. The thermal disorder could not be tackled and hence, it led to the large value of the R-factor.

In the crystal structure, intramolecular hydrogen bonds (O3–H3…O1 and C13–H13….O3) helps in stabilizing the molecule. Intermolecular interactions N1–H1…O2 play a crucial part in assembling the molecules in three-dimensional network Table 3. Packing of the molecules in the unit cell down the c-axis is shown in Figure 3.

Acknowledgements

Rajni Kant is thankful to the Indian Council of Medical Research and the Department of Science and Technology, New Delhi for funding under sponsored research project (No. BIC/12(14)/2012 and EMR/2014/000467).

References

[1]Wroblewska, A., Huta, O. M., Patsay, I. A., Petryshnand, R. S. and Blazejowski, J., *Anal. Chim. Acta.*, **2004,** *507*, 229. https://doi.org/10.1016/j.aca.2003.11.032

[2]Shchekotikhin, Y. M., Nikolaeva, T. G., Shub, G. M., and Kriven'ko, A. P., *Pharm. Chem.* J., **2001,** *35*, 206. https://doi.org/10.1023/A:1010484013306

[3]Kidwai, M. and Bhatnagar, D., *Tetrahedron Lett*., **2010**, 51, 2700. https://doi.org/10.1016/j.tetlet.2010.03.033

[4]Tu, S., Zhang, X., Shi, F., Li, T., Wang, Q., Zhu, X., Zhang, J., and Xu, J., *J. Heterocycl. Chem*., **2005**, *42*, 1155. https://doi.org/10.1002/jhet.5570420618

[5]Gamage, S. A., Spicer, J. A., Atwell, G. J., Finlay, G. J., Baguley, B .C and Denny, W. A., *J. Med. Chem*. **1992**, *42*, 2383. https://doi.org/10.1021/jm980687m

[6]Palani, K., Thirumalai,D., Ambalavanan, P., Ponnuswamy, M. N., and Ramakrishnan, V. T., *J. Chem. Crystallogr*., **2005**, *35***,** 751. https://doi.org/10.1007/s10870-005-3880-2

[7]Wainwright, M. J., *Antimicrob. Chemother*., **2001**, *47*, 1. https://doi.org/10.1093/jac/47.1.1

[8]Venkatesan, K., Pujari, S. S., Srinivivasan, K. V., *Synth. Commun*., **2009**, *39*, 228. https://doi.org/10.1080/00397910802044306

[9]Kidwai, M., and Bhatnagar, D., *Tetrahedron Lett*., **2010**, *51*, 2700. https://doi.org/10.1016/j.tetlet.2010.03.033

[10]Venkatesan, K., Pujari, S. S., and Srinivivasan, K. V., *Synth. Commun*., **2009**, *39*, 228. https://doi.org/10.1080/00397910802044306

[11]Kour, D., Patil, D. R., Deshmukh, M. B., Gupta, V. K. and Kant, R., *Eur. Chem. Bull*. **2014**, *3(2)*, 173-175. DOI: 10.17628/ecb.2014.3.173-175

[12]Kour, D., Patil, D. R., Deshmukh, M. B. and Kant, R., *Eur. Chem. Bull.*, **2014**, *3(6)*, 552-554. DOI: 10.17628/ecb.2014.3.552-554

[13]Kour, D., Patil, D. R., Deshmukh, M. B., Gupta, V. K. and Kant, R., *J. Crystallogr*., **2014,** Article ID 914504.

[14]Sheldrick, G. M., *Acta Cryst*.,**2008,** *A64*, 112-122. https://doi.org/10.1107/S0108767307043930

[15]Farrugia, L., *J. Appl. Crystallogr*.,**1999**, *32*, 837-838. https://doi.org/10.1107/S0021889899006020

[16]Nardelli, M., *J. Appl. Cryst*., **1995**, *28*, 659. https://doi.org/10.1107/S0021889895007138

[17]Spek, A. L., *Acta Cryst D*., **2009**, *65*, 148-155. https://doi.org/10.1107/S090744490804362X

[18]Farrugia, L. J., *J. Appl. Cryst*., **2012**, *30*, 565. https://doi.org/10.1107/S0021889897003117

[19]Allen, F. H., Kennard, O., Watson, D. G., Brammer L., Orpen, A. G., Taylor, R., *J. Chem. Soc., Perkin Trans*., **1987**, *2*, S1–19. https://doi.org/10.1039/p298700000s1

[20]Duax W. L. and Norton, D. A., *Atlas of Steroid Structures*, **1975**, Plenum Press, New York, NY, USA. https://doi.org/10.1007/978-1-4684-6150-3

Received: 28.12.2017.
Accepted: 10.01.2018.

ANTIOXIDATIVE AND ANTIRADICAL SEASONAL DISTINCTIVES OF SEA BUCKTHORN SPROUTS

Inara Nokalna,[a]* Alise Silova,[b] Ilona Vanaga,[c,d] Imants Kalnins[e] and Andrejs Skesters[b]

Keywords: sea buckthorn, antioxidants, antiradicals.

More than 40 volatile compounds with pharmacological effects (including antioxidant, anti-inflammatory, anticancer, radioprotective activity and improvement of cardiovascular risk factors, etc) are detected in the sea buckthorn. The most thoroughly investigated parts of sea buckthorn are berries – their juice and oil, but less is known about the bioactives of the other plant parts. This study aims to determine antioxidative (AO) and antiradical (AR) properties of sea buckthorn sprouts. The study results show differences between spring and autumn sprouts' collection as well as water and 70% ethanol extracts. Further, *in vivo* research needs to be done to provide a full understanding of sea buckthorn sprouts' AO and AR effects.

* Corresponding Authors
Fax:
E-Mail: Inara.Nokalna@rsu.lv
[a] Dept. of Physiology and Biochemistry of Riga Stradinš University, Riga, Latvia
[b] Laboratory of Biochemistry of Riga Stradinš University, Riga, Latvia
[c] SilvEXPO, Nature, Driven, Technologies, Ltd.
[d] Faculty of Medicine, University of Latvia, Riga, Latvia
[e] Department of Physics of Riga Stradinš University, Riga, Latvia

Introduction

Studies on the effects of natural polyphenols, which are also present in sea buckthorns (*Hippophae rhamnoides L*, have evolved significantly over the last 15 to 20 years and have proven thereof role in the prevention of cardiovascular, cancer, degenerative and other diseases.

These polyphenolic compounds are a major group of phytochemicals that have antioxidative activity by inducing body's antioxidative systems – hydrophilic and lipophilic, both of these systems show antibacterial, antiviral, antitumor and anti-inflammatory properties and play a significant role in protection against oxidative stress (OS).[1] OS essentially is an imbalance between the production of free radicals (FR), reactive oxygen species (ROS), and/or reactive nitrogen species (RNS), and the body's possibility to detoxify or counteract FR and/or ROS harmful effects on cells membranes and other organism systems through the neutralization via antioxidants (AO). ROS can damage any components of the cell membrane, such as the DNA proteins and lipids, and give rise to different pre-pathological and pathophysiological conditions.[2] Thus, OS plays direct and indirect role in pathophysiology of several diseases such as neurodegenerative (Parkinson's Disease, Alzheimer's Disease, Multiple sclerosis), cancer, Diabetes Mellitus, cardio-vascular diseases and others.[3] Chemical content of various parts of sea buckthorn (mainly berries) and its products have been studied, but there is not a lot of data regarding separate components that describe antioxidative and/or antiradical activity of this plant. There has never been a complex approach to antioxidants as their possible potential to regulate active forms of oxygen and nitrogen free radicals, thus stopping development of oxidative and/or nitrosative stress *in vitro.* Herbal remedies made of sea buckthorn are most frequently used for the treatment of-cancer therapy side effects, cardiovascular diseases, gastric ulcers, liver cirrhosis, skin diseases, such as damaging effects of sun, therapeutic radiation treatment and cosmetic laser surgery, and some other pathological conditions.[4] However, until now, little evidence has been obtained to indicate, whether biologically active compounds are consistently present throughout the plant growth stages or whether the compounds are affected by the seasonal changes. Also, the significant differences in chemical composition and biological activity of sea buckthorn leaves, shoots, berries, and buds indicate a need for detailed studies of their extracts, specific fractions and compounds during a whole vegetative season.

This study aimed to characterize the sea buckthorn sprouts, which were harvested in spring and autumn seasons, and their aqueous and 70 % ethanol extracts according to their antioxidative and antiradical properties *in vitro.*

Materials and methods

Extracts preparing

For this study, the extraction and determination of antioxidants present in sea buckthorn sprouts which were collected in spring (April) and autumn (October) season were determined via two different solvent systems: 70 % ethanol (ethanol solution in water) and water.

For extraction air-dried sea buckthorn sprouts were used (dry matter 89-91 %) were used. The sprouts were first ground in a mechanical grinder. The gravity separation was used to extract the dry matter of sea buckthorn. The matter was put in the flask and the solvent was added, then the

flask was put in the water bath, and kept there for 3 hours while stirring. The temperature in the bath was about 60 °C. After the extraction, the solution was filtered in order to obtain a particle-free solution and then evaporated. Two types of extracts were obtained – water (aqueous) extract (extracted with distilled water) and ethanol extract (extracted with 70 % ethanol). The solvent and sea buckthorn ratio was 10:1, e.g., 50 g of air-dried sea buckthorn doused with 500 g of solvent.

Nitric Oxide Scavenging Assay

The nitric oxide scavenging ability was determined by Griess reaction adapted from Santiago and Valerio.[5] A hundred microliters of each sample were added with 400 µL 10 mM sodium nitroprusside and 100 µl phosphate buffered saline (PBS), pH 7.4. The solutions were incubated for 150 min at 25 °C. After which, 100 µL of each solution was transferred to a new tube and 200 µL 0.33 % sulfanilamide was added. The resulting solutions were incubated for 5 min at 25 °C.

Then, 200 µL 0.1 % naphthyl ethylenediamine was added. Again, they were incubated for 30 min at 25 °C. One hundred fifty microliters of the resulting mixture was transferred to a 96-well microplate in six replicates and was read at 540 nm using absorbance reader SunriseTM (TECAN).

An "empty" sample without the active compound is prepared at the same time. Inhibition is calculated by the following equation: % (inhibition) = $100*(A_0 - A_1)/A_0$. where, A_0 – average absorption for the "empty" sample (contains solvent), A_1 – average absorption for the real sample.

Radical cation ABTS+ scavenging activity

On the basis of the modified method by Re R. (1999), a mixture of 7 mM ABTS•+ (2,2'-azinobis(3-ethylbenzothiazoline-6-sulfonic acid)) and 2.45 mM potassium persulfate was kept in the dark for 16 hours at room temperature.[6] Before the measurement, it was essential to dilute the ABTS•+ solution with methanol in order to obtain the absorption of 0.700 ± 0.025 at 734 nm. The measurement (A_0) of 2970 µL of ABTS•+ solution was taken, then 30 µl of the sample was added. The mixture was incubated at 37 °C and a second absorbance (A_1) after 6 min was taken. Using the difference between the two absorptions A_0 and A_1, the concentration of the sample was calculated. The result was expressed in millimoles of Trolox equivalent (TE mmol L^{-1}) of the sample solution.

Total Antioxidant Status

Total antioxidant status (TAS) in samples was measured using Randox Total Antioxidant status kit (Randox Laboratories Ltd.) adapted to the RX Daytona automated chemistry analyzer (Randox Laboratories Ltd).[7]

ABTS® [2,2'-azino-bis(3-ethylbenzothiazoline-6-sulphonic acid)] incubated with H_2O_2 and peroxidase (metmyoglobin), generated the ABTS® radical cation. It has a relatively stable color of green and blue, which absorbs at 600 nm. The antioxidants present in the sample prevent the formation of the cation, therefore the color is proportional to its concentration. The result was expressed in millimoles of Trolox equivalent (TE mmol L^{-1}) of the sample solution.

Total polyphenol

An aliquot of 500 µl of an extract was mixed with 2.5 ml of Folin-Ciocalteu phenol reagent (10x dilution) and allowed to react for 5 min. Then 2 ml of 7.5 % Na_2CO_3 solution was added and allowed to stand for 1 h before the absorbance of the reaction mixture was read at 765 nm. All tests were performed six times. The total polyphenol contents of the extract was evaluated from gallic acid standard curve and expressed as mg of gallic acid (GAE) per gram of plant material.[8]

Ferrum reducing antioxidant potential (FRAP) activity

Fe(III) ion reduction to Fe(II) ion in the presence of 2,4,6-tri(2-pyridyl)-s-triazine (TPTZ) gives intense blue color with maximum absorption at 593 nm. The ability to reduce ferric ions was measured using a modified version of the method described by Benzie and Strain (1996).[9,10] An aliquot (100 µl) of an extract (with appropriate dilution, if necessary) was added to 3 ml of FRAP reagent (10 parts of 300 mM sodium acetate buffer at pH 3.6, 1 part of 10 mM TPTZ – HCl (40 mM) solution and 1 part of 20 mM $FeCl_3.6H_2O$ solution). The reaction was monitored up to 5 min at 593 nm, at 37 °C. FRAP reagent was used as a blank. The aqueous solution of a known amount of Fe(II) was used for calibration.

The antioxidant capacity based on the ability to reduce ferric ions of the extract was expressed as FRAP value in mmol Fe (II) per liter of the sample solution.

DPPH free radical scavenging activity

DPPH is a stable organic radical. In a chemical reaction, it functions as a radical and it is a scavenger of antioxidants. DPPH solution is violet with a maximum absorption at 515 nm, while its reduced form is yellow.[11,12] Therefore, the decreased level of absorption at 515 nm when adding extracts, was proportional to the natural substance antioxidant activity.

The antiradical activity (six replicates per treatment) was expressed as IC50 (mg mL^{-1}) - the concentration required to cause a 50 % DPPH inhibition. The ability to scavenge the DPPH radical was calculated by using the following equation: %(inhibition) = $100*(A_0 - A_1)/A_0$, where A_0 – average absorption for the "empty" sample (contains solvent), A_1 – average absorption for the test sample.

The calibration curve was obtained with TROLOX/methanol. The free radical scavenging activity for the sample was calculated after the Trolox equivalent and expressed in millimoles of Trolox equivalent (TE mmol L^{-1}) of the sample solution.

Statistical analysis

The results were expressed as the mean ± standard deviation (SD), and experiments were carried out in six replicates. The results corresponded to a normal distribution and were processed with a two-sample T Test assuming Equal Variance in MS Office Excel 2013.

All statistical calculations and image creation were carried out using IBM SPSS 20.0 and MS Excel.

Results and Discussion

Sea buckthorn is a dioecious plant, e.g., it has distinct male and individual female organisms with quite different biologically active species. This study aimed to characterize the antioxidative and antiradical properties of sea buckthorn sprouts which were collected in spring and autumn season and extracted in water and 70 % ethanol. In order to characterize the activity of natural antioxidant substances, several approved standard methods were applied. Each method allowed to detect some of the antioxidative system parameters, as there is no universal method to give an entire system overview. Some of the indicators helped to assess the general water-soluble antioxidants, without assessing the lipid-soluble ones.[13] Some methods require a low pH level, which actually stems the antioxidant activity. Also in the case of bioflavonoids low water solubility should be taken into account, and thus organic solvents acquired from plants – like ethanol – are preferable.[14]

The ABTS method was applied in order to determine radical scavenging activity of hydrogen contributors and chain disintegrating antioxidants in many plant extracts.

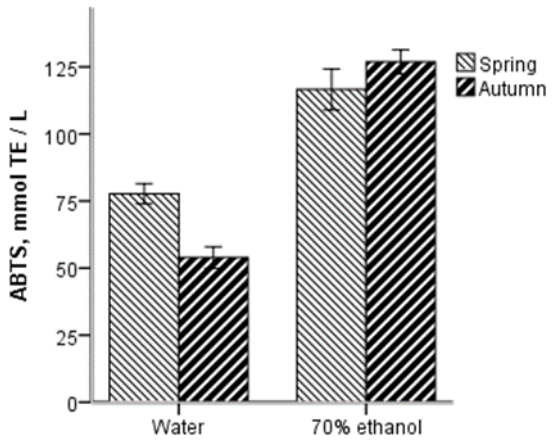

Figure 1. Anti-oxidant activity of sea buckthorn sprouts in 70% ethanol extract by ABTS method

As seen in Figure 1, all samples showed a higher value for ABTS when extracted with 70% ethanol, especially in the autumn sample, followed by water. It was detected, that autumn samples extracted with 70 % ethanol recorded a 126.71 ± 1.88 TE mmol L^{-1} followed by spring sample 116.50 ± 1.75 TE mmol L^{-1} ($p < 0.001$). Contradictory data was obtained in aqueous extracts of the samples. The radical cation $ABTS^{+}$ scavenging activity in spring samples of the aqueous extract was significantly higher, compared to autumn samples, respectively, 77.97 ± 1.75 and 52.99 ± 14.06 TE mmol L^{-1} ($p < 0.001$). Similar changes were found in the samples, determining their radical scavenging activity using the total antioxidant status kit (Randox Laboratories Ltd).

As seen in Figure 2, the amount of TAS in spring samples of water extract was significantly higher, compared to autumn samples, i.e. 155.00±1.58 and 149.00±1.52 TE mmol L^{-1} ($p < 0.001$), respectively. The amount of TAS was significantly ($p < 0.001$) increased in 70 % ethanolic of autumn sample, i.e. 282.00 ± 3.50 compared with spring sample, i.e. 264.00±2.98 TE mmol L^{-1}.

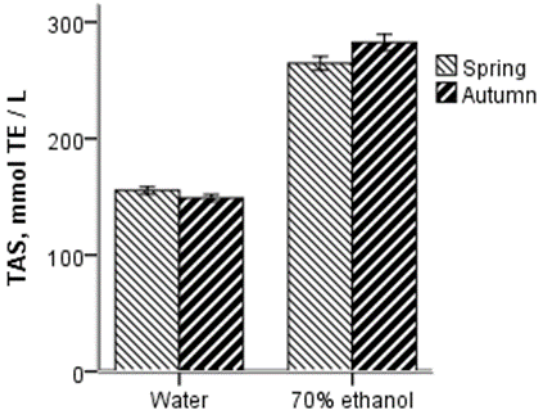

Figure 2. Anti-oxidant activity of sea buckthorn sprouts in 70 % ethanol and water extracts by TAS method

The FRAP assay is used in order to measure the potency of the chemical compounds present in the extract to challenge ferrozine for the ferrous ion. FRAP method is based on Fe(III) ion reduction to Fe(II) ion in the presence of TPTZ when a deep blue color forms with an absorption maximum of 593 nm. The absorption rate falls due to the added antioxidant extracts and is directly proportional to the antioxidative capacity. The higher the FRAP value, the greater its antioxidant activity. The given method shows the amount of low molecular weight antioxidants but does not include any compounds with thiol groups.[15]

Based on Figure 3, ethanolic extracts had the highest reducing power followed by water. Autumn sample had the significantly highest reducing power in the range of 165.00±3.66 mmol Fe(II) L^{-1} compared to spring sample from the range of 159.90±4.09 mmol Fe(II) L^{-1} ($p = 0.010$). In respect to the aqueous extracts their detected FRAP value was significantly ($p < 0.001$) higher in spring samples, i.e. 108.12±0.92 Fe (II) L^{-1} compared to the autumn samples, i.e. 97.78±0.66 Fe (II) L^{-1}.

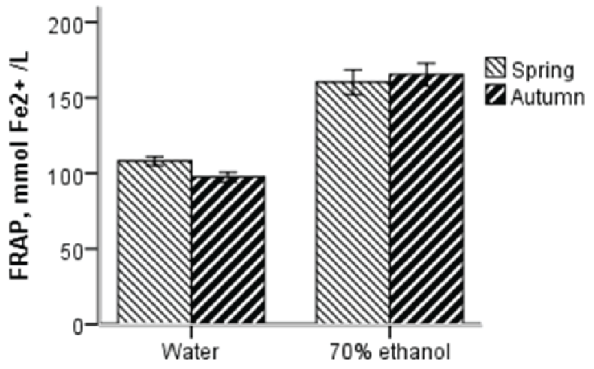

Figure 3. Anti-oxidant activity of sea buckthorn sprouts extracts in 70 % ethanol and water extract by FRAP method

The Folin-Ciocalteau method was used as it is a rapid, easy and relatively simple method to identify total phenolic content in natural samples. A close interdependence between the composition of phenolic compounds and antioxidant activity is expected as phenolic compounds are potent antioxidants and free radical scavengers.[16]

Polyphenols as antioxidants can neutralize active oxygen species and thereby regulate the oxidative stress. Polyphenols do not have only the direct antiradical activity, but they are also able to link metals of variable valence to form chelate complexes, thereby stopping the emission of free radicals.[17,18] All tests were carried out in six replicates, and the results were expressed as mg gallic acid equivalent (GAE) g^{-1} extract.

Table 1. Total phenolic content of the sea buckthorn (*Hippophae rhamnoides L.)* sprouts in 70% ethanol and water extracts

Samples	Solvent	mg of GAE g^{-1}
Autumn	70 % ethanol	4.89 ± 0.06*
Spring		4.73 ± 0.08
Autumn	water	2.92 ± 0.13
Spring		2.92 ± 0.06

*p = 0.001 *vs* spring 70 % ethanolic extract sample

As seen in Table 1, the most effective solvent for extracting polyphenols is ethanol and it has proven to be more effective, respectively, 67 % for autumn samples and 63 % for spring samples, compared to water. It was found that 70 % ethanolic extracts yielded the highest total polyphenol content in autumn samples compared to the spring samples (p = 0.001).

No significant differences between autumn and spring samples were found for the water extracts. DPPH radical scavenging method is widely used as it is an easy, fast and convenient method for determining radical scavenging activity of many samples without being dependant on sample polarity.[19] DPPH method is widely used to determine the antiradical activity of an analyte. •DPPH is a stable organic radical that gets scavenged by an antioxidant "trap"[20]

Nitric oxide is formed in normal physiological processes and sustains a metabolic pace. During pathophysiological situations its production increase. As a result, it enables the generation of a much more active oxidant – peroxynitrite.[21,22]

Scores for DPPH and NO anti-oxidative activity were calculated by IC_{50} %, e.g., a concentration of antioxidant (mg/ml) at which 50 % inhibition of the radical takes place and the lower the given value is, the greater the anti-oxidative capacity. The lower IC_{50} value indicates a higher antioxidant activity.

Table 2. The IC_{50} values of sea buckthorn *(Hippophae rhamnoides L.)* sprouts in 70 % ethanol and aqueous extract by DPPH radical scavenging and nitric oxide free radical scavenging method

Samples	Solvent	DPPH radical	NO radical
		IC_{50}, mg mL^{-1}	
Autumn	70 % ethanol	0.39 ± 0.002 *	1.36 ± 0.026
Spring		0.48 ± 0.002	0.60 ± 0.01 **
Autumn	water	0.74 ± 0.002	2.47 ± 0.021
Spring		0.63 ± 0.01^{+}	1.59 ± 0.011^{+}

*p < 0.001 *vs* spring extract sample in 70% ethanolic solution; **p< 0.001 *vs* spring extract sample in 70% ethanolic solution; +p < 0.001 *vs* autumn extract sample in water

Table 3. DPPH radical scavenging activity compared with standard Trolox (vitamin E analog)

Samples	Solvent	DPPH µmol Trolox L^{-1} (100 g L^{-1})
Autumn	70 % ethanol	156.2 ± 0,40 *
Spring		125.9 ± 0,70
Autumn	water	83.1 ± 0,53
Spring		95.9 ± 1,45^{+}

*p < 0.001 *vs* spring extract sample in 70% ethanolic; ^{+}p < 0.001 *vs* autumn extract sample in water.

The ethanol extracts showed the highest capacity to neutralize DPPH radical. In this study, DPPH radical scavenging activity of the tested samples in decreasing order was: autumn 70 % ethanol > spring 70 % ethanol > spring water extract > autumn water extract (Table 2, Table 3)

This antiradical activity could be due to the phenolic compounds. In fact, it has been found that antioxidant molecules such as polyphenols, flavonoids, and tannins reduce and discolor DPPH due to their hydrogen donating ability.[23]

Using NO radical scavenging method, the obtained results recorded in Table 2 revealed that 70 % ethanolic of spring samples expressed the highest antiradical activity of 50 % at the concentration of 0.60 mg mL^{-1}, followed by autumn sample at the concentration of 1.36 mg mL^{-1} (p < 0.001) and then aqueous extracts of spring samples at 1.59 mg mL^{-1} and autumn samples at 2.47 mg mL^{-1} (p < 0.001). This study portrays that both ethanol and aqueous extracts of sea buckthorn sprouts collected in spring exhibited high nitric oxide radical scavenging activities.

Conclusion

70 % Ethanol extracts of the Sea buckthorn sprout samples collected in autumn had the highest total phenolic content and thereby higher anti-oxidant and anti-radical activities, except for NO radical scavenging activity.

Therefore, the use of sea buckthorn sprouts could be relevant in the prevention and treatment of such diseases, whose pathogenesis implicates oxidative stress, as well as in the food industry as a good preservative owing to its anti-oxidative potential.

Declaration

Authors report that they do not have competing interests.

References

[1]Gornaš, P., Šne, E., Siger, A., Seglina, D. *Ind. Crops Prod*., **2014**, *60, 1-7*. https://doi.org/10.1016/j.indcrop.2014.05.053

[2]Lobo, V., Patil, A., Phatak, A., Chandra, N., *Pharmacogn. Rev*., **2010**, *4(8)*, 118-126. https://doi.org/10.4103/0973-7847.70902

[3]Uttara, B., Singh, A. V., Zamboni, P., Mahajan, R. T., *Curr Neuropharmacol*., **2009**, *7(1)*, 65–74. https://doi.org/10.2174/157015909787602823

[4]Zeb, A., *J. Biol. Sci*., **2004**, *4(5)*, 687-693. https://doi.org/10.3923/jbs.2004.687.693

[5]Santiago, L. A., Valerio, V. L. M., *Int. J. Pharm. Front. Res*., **2013**, *3(1)*, 15-25.

[6]Re, R., N., Pellegrini, A., Proteggente, A. P., Yanh, M., Rice-Evans, C., *Free Radicals Biol. Med*., **1999**, *26(9-10)*, 1231-1237. https://doi.org/10.1016/S0891-5849(98)00315-3

[7]Miller, N. J., Rice-Evans C., Davies, M. J., *Clin. Sci*., **1993**, *84*, 407−412. https://doi.org/10.1042/cs0840407

[8]International Standard *ISO 14502-1:2005* (E). *Determination of substances characteristic of green and black tea – Part 1: Content of total polyphenols in tea – a Colorimetric method using Folin-Ciocalteu reagent.*

[9]Benzie, F. F., Strain, J. J., *Methods in Enzymology*, **1999**, *299*, 15-23. https://doi.org/10.1016/S0076-6879(99)99005-5

[10]Lado, C., Then, M., Varga, I., Szoke, E., Szentmihaly, K., *Z. Naturforsch.*, **2004**, *59c*, 354-358.

[11]Brand – Williams, W., Cuvelier, M. E., Berset C., *J. Agric. Food Chem.*, **2007**, *55 (1)*, 165–169.

[12]Rebiai, A., Lanez, T., Belfar, M. L., *Int. J. Pharm. Pharmac. Sci.*, **2014**, *6(1)*, 395-400.

[13]Terashima, M., Nakatani, I., Harima, A., Nakamura, S., Shiiba, M., *J. Agric. Food Chem.*, **2007**, *55 (1)*, 165–169. https://doi.org/10.1021/jf062700e

[14]Zhijun, L., *Endocrin. Metab. Immune Disorder Drug Targets*, **2008,** *8(2)*, 112–121. https://doi.org/10.2174/187153008784534358

[15]Rubio, C. P., Hemandez - Ruiz, J., Martine-Subiela, S., Tvarijonaviciute, A., Ceron, J. J., *BMC Vet. Res.*, **2016,** *12*, 166. https://doi.org/10.1186/s12917-016-0792-7

[16]Kumar S., Kumar D., Manjusha, Saroha K., Singh N., Vashishta B. *Acta Pharm*, **2008,** *58(2)*,215-20.

[17]Perron, N. R., Brumaghim, J. L., *Cell Biochem Biophys*, **2009**, *53*, 75–100. https://doi.org/10.1007/s12013-009-9043-x

[18]Antioxidant Enzyme Edited by Mohammed Amr El-Missiry. *InTech: Biochemistry, Genetics and Molecular Biology*, **2012**, *October 03*. https://doi.org/10.5772/2895

[19]Koleva, I. I, Teris, A. B., Jozef, P. H., Linssen, A. G., Luyba, N. E., *Phytochem Anal*., **2002**, *13*, 8 -17. https://doi.org/10.1002/pca.611

[20]Behrendorff, J., Vickers, C. E., Chrysanthopoulus, P., Nielsen, L. K., *Microbial. Cell Fact*., **2013**; *12*, 76. https://doi.org/10.1186/1475-2859-12-76

[21]Pacher, P., Beckman, J., Liaudet, L., *Physiol. Rev.*, **2007**, *87*(1), 315-424. https://doi.org/10.1152/physrev.00029.2006

[22]Hogg, N., Kalyanaraman, B., Biochim. Biophys. Acta – Bioenergetics, **1999**, 2/3, 378-384.

[23]Kumaran, A., Karunakaran, R. J., *Food Sci. Technol.* **2007**, *40*, 344–352.

Received: 05.12.2017.
Accepted: 12.01.2018.

SYNTHESIS OF BIOACTIVE HETEROCYCLES FROM 6-AMINO-4-(2-CHLORO-5-NITROPHENYL)-3-METHYL-1,4-DIHYDROPYRANO[2,3-*c*]PYRAZOLE-5-CARBONITRILE

A. K. Elziaty,[a] G. Bassioni,[b] A. M. A. Hassan[a] and H. A. Derbala[a]

Keywords: Enaminonitrile, pyranopyrazole, pyrimidinone, oxazinone, antimicrobial agents.

Enaminonitrile derivative, 6-amino-4-(2-chloro-5-nitrophenyl)-3-methyl-1,4-dihydropyrano[2,3-*c*]pyrazole-5-carbonitrile (**1**) was synthesized. This compound was utilized as a building block for the synthesis of new 3-methylpyrazolopyran moiety incorporated with different heterocycles involving pyrimidinone, oxazinone, and iminopyrimidine, in addition to novel derivatives including diacetyl derivative (**5**), benzoyl derivative (**6**), carbamodithioic acid (**10**) and urea derivative (**13**). Spectral techniques, FT-IR, ^{1}H-NMR and mass spectroscopy and elemental analysis were used to characterize the synthesized compounds. Screening and evaluation of these products as antimicrobial agents showed that the derivatives **5**, **6**, **10**, and **13** possess a potent activity.

* Corresponding Authors
Fax:
E-Mail:
[a] Chemistry department, Faculty of Science, Ain Shams University, Abbassia, Cairo Egypt 11566
[b] Chemistry department, Faculty of Engineering , Ain Shams University, Abbassia, Cairo Egypt 11566

Introduction

It has been reported that pyran derivatives posses hypotensive effect,[1] anticancer activity,[2] antifungal effect,[3,4] plant growth regulation activity.[5] Pyranopyrazoles are important compounds for the preparation of many biological active heterocyclic compounds[6] and they proved to have useful properties as therapeutics in clinical application.[7-9] A literature survey revealed that pyrazole derivatives have received much attention during the recent years on account of their utilization as antioxidant,[10] antihypertensive,[11] antifungal[12,13] and vasodilator.[14] As well as, pyrimidinone derivatives have extensive applications as structural units of various biologically important molecules and as useful intermediates in medicinal chemistry[15] and pyranopyrimidinones compounds showed considerable pharmaceutical and biological activities, including anticancer, antitumor, antimalarial, antibacterial, antihypertensive, anti-inflammatory, hepatoprotective, cardiotonic, vasodilator, bronchiodilator, antifolate, and antiallergic activities.[16-28] They are also used in the preparation of dyes and pigments flavoring agents,[29,30] and in luminescence chemistry.[31] Over the past decades, significant efforts have been devoted to develop the synthesis of pyrimidinethione derivatives,[32,33] as they are considered versatile synthons for the construction of many heterocycles of synthetic and biological importance.[34-37] Thus, in view of the above facts and in continuation of our efforts to construct heterocyclic compounds from pyran derivatives, and to study their biological potency,[38-45] it was of interest to synthesize a ring system combine both the pyrazole and the pyran moieties which might have good biological activity.

Results and Discussion

Syntheses

The previously reported[46] pyranopyrazole derivative (**1**) was allowed to react with different reagents aiming to synthesize antimicrobial heterocycles. Reaction of **1** with formic acid afforded the pyrimidinone derivative **2** whose structure was confirmed from IR spectral data which revealed the absence of absorption bands of C≡N and NH_2 groups and the appearance of bands characteristic to carbonyl and NH groups at υ1682 cm^{-1} and 3182 cm^{-1}, respectively. The ^{1}H-NMR spectrum showed a singlet at δ11.08 ppm, disappeared by D_2O due to NH group proton. Acid hydrolysis of the cyano functionality was carried out by addition of concentrated sulphuric acid onto pyranopyrazole derivative **1** at room temperature to give the amide derivative **3**. The structure of the amide **3** was elucidated by the FTIR spectra which showed no absorption band of C≡N and appearance of a new band due to C=O group at υ1685 cm^{-1}.

In our previously reported work for the synthesis of oxazinone derivatives,[46] the pyranopyrazole derivative **1** was allowed to react with acetic anhydride and/or benzoyl chloride under solvent-free conditions and afforded the pyrazolopyranooxazinones **4a**, **b**. On the contrary, herein, the reaction of **1** with acetic anhydride in pyridine gave the diacetyl derivative **5** and benzoylation with benzoyl chloride in dry toluene as a solvent afforded the benzoyl derivative **6**. The IR spectra of both products **5** and **6** revealed the presence of cyano group absorption that proved no cyclization has occurred (Scheme 1).

To make use of nucleophilic character of the amino group, it was subjected to react with various electrophiles. Thus, when enaminonitrile **1** was treated with triethyl orthoformate, it gave the imidoformate derivative **7**. The latter product was utilized as a precursor for the synthesis of pyrazolopyranopyrimidine **8** by reaction with hydrazine hydrate in ethanol. The structure of **7** was confirmed from its IR spectrum that did not show the absorption frequency of NH_2 group but showed the C=N group band at 1632 cm^{-1}.

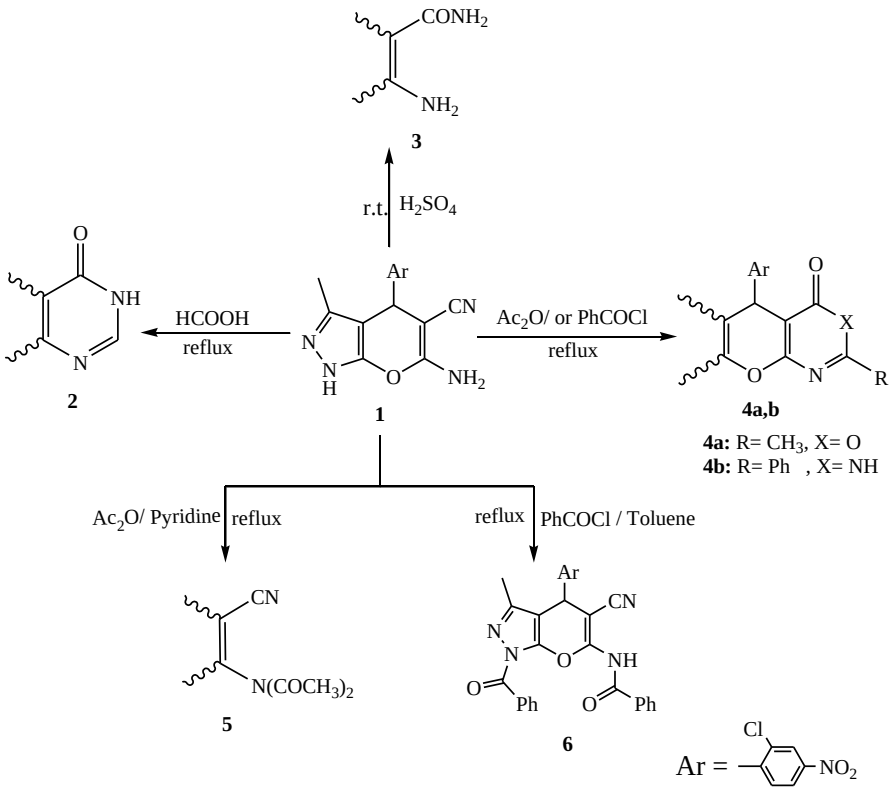

Scheme 1. Reactions of pyranopyrazole derivative.

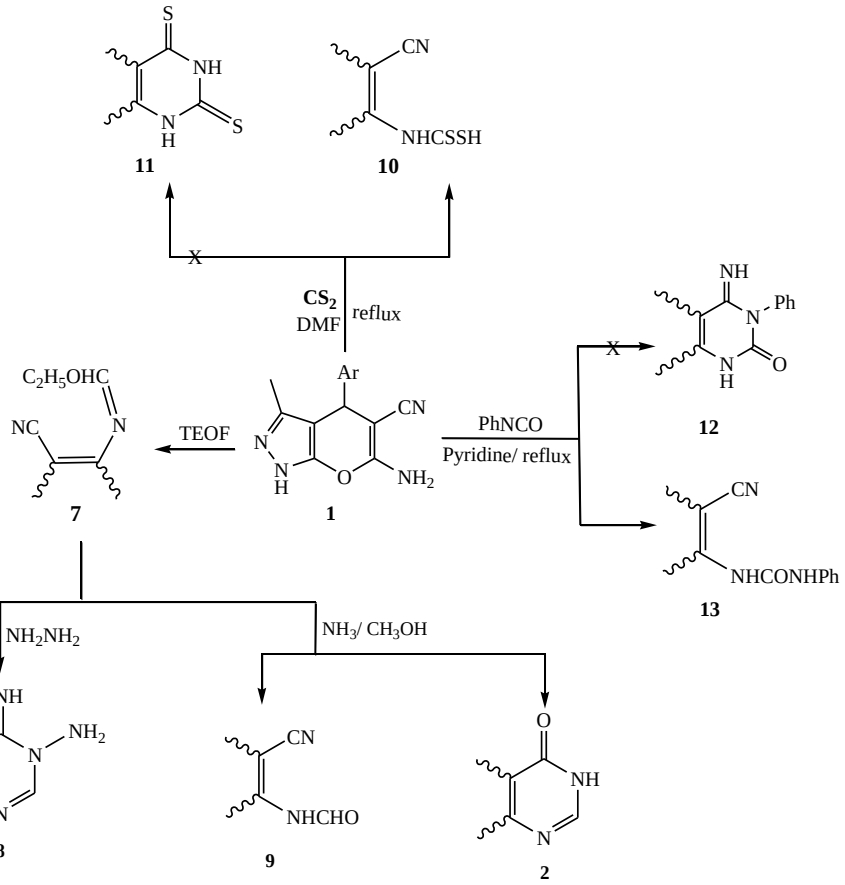

Scheme 2. Further reactions of pyranopyrazole derivatives

Further, the ^{1}H-NMR spectrum showed a singlet at δ12.36 ppm which disappeared in D_2O and is due to NH group, a quartet peak owing to CH_2 group at δ 4.34-4.28 ppm and a triplet peak at δ 1.31-1.28 ppm due to CH_3 protons.

The structure of **8** has been elucidated on the basis of IR spectrum which showed a coupling band at 3188, 3119 cm^{-1}due to NH_2 group and two peaks for NH pyrazole and NH imino at 3349 and 3309 cm^{-1}, respectively. Its ^{1}H-NMR spectrum showed a singlet at δ 12.57 ppm NH of pyrazole group and 10.25 ppm for C=NH. However, when the imidoformate derivative **7** was subjected to react with ammonium hydroxide in methanol, hydrolysis of the imidoformate functionality to the formamide derivative **9** occurred instead of the formation of the pyrimidinone derivative **2**.

Further, treatment of the enaminonitrile **1** with carbon disulfide afforded carbamodithioic acid **10** instead of pyrimidenedithione derivative **11**.The IR spectrum of **10** revealed the absorption band attributable to C≡N group at 2215 cm^{-1} and a sharp band at 1390 cm^{-1}due to C=S group. The reaction of the compound **1** with phenylisocyanate in pyridine provided the urea derivative **13** instead of the pyrimidinone derivative **12**. The structure of **13** was confirmed from its elemental and spectral analysis (Scheme 2).

Antimicrobial Study

The antibacterial activity of the synthesized compounds 2, **3**, **7**, **8**, **1**0 and **13** was tested against a panel of two gram positive bacteria (*Staphylococcus aureus* and *Bacillus subtilis*) and two Gram-negative bacteria (*Escherichia coli* and *Pseudomonas aeuroginosa*). The antifungal activities of the compounds were tested against two fungi (*Candida albicans* and *Aspergillus flavus*).

Each compound was dissolved in DMSO and a solution of concentration 1 mg mL^{-1} were prepared. Separately paper discs (5cm) were cut and sterilized in an autoclave. The paper discs, soaked in the solution of the compound, were placed aseptically in the petri dishes containing nutrient agar media (agar 20g + beef extract 3g +peptone 5g) seeded with *Staphylococcus aureus, Bacillus subtilis, Escherichia coli, Pseudomonas aeuroginosa, Candida albicans and Aspergillus flavus*. The petri dishes were incubated at 36 °C and the inhibition zones were recorded after 24 h of incubation. Each treatment was replicated three times. The antibacterial activity of a common standard antibiotic ampicillin and antifungal colitrimazole was also recorded using the same procedure as above at the same concentration and solvents.

The % activity index for the complex was calculated by the formula as shown below:

$$\text{Activity index (\%)} = 100\,\frac{\text{zone of inhibition by test compound}}{\text{zone of inhibition by standard}}$$

The antimicrobial activity of the synthesized heterocycles was shown in Table 1.

Minimum inhibitory concentration (MIC) measurements

The MIC was determined using the disc diffusion technique by preparing discs containing 1.9-1000 µg/ml of each compound against gram positive *Staphylococcus aureus* and *Bacillus subtilis* and gram negative *Escherichia coli* and *Pseudomonas aeuroginosa*. The antifungal activities of the compounds were tested against two fold fungi *Candida albicans* and *Aspergillus flavus* and applying the protocol. The two fold dilutions of the solution were prepared. The microorganism suspensions at 10 CF-U/ mL (colony forming unit/ml) concentration were inoculated to the corresponding wells. The plates were incubated at 36C for 24 h. for the bacteria.The standard antibiotic ampicillin and Antifungal Colitrimazole was also recorded using the same procedure as above at the same concentration and solvents. At the end of the incubation period, the minimum inhibitory concentration (MIC) values were recorded as the lowest concentration of the substance that had no visible turbidity. Control experiments with DMSO and uninoculated media were run parallel to the test compounds under the same condition. The results of MIC measurements of the synthesized heterocycles compounds are shown in Table 2.

Experimental

All melting points were determined on an electrothermal apparatus and are uncorrected. The FT-IR were recorded in potassium bromide disks on Pye Unicam SP3-300 and Shimdazu FTIR 8101PC Infrared spectrophotometers. The ^{1}H-NMR was recorded on a Varian Mercury VX-300 NMR spectrometer. ^{1}H-NMR spectra were run at 300 MHz and on a Varian Gemini 200 MHz, Bruker AC 200 MHz using TMS as internal standard in deuterated chloroform ($CDCl_3$) or deuterated dimethyl sulfoxide (DMSO-d_6). Chemical shifts are quoted in δ and were related to that of the solvents. The mass spectra were recorded on a Shimadzu GC-MS QP1000 EX mass spectrometer at 70 eV. Elemental analyses were carried out at the Micro analytical Center of Cairo University. All the reactions and the purity of the new compounds were followed and cheeked by TLC.

Synthesis

4-(2-Chloro-5-nitrophenyl)-3-methyl-4,6-dihydropyrazolo-[4',3':5,6]pyrano[2,3-d]pyrimidin-5(1H)-one (2)

A mixture of **1** (5 mmol, 1.66 g) and formic acid (20 mL) was refluxed for 2 h, the reaction mixture was poured after cooling into water and crushed ice, the solid formed was filtered off, washed with cold water and crystallized from ethanol to give compound **2** as a pale yellow solid (72 %). m.p. 229-230 °C. IR (KBr): 3403 (NH pyrraz.), 3182 (NH pyrim.), 1682 (CO) cm^{-1}. MS *m/z* (%) 359 (M^{+}, 7.35), 360 (3.42), 230 (74.53), 179 (2.15), 43(100). ^{1}H-NMR (DMSO-d_6) δ = 11.4 (s, 1H, NH), 11.08 (s, 1H, NH), 8.49 (s, 1H, CH, N = C2-H), 8.07–7.70 (m, 3H, aromatic), 4.64 (s, 1H, benzylic), 2.12 (s, 3H, CH_3). Anal. Calcd. for $C_{15}H_{10}N_5O_4Cl$ (359.73): C, 20.08; H, 2.80; Cl, 9.85; N, 19.47. Found: C, 20.06; H, 2.82; Cl, 9.83; N, 19.48.

Table 1. Antimicrobial study of the synthesized heterocycles compounds

Compound	*E. coli*, mg mL^{-1}		*P. aeuroginosa*, mg mL^{-1}		*S. aureus* mg mL^{-1}		*B. subtilis* mg mL^{-1}		*C. albicans* mg mL^{-1}		*A. flavus* mg mL^{-1}	
	DIZ, mm	% AI	DIZ, mm	% AI	DIZ, mm	% AI	DIZ, mm	% AI	DIZ, mm	% AI	DIZ, mm	% AI
2	9	36.0	16	69.6	14	60.9	16	69.6	8	30.8	12	48.0
3	13	52.0	20	86.9	15	65.2	18	78.3	21	80.8	20	80.0
7	NA	----	2	8.7	2	8.7	NA	----	NA	----	NA	----
8	NA	----	5	21.7	4	17.4	6	26.1	NA	----	7	28.0
10	5	20.0	9	39.1	9	39.1	10	43.5	5	19.2	9	36.0
13	7	28.0	11	47.8	10	43.5	13	56.5	10	38.5	18	72.0
Ampicillin	25	100	23	100	23	100	23	100	NA	----	NA	----
Colitrim-azole	NA	----	NA	----	NA	----	NA	----	26	100	25	100

DIZ = Diameter of inhibition zone; % AI = % Activity index; NA = No activity

Table 2. Antimicrobial and antimycotic activities in terms of MIC (μg mL^{-1}).

Compound	*E. coli*	*P. aeuroginosa*	*S. aureus*	*B. subtilis*	*C. Albicans*	*A. flavus*
2	250	187.5	93.7	187.5	93.7	46.9
3	187.5	125	62.5	187.5	23.4	7.8
7	NA	750	500	NA	NA	NA
8	NA	500	375	750	NA	250
10	750	375	250	375	187.5	62.5
13	375	250	187.5	250	46.9	23.4
Ampicillin	125	187.5	93.7	187.5	----	----
Colitrimazole	----	----	----	----	7.8	5.8

6-Amino-4-(2-chloro-5-nitrophenyl)-3-methyl-1,4-dihydro-pyrano[2,3-*c*]pyrazole-5-carboxamide (3)

Compound **1** (5 mmol, 1.66 g) was added drop wise with stirring to concentrated cold sulphuric acid (6 mL) at 20 °C, the temperature did not exceed 40 °C during the addition, then the solution was stirred for further 1 h at room temperature and poured onto ice cold water (10 mL). The reaction mixture was left overnight in the refrigerator. The yellow precipitate was filtered off and crystallized from water to give compound **3** as a pale yellow solid (68 %). m.p. 175-176 °C. FTIR (KBr): 3588 (NH pyrraz.), 3567-3370 (NH_2), 3191-3108(amide NH_2), 1685 (CO) cm^{-1}. MS *m/z* (%): 350(M^{+};1.36), 351(4.93), 307 (67.39), 230(70.44), 151 (43.39), 43(100). ^{1}H-NMR (DMSO-d_6) δ = 11 (s, 1H, NH, pyraz., exchanged with D_2O), 7.38- 6.67 (s, 4H, C2-N$\underline{H}_2$; CON$\underline{H}_2$, exchanged with D_2O), 8.63–7.60 (m, 3H, aromatic), 4.68 (s, 1H, benzylic), 2.1 (s, 3H, CH_3). Anal. Calcd. for $C_{14}H_{11}N_4O_5Cl$ (350.72): C, 47.95; H, 3.16; Cl, 10.11; N, 15.98. Found: C, 47.93; H, 3.15; Cl, 10.11; N, 15.99.

N-Acetyl-N-[4-(2-chloro-5-nitrophenyl)-5-cyano-3-methyl-1,4-dihydropyrano[2,3-*c*]pyrazol-6-yl]acetamide (5)

A solution of **1** (5 mmol, 1.66 g) in acetic anhydride-pyridine mixture (30 mL, 2:1 v/v) was heated on a water bath for 8 h, then cooled and poured into ice/ water mixture. The precipitate thus formed was filtered off, washed several times with water, dried and crystallized from dioxane to give compound **5**, as a deep brown solid (50 %). m.p. > 300 °C. FTIR (KBr): 3355(NH pyrrazole), 1787, 1739 (C═O), 2223(C ≡N) cm^{-1}. ^{1}H-NMR (DMSO-d_6) δ = 11.28 (s, 1H, NH, pyrazole, exchanged with D_2O), 8.42-7.70 (m, 3H, aromatic), 4.62 (s, 1H, benzylic), 2.12 (s, 6H, $2CH_3$), 2.55 (s, 3H, CH_3). MS *m/z* (%): 415 (M^{+};100), 417(32), 416 (19.5). Anal. Calcd. for $C_{18}H_{14}N_5O_5Cl$ (415.79): C, 52; H, 3.39; Cl, 8.53; N, 16.84. Found: C, 52.01; H, 3.38; Cl, 8.52; N, 16.85.

N-[4(2-Chloro-5-nitrophenyl)-5-cyano-3-methyl-1,4-dihydro-pyrano[2,3-c]pyrazol-6-yl]benzamide (6)

A mixture of **1** (5 mmol, 1.66 g) and benzoyl chloride (5 mmol) in toluene was refluxed for 24 h. The excess of solvent was removed under vacuum, the remaining solid was crystallized from ethanol-dioxane (1:1) to give compound **6** as a brown solid (53 %). m.p. 261-262 °C. FTIR (KBr): 3452 (NH pyrrazole), 3168 (NH-amide), 1708 (C═O, cyclic amide), 2193 (C≡N), 1641 (C═O, amide) cm^{-1}. ^{1}H-NMR (DMSO-d_6) δ = 8. 35 (s, 1H, NH, amide), 8.19-7.40 (m, 13H, aromatic), 5.41 (s, 1H, benzylic), 1.79 (s, 3H, CH_3). MS *m/z* (%): 539 (M^{+}; 3.40), 541 (2.38), 426 (15.76), 220 (28.65), 41(100). Anal. Calcd. for $C_{28}H_{18}N_5O_5Cl$ (539.93): C, 62.29; H, 3.36; Cl, 6.57; N, 12.97. Found: C, 62.27; H, 3.35; Cl, 6.56; N, 12.98.

Ethyl-4-(2-chloro-5-nitrophenyl)-5-cyano-3-methyl-1,4-dihyd-ropyrano[2,3-c]pyrazol-6-ylimidoformate (7)

A mixture of **1** (5 mmol, 1.66 g) and triethyl orthoformate (20 mL) was refluxed for 24 h. After completion of the reaction, the excess of triethyl orthoformate was removed under vacuum. The remaining solid was washed with n-hexane several times and crystallized from benzene to give

compound **7** as a pale brown solid (60 %). m.p. 233-234 °C. FTIR (KBr,): 3180 (NH pyrrazole), 1632 (C═N), 2210 (C≡N) cm^{-1}. ^{1}H-NMR (DMSO-d_6) δ = 12.36 (s, 1H, NH, pyrazole, exchanged with D_2O), 8.59 (s, 1H, N═CH), 8.17–7.77 (m, 3H, aromatic), 5.47 (s, 1H, benzylic), 4.34-4.28 (q, 2H, CH_2), 1.77 (s, 3H, CH_3, pyrazole), 1.31-1.28 (t, 3H, CH_3). MS *m/z* (%): 386.87(M^{+}; 11.08), 389(5.67), 283(25.01), 259(34.62), 202(32.17), 146 (82.33), 82 (100). Anal. Calcd. for $C_{17}H_{14}N_5O_4Cl$ (387.78): C, 52.66; H, 3.64; Cl, 9.14; N, 18.06. Found: C, 52.64; H, 3.62; Cl, 9.13; N, 18.08.

4-(2-chloro-5-nitrophenyl)-5-imino-3-methyl-1,4-dihydropyr-azolo-[4',3':5,6]pyrano[2,3-d]pyrimidin-6- (5H)-amine (8)

To a well stirred cold solution of compound **7** (20 mmol, 7.76 g) in ethanol (20 mL), hydrazine monohydrate (99 %) (3 mL) was added drop wise and then the mixture was stirred at room temperature for 6 h and left overnight. The solid that precipitated was filtered off and and crystallized from ethanol to give compound **8** as a pale yellow solid (66 %). m.p. > 300 °C. FTIR (KBr,): 3349 (NH pyrrazole), 3309 (NH, imino), 3188, 3119 (NH_2), 1638 (C═N) cm^{-1}. ^{1}H-NMR (DMSO-d_6) δ = 12.57 (s, 1H, NH, pyrazole), 10.25 (s, 1H, C═NH), 8.44 (s, 1H, CH═N), 8.18-7.67 (m, 3H, aromatic), 5.89 (s, 1H, benzylic), 4.40 (s, 2H, NH_2), 1.93 (s, 3H, CH_3). MS *m/z* (%): 373 (M^{+}; 2.43), 290 (13.60), 221 (21.71), 161 (65.56), 60 (100). Anal. Calcd. for $C_{15}H_{12}N_7O_3Cl$ (373.76): C, 48.20; H, 3.24; Cl, 9.48; N, 26.23. Found: C, 48.21; H, 3.23; Cl, 9.47; N, 26.24.

4-(2-Chloro-5-nitrophenyl)-5-cyano-3-meth- yl-1,4-dihydro-pyrano[2,3-c]pyrazol-6-yl formamide (9)

Compound **7** (2 mmol, 0.78 g) was added to a mixture of methanol (15 mL) and 25% aqueous ammonia solution (15 mL). The reaction mixture was stirred for 24 h, cooled, and the precipitated solid was filtered off and crystallized from toluene to give compound **9** as a pale brown solid (51 %). m.p. > 300 °C. FTIR (KBr,): 3271(NH pyrrazole), 2205 (C≡N), 1669 (CO) cm^{-1}. ^{1}H-NMR (DMSO-d_6) δ = 12.57 (s, 1H, NH, pyrazole), 8.21 (s, 1H, CHO), 8.32-7.68 (m, 3H, aromatic), 7.2 (s, 1H, NH), 4.74 (s, 1H, benzylic), 1.9 (s, 3H, CH_3). Anal. Calcd. for $C_{15}H_{10}N_5O_4Cl$ (359.73): C, 50.08; H, 2.80; Cl, 9.48; N, 26.23. Found: C, 48.21; H, 3. 2 3; Cl, 9.47; N, 26.24.

4-(2-Chloro-5-nitrophenyl)-5-cyano-3-methyl-1,4-dihydro-pyrano[2,3-c]pyrazol-6-yl carbamodithioic acid (10)

To a solution of **1** (10 mmol, 3.31 g) in DMF (20 mL), carbon disulfide (15 mmol) and 10 mL of sodium methoxide (prepared from 0.59 gm of sodium metal and 30 ml methanol) were added. The mixture was refluxed for 20 h and then poured into ice cold water. A solution of sodium hydroxide (20 mL, 1M) was added to it and left overnight. The solution was filtered and acidified with dilute acetic acid to give yellow precipitate, which was collected, washed with dilute acetic acid, dried and crystallized from ethanol to give compound **11** as a deep yellow solid (52 %). m.p. > 300 °C. FTIR (KBr): 3261 (NH pyrrazole), 3151(NH), 2966 (SH), 2215 (C≡N), 1390 (C═S) cm^{-1}. ^{1}H-NMR (DMSO-d_6) δ = 12.02 (s, 1H, NH, pyrazole), 7.70-7.14 (m, 3H, aromatic), 5.52 (s, 1H, benzylic), 10.89 (s, 1H, NH), 1.2(s, 1H, SH), 1.9 (s, 3H, CH_3). MS *m/z* (%):406.9 (M^{+}; 6.07), 409 (4.64), 358 (32.16), 281 (25.37), 64 (100). Anal. Calcd. for $C_{15}H_{10}N_5O_3S_2Cl$ (407.85): C, 44.17; H, 2.47; Cl, 8.69; N, 17.17. Found: C, 44.16; H, 2.46; Cl, 8.68; N, 17.18.

N-[4-(2-Chloro-5-nitrophenyl)-5-cyano-3-methyl-1,4-dihydro-pyrano[2,3-c]pyrazol-6-yl]-N'-phenyl- urea (13)

A mixture of **1** (10 mmol, 3.31 g) and phenylisocyanate (10 mmol) in pyridine (20 mL) was refluxed for 12 h. The reaction mixture was cooled and poured onto ice/ water mixture and neutralized with diluted HCl. The solid product so formed was collected by filtration and crystallized from methanol to give compound **13** as a deep yellow solid (56 %). m.p. > 300 °C. FTIR (KBr): 3371 (NH pyrrazole), 3213, 3101 (2NH, amide), 1745 (C=O), 2210 (C≡N) cm^{-1}. ^{1}H-NMR (DMSO-d_6) δ = 11.5 (s, 1H, NH, pyrazole), 8.58-7.11 (m, 8H, aromatic), 4.7(s, 1H, benzylic), 8.9 (s, 1H, NH), 6.7 (s, 1H, NH), 1.9 (s, 3H, CH_3). MS *m/z* (%):450 (M^{+}; 3.47), 451.85 (4.90), 244 (22.11), 219 (41.50), 198 (79.99). Anal. Calcd. for $C_{21}H_{15}N_6O_4Cl$ (450.84): C, 55.95; H, 3.35; Cl, 7.86; N, 18.64. Found: C, 55.94; H, 3.33; Cl, 7.87; N, 18.65.

References

[1]Goel, A., Singh, F. V., *Tetrahedron Lett.*, **2005**, *46*, 5585-5587. https://doi.org/10.1016/j.tetlet.2005.06.034

[2]EL-Far, M., EL megeed, F. V. G. A., Eskander, E. F., Rady, H. M., Tantawy, M. A., Eur. *J. Med. Chem*., **2009**, *44* (10), 3936-3946. https://doi.org/10.1016/j.ejmech.2009.04.020

[3]Pasternak, P. V., Averkiev, Antipin, B. B. M. Y., Peregudov, A. S., Chkanikov, N. D. *J. Fluorine Chem*., **2004**, *125*, 1853-1868.https://doi.org/10.1016/j.jfluchem.2004.06.008

[4]Ballini, R., Sartori, G., Sartorio, R., *Tetrahedron Lett*., **2004**, *45*, 2297-2299. https://doi.org/10.1016/j.tetlet.2004.01.115

[5]Abdel hamid, A. O., Afifi, M. A. M., *J. Adv. Res.*, **2010**, *1*, 137-144. https://doi.org/10.1016/j.jare.2010.03.005

[6]Al-Amiery, A. A., Al-Bayati, R. I., Saed, F. M., Ali, W. B., Kadhum, A. A. H., Mohamad, A. B., *Molecules*, **2012**, *17*, 10377-10389. 10.3390/molecules170910377

[7]El-Gazzar, A. B. A., El-Enany, M. M., Mahmoud, M. N., *Bioorg. Med. Chem*., **2008**, *16*, 3261-3273. https://doi.org/10.1016/j.bmc.2007.12.012

[8]Fayed, A. A., Hosni, H. M., Flefel, E. M., Amr, A. E. E., *World J. Chem*., **2009**, *4*, 58-65.

[9]Sondhi, S. M., Singh, N., Johar, M., Kumar, A., *Bioorg. Med. Chem*., **2005**, *13*, 6158-6166. https://doi.org/10.1016/j.bmc.2005.06.063

[10]Abu-Hashem, A. A., El-Shehry, M. F., Badria, F. A., *Acta Pharm*., **2010**, *60*, 311-323. https://doi.org/10.2478/v10007-010-0027-6

[11]Svetlik, J., Veizerova, L., Liptaj, T., Kubista, J., *ARKIVOC*, **2009**, *2009*, 79-86.

http://dx.doi.org/10.3998/ark.5550190.0010.a09

[12]Fathalla, O. A., Zeid, I. F., Haiba, M. E., Soliman, A. M.; Abd-Elmoez, S. I.; Serwy, W. S. *World J. Chem*., **2009**, *4*, 127-132.

[13]El-Assiery, S. A., Sayed, G. H., Fouda, A., *Acta Pharm*., **2004**, *54*, 143-150.

[14]Li, M., Wang, S. W., Wen, L. R., Qi, W. Y., Yang, H. Z., *J. Chin. Chem. Soc.*, **2005**, *52*, 1021-1028. 10.1002/jccs.200500143

[15]Wannberg, J., Dallinger, D., Kappe, C.O., Larhed, M. J., *Comb. Chem.*, **2005**, *7*, 574-583. http://dx.doi.org/10.1021/cc049816c

[16]Alqasoumi, S. I., Al-Taweel, A. M., Alafeefy, A. M., Noaman, E., Ghorab, M. M., *Eur. J. Med. Chem.*, **2010**, *45*, 738-744. https://doi.org/10.1016/j.ejmech.2009.11.021

[17]Broom, A. D., Shim, J. L., Anderson, G. L., *J. Org. Chem.*, **1976**, *41*, 1095-1099.10.1021/jo00869a003

[18]Joshi, A. A., Viswanathan, C. L., *Anti-Infect. Agents Med. Chem.*, **2006**, *5*, 105-122. https://doi.org/10.2174/187152106774755626

[19]Ghorab, M. M., Hassan, A. Y., *Phosphorus, Sulfur Silicon Relat. Elem.*, **1998**, *141*, 251-261. https://doi.org/10.1080/10426509808033737

[20]Sharma, P., Rane, N., Gurram, V. K., *Bioorg. Med. Chem. Lett.*, **2004**, *14*, 4185-4190. https://doi.org/10.1016/j.bmcl.2004.06.014

[21]El-Gazzar, A. B. A., Hafez, H. N., Nawwar, G. A. M., *Eur. J. Med. Chem.*, **2009**, *44*, 1427-1436. https://doi.org/10.1016/j.ejmech.2008.09.030

[22]De la Cruz, J. P., Moreno, A., Mérida, F., García-Campos, J., de la Cuesta, F. S., *Pharmacol. Toxicol.*, **1994**, *75*, 250-254.10.1111/j.1600-0773.1994.tb00356.x

[23]Gupta, R., Jain, A., Joshi, R., Jain, M., *Bull. Korean Chem. Soc.*, **2011**, *32*, 899-904. 10.5012/bkcs.2011.32.3.899

[24]Hanna, M. M., *Eur. J. Med. Chem.*, **2012**, *55*, 12-22. https://doi.org/10.1016/j.ejmech.2012.06.048

[25]Shinde, S. V., Jadhav, W. N., Karade, N. N., *Orient. J. Chem.*, **2010**, *26*, 307-317.

[26]Lichtner, R. B., Hutchinson, G., Hellmann, K., *Eur. J. Cancer Clin. Oncol.*, **1989**, *25*, 945-951. https://doi.org/10.1016/0277-5379(89)90152-1

[27]DeGraw, J. I., Christie, P. H., Clowell, W. T., Sirotnak, F. M., *J. Med. Chem.*, **1992**, *35*, 320-324. 10.1021/jm00080a017

[28]Thomas, H. D., Saravanan, K., Wang, L. Z., Lin, M. J., Northen, J. S., Barlow, H., Barton, M., Newell, D. R., Griffin, R. J., Golding, B. T., Curtin, N. J., *Mol. Cancer Therapy*, **2009**, *8*, 1828-1837. 10.1158/1535-7163.MCT-08-1208

[29]Petal, N. C., Mehta, A. G., *Asian J. Chem.*, **2001**, *13*, 1385-1388.

[30]Holla, B. S., Mahalinga, M., Karthikeyan, M. S., Akberali, P. M., Shetty, N. S., *Bioorg. Med. Chem.*, **2006**, *14*, 2040-2047. https://doi.org/10.1016/j.bmc.2005.10.053

[31]Całus, S., Gondek, E., Danel, A., Jarosz, B., Pokładko, M., Kityk, A. V., *Mater. Lett.*, **2007**, *61*, 3292-3295. https://doi.org/10.1016/j.matlet.2006.11.055

[32]Yousif, N. M., Gad, F. A., Sayed, H. H., *Egypt. J. Chem.*, **1992**, *35*, 101-110.

[33]Yousif, N. M., Gad, F. A., Sayed, H. H., *Egypt. J. Pharm. Sci.*, **1996**, *37*, 145-156.

[34]Sayed, H. H., *Indian J. Chem.*, **1998**, *37B*, 1054-1058.

[35]Sayed, H. H., Fahmy, F. A., *Egypt. J. Chem.*, **2001**, *44*, 365-372.

[36]Rashad, A. E., Sayed, H. H., Shamroukh, A. H., Awad, H. M., *Phosphorus Sulfur*, **2005**, *180*, 2767-2777. https://doi.org/10.1080/104265090968118

[37]Abdel-Megeid, F. M. E., Hassan, N. A., Zahran, M. A., Rashad, A. E., *Sulfur Lett.*, **1998**, *21*, 269-284.

[38]El-Ziaty, A. K., Abdalha, A. A., Hamed, A. A., Shiba, S. A., Abdulalh, A. A., *Eur. J. Chem.*, **2012**, *3*(1), 65-70. 10.5155/eurjchem.3.1.65-70.518

[39]El-Ziaty, A. K., Shiba, S. A., *Synth. Commun.*, **2007**, *27*, 4043-4057. https://doi.org/10.1080/00397910701575491

[40]Abou-Elmagd, W. S. I., EL-Ziaty, A. K., Abdalha, A. A., *Heterocycl. Commun.*, **2015**, *21*(13), 179-185. https://doi.org/10.1515/hc-2015-0008

[41]Elziaty, A. K.; Mostafa, O. E. A.; El-Bordany, E. A.; Nabil, M.; Madkour, H.M.F. *Int. J. Sci. Eng. Res.* **2014**, *5*, 727-735.

[42]Ismail, M. F., Mahmoud, M. R., Shiba, S. A., El-Ziaty, A. K., Abu El-Azm, F. S. M., *Synth. Commun.*, **2014**, *44*, 1094-1102. https://doi.org/10.1080/00397911.2013.846381

[43]El-Ziaty, A. K., Hussein, A. M., Mahmoud, M. R., *World Appl. Sci. J.*, **2012**, *17*(1), 101-108.

[44]Morsy, J. M., Aly, A. F., Elshahawi, M. M., EL-Ziaty, A. K., *J. Heterocycl. Chem.*, **2016**, *53* (5), 1443-1448. 10.1002/jhet.2445

[45]EL-Ziaty, A. K, El-Shahawi, M. M., *J. Chem.* **2017**. https://doi.org/10.1155/2017/5610707

[46]EL-Ziaty, A. K., Abdel-Aziz, M. S., Bassioni, G., Hassan, A. M. A., Derbala, H. A., *J. Chem.*, **2016**. http://dx.doi.org/10.1155/2016/5286462

Received: 23.12.2017.
Accepted: 21.01.2018.

SYNTHESIS, REACTIONS AND SPECTRAL CHARACTERIZATION OF NOVEL THIENOPYRAZOLE DERIVATIVES

Adel M. Kamal El-Dean[a], Remon M. Zaki[a]*, Shaban M. Redwan[a] and Ahmed F. Saber[a]*

Keywords: Pyrazole, thienopyrazole, pyrimidothienopyrazole, synthesis.

4-Amino-3-methyl-1-phenyl-*1H*-thieno[2,3-*c*]pyrazole-5-carboxamide has been synthesized by an innovative method. The aminoamide derivative was gently refluxed with chloroacetyl chloride under neat conditions followed by neutralization with sodium carbonate solution to afford the chloromethyl pyrimidinone compound. The chloromethyl pyrimidinone derivative was converted to the thiol derivative by the reaction with thiourea in ethanol. The thiol compound was alkylated with α-halocompounds such as ethyl chloroacetate, chloroacetone, phenacyl bromide and 2-chloro-4,6-dimethylnicotinonitrile to afford the corresponding S-alkylated compounds. The chemical structures of the newly synthesized compounds were elucidated on the basis of elemental and spectral analyses containing FT-IR, ^{1}H-NMR, and mass spectroscopy.

*Corresponding Authors
E-Mail: remonch@yahoo.com; ahmed.fathi_91@yahoo.com
[a] Chemistry Department, Faculty of Science, Assiut University, Assiut 71516, Egypt

INTRODUCTION

Many of pyrazoles and related compounds are known to possess biological activity.[1-6] Thieno[3,4-*c*]pyrazoles are a class of biologically active compounds, currently employed in the field of medicinal chemistry owing to their remarkable anti-inflammatory,[7,8] analgesic and antithrombotic activities, also for the treatment of cardiovascular or cerebrovascular diseases, and hyperglycemia.[9] Thieno[3,2-*c*]pyrazoles are used in the treatment of hypertension and glaucoma.[10] Thieno[2,3-*c*]pyrazoles on the other hand, represent a class of heterocyclic compounds which have antifungal, antibacterial and anti-inflammatory activities.[11-21]

RESULT AND DISCUSSION

4-Amino-3-methyl-1-phenyl-*1H*-thieno[2,3-*c*]pyrazole-5-carboxamide was synthesized by an innovative method according to literature procedure.[19-21] All attempts to displace the chloride ion by the thiol group in the previously prepared 5-chloro-3-methyl-1-phenyl-*1H*-pyrazole-4-carbonitrile compound **(1)** by the reaction of thiourea in ethanol and with other moieties to obtain 5-mercapto-*N*-phenylpyrazole-4-carbonitrile **(2)** failed, giving the chloropyrazole carbonitrile starting material **(1)**. The previous results forced us to search for another method to prepare the target amino thienopyrazole carboxamide compound **(5)**. The desired results were achieved by the reaction of elemental sulfur with chloropyrazole in the presence of sodiumborohydride to give the non-isolated sulfanyl sodium salt **(3)** which underwent an *in situ* reaction with chloroacetamide to afford the pyrazole sulfanyl acetamide derivative **(4)**. The latter compound underwent Thorpe-Zeigler cyclization on heating in ethanolic sodium ethoxide solution yielding the amino thienopyrazole carboxamide **(5)** (Scheme 1). The chemical structure of compound **(5)** was elucidated on the basis of elemental and spectral data. IR spectrum of compound **(5)** revealed appearance of absorption band at 3400, 3305, 3190 cm^{-1} due to two NH_2 group. ^{1}H NMR spectrum showed two singlet signals at δ 2.60, 6.90 and 7.00 ppm characteristic for CH_3 and NH_2 groups respectively. ^{13}C NMR spectrum displayed signals at 15.2 and 169.80 ppm attributed to CH_3 and $CONH_2$ groups respectively.

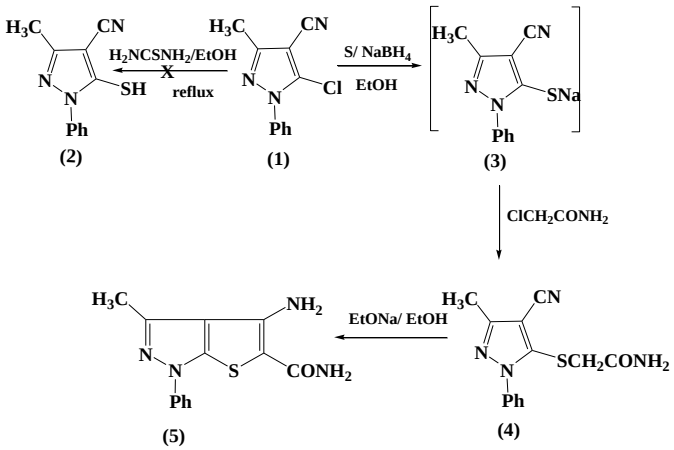

Scheme 1. Synthesis of aminoamide derivative of thienopyrazole.

Heating the amino carboxamide compound **(5)** with chloroacetyl chloride on a water bath under neat conditions followed by neutralization with diluted sodium carbonate solution afforded the chloromethylpyrazolo-thienopyrimidinone **(6)**. The latter compound was characterized on the basis of elemental and spectral analysis. IR spectrum revealed the disappearance of absorption bands for NH_2 groups in the amino amide compound **(5)** and appearance of a broad absorption band at 3480-3300 cm^{-1} for NH group. ^{1}H NMR spectrum showed singlet signal at δ 4.60 ppm for CH_2 group and singlet signal at 10.60 ppm for NH pyrimidine.

5-(Chloromethyl)-3-methyl-1-phenyl-*1H*-pyrazolo[4',3':4,5]-thieno[3,2-*d*]pyrimidin-7(*6H*)-one **(6)** was converted into corresponding 5-(mercaptomethyl)-3-methyl-1-phenyl-*1H*-pyrazolo[4',3':4,5]thieno[3,2-*d*] pyrimidin-7(*6H*)-one **(7)** by refluxing with thiourea followed by treatment with sodium hydroxide and then acidification with HCl. Mercapto-methylpyrazolothienopyrimidine **(7)** was alkylated using α-halogenated compounds namely, ethyl chloroacetate, phenacyl bromide and chloroacetone to give S-alkylated mercaptomethylpyrazolothienopyrimidine derivatives respectively (**8-10**) (Scheme 2). While the reaction with 2-chloro-4,6-dimethylnicotinonitrile, afforded thienopyridinyl of pyrazolothienopyrimidine compound **(11)**. The structure of compound **(7)** was confirmed using elemental and spectral data. IR spectrum revealed absorption bands at 3428 cm^{-1} characteristic of the NH group and 1655 cm^{-1} for CO group. ^{1}H NMR spectrum of the thiol derivative **(7)** in DMSO-d_6 displayed singlet signals at δ: 3.70 ppm for CH_2, at 1.20 ppm for SH group and at 3.90 ppm attributed to NH group.

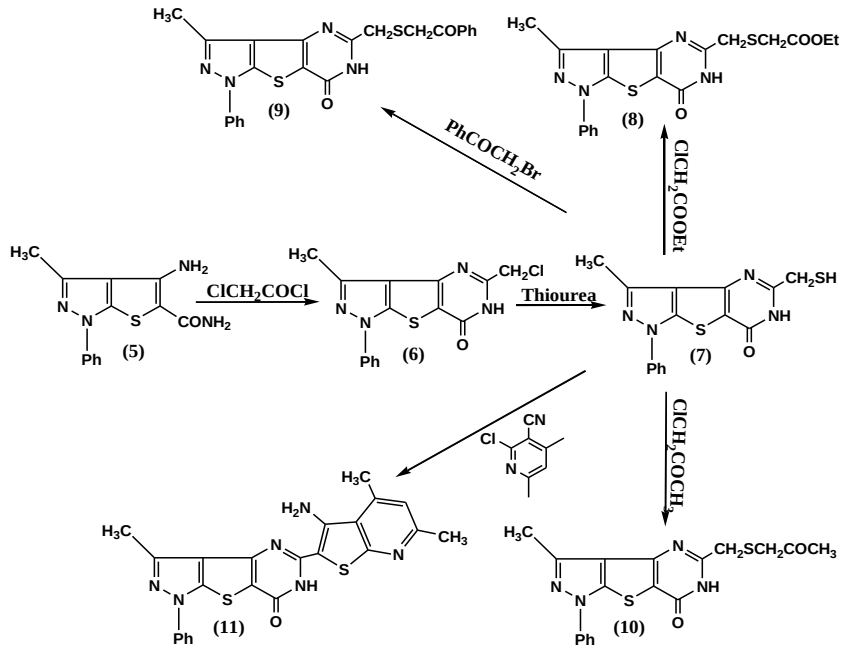

Scheme 2. Synthesis and reactions of mercaptomethylpyrimidothienopyrazole derivative.

Experimental

All melting points were uncorrected and recorded on a Gallen Kamp electric melting point apparatus. The elemental analyses were carried out at the Micro Analytical Center of Chemistry Department- Assiut University.

The FT-IR spectra were recorded using potassium bromide disks on a FT-IR 8201 PC Shimadzu. ^{1}H NMR and ^{13}C NMR spectra were obtained on a Bruker (^{1}H NMR: 400 and 300 MHz, ^{13}C NMR: 100 and 75 MHz) spectrometers in $CDCl_3$ and DMSO-d_6 using Me_4Si as internal standard and chemical shifts are expressed as ppm. Mass spectra were measured on a Jeol-JMS 600 and Shimadzu Qp-2010 plus spectrometer at the Micro Analytical Center –Cairo University- Giza.

All reactions were monitored by TLC on silica gel coated aluminum sheets (Silica Gel 60 F254, Merck). Compounds **(1)**, **(4),** and **(5)** were prepared according to literature procedure[22-27] with m.p. 120-122 °C, 144-146 °C and 214-216 °C, respectively.

Synthesis of 3-methyl-1-phenyl-5-sulfanylacetamidopyrazole-4-carbonitrile (4)

Sodium borohydride (4 g, 0.105 mol) was added to a suspension of finely powered sulfur (4 g, 0.125 mol) in absolute ethanol (60 ml), kept in an ice bath, in small portions till all sulfur powder dissolved, then chlorocyanopyrazole **(1)** (10 g, 46 mmol) was added to the reaction mixture with stirring in an ice bath for 1 h. The reaction mixture was refluxed for 4 h followed by cooling. Then, the chloroacetamide (4.30 g, 46 mmol) was added to the mixture. The reaction mixture was left overnight with stirring. The solid precipitate which is formed was filtered off, dried, and recrystallized from ethanol as white crystals in (10 g, 80 %). m.p. 144–146 °C. IR (KBr): 3450, 3300 (NH_2), 3050 (CH aromatic), 2920, 2850 (CH aliphatic), 2220 (CN), 1660 (CO amide), 1590 (C=N) cm^{-1}. ^{1}H NMR (400 MHz, DMSO-d_6): δ = 2.35 (s, 3H, CH_3), 3.30 (s, 2H, CH_2), 7.15 (s, 2H, NH_2), 7.30–7.70 (m, 5H, ArH). Anal. Calcd. for $C_{13}H_{12}N_4OS$: C, 57.34; H, 4.44; N, 20.57; S, 11.77, Found: C, 57.26; H, 4.50; N, 20.60; S, 12.00.

Synthesis of 4-Amino-3-methyl-1-phenyl-*1H*-thieno[2,3-*c*]pyrazole-5-carboxamide (5)

To a solution of acetamido-pyrazole carbonitrile compound (**4**) (4 g, 16 mmol) in absolute ethanol (20 ml), sodium ethoxide solution (2.5 ml) was added. The mixture was gently refluxed for 10 min. The solid precipitate which separated out during reflux was filtered off, dried, and recrystallized from the mixture of ethanol–dioxane 2:1 as white crystals in (2.80 g, 70 %). m.p. 214-216 ºC. IR (KBr): 3400, 3305, 3190 (NH_2), 3050 (CH aromatic), 2910 (CH aliphatic), 1635 (CO amide), 1580 (C=N) cm^{-1}. ^1H NMR (DMSO-d_6): δ = 2.60 (s, 3H, CH_3), 6.90 (s, 2H, NH_2 amide), 7.00 (s, 2H, NH_2), 7.30-7.70 (m, 5H, ArH). ^{13}C NMR (100 MHz, DMSO-d_6): 15.2 (CH_3 pyrazole), 109.3, 121.5, 145.4, 145.4, 149.9 (C), 124.4, 128.2, 129.8, 133.1 (Ph pyrazole), 169.8 ($CONH_2$). EI-MS: m/z 272.14 [M^+]. Anal. Calcd. for $C_{13}H_{12}N_4OS$: C, 57.34; H, 4.44; N, 20.57; S, 11.77. Found: C, 57.44; H, 4.55; N, 20.47; S, 11.65.

Synthesis of 5-chloromethyl-3-methyl-1-phenyl-pyrimido-[4',5':4,5]thieno[2,3-*c*]pyrazol-7(*6H*)-one (6)

A mixture of compound (**5**) (4.00 g, 15 mmol) and an excess of chloroacetyl chloride (8 ml, 70 mmol) was heated on water bath for 3 h, then poured into cold water (100 ml), neutralized with sodium carbonate solution (10 %) to just alkaline. The solid product was filtered off, dried and recrystallized from dioxane as pale yellow crystals (3.8 g, 78%). m.p. 304-306 ºC. IR (KBr): 3480-3300 (NH), 3050 cm^{-1} (CH aromatic), 2920, 2850 cm^{-1} (CH aliphatic), 1645 cm^{-1} (CO amide) cm^{-1}. ^1H NMR (DMSO-d_6): δ = 2.60 (s, 3H, CH_3), 4.60 (s, 2H, CH_2), 7.20-7.90 (m, 5H, ArH), 10.60 (s, 1H, NH). Anal. Calcd. for $C_{15}H_{11}ClN_4OS$: C, 54.46; H, 3.35; Cl, 10.72; N, 16.94; S, 9.69. Found: C, 54.69; H, 3.50; Cl, 10.50; N, 17.00; S, 9.50.

Synthesis of 5-(mercaptomethyl)-3-methyl-1-phenyl-*1H*-pyrazolo[4',3':4,5]thieno[3,2-*d*]pyrimidin-7(*6H*)-one (7)

A mixture of compound (**6**) (1.89 g, 5.75 mmol) and thiourea (1.30 g, 0.01 mol) in ethanol was refluxed for 2 h. The yellow precipitate which obtained on heating, was filtered off and dissolved in sodium hydroxide (5 %), then acidified with (0.01 N) HCl until acidic. The solid product was collected as faint yellow crystals (1.37 g, 73%). m.p>360 ºC. IR (KBr): 3428 (NH), 1655 (CO), 2923, 2853 (CH aliphatic) and 1594 (C=N) cm^{-1}. ^1H NMR (DMSO-d_6): δ = 1.20 (s, 1H, SH), 2.50 (s, 3H, CH_3), 3.70 (s, 2H, CH_2), 3.90 (s, 1H, NH), 7.20-7.70 (m, 5H, ArH) ppm. EI-MS: m/z 328 [M^+]. Anal. Calcd. for $C_{15}H_{12}N_4OS_2$: C; 54.86; H, 3.68; N, 17.06; O, 4.87; S, 19.52. Found: C; 54.74; H, 3.75; N, 17.13; S, 19.44.

Synthesis of ethyl-2-(((3-methyl-7-oxo-1-phenyl-6,7-dihydro-*1H*-pyrazolo[4',3':4,5]thieno[3,2-*d*]pyrimidin-5-yl)methyl)thio)-acetate (8)

A mixture of compound (**7**) (1.60 g, 3.87 mmol), ethyl chloroacetate (0.47 ml, 3.87 mmol) and sodium acetate (0.7 g, 8.5 mmol), were refluxed in ethanol (20 ml) for 3hrs. then allowed to cool. The solid product was collected and recrystalized from ethanol as yellowish white crystals (1.30 g, 65 %), m.p. 190-192 ºC. IR (KBr): 3435 (NH), 2923, 2852 cm^{-1} (CH aliphatic), 1663, 1727 cm^{-1} (2CO) and 1595 cm^{-1} (C=N). ^1H NMR (DMSO-d_6): δ= 1.20 (t, 3H, CH_3), 2.60 (s, 3H, CH_3 pyrazole), 3.60 (s, 2H, CH_2-S), 3.70 (s, 2H, -SCH_2) 3.90 (q, 2H, CH_2 ester), 7.40-7.80 (m, 5H, ArH) and 12.80 (s, 1H, NH). Anal. Calcd. for $C_{19}H_{18}N_4O_3S_2$: C; 55.06; H, 4.38; N, 13.52; O, 11.58; S, 15.47. Found: C; 55.18; H, 4.30; N, 13.41; S, 15.39.

Synthesis of 3-methyl-5-(((2-oxo-2-phenylethyl)thio)methyl)-1-phenyl-*1H*-pyrazolo[4',3':4,5]thieno[3,2-*d*]pyrimidin-7(*6H*)-one (9)

A mixture of the mercapto compound (**7**) (0.86 g, 1.93 mmol), phenacyl bromide (0.38 ml, 1.90 mmol) and sodium acetate (0.40 g, 4.87 mmol), were refluxed in ethanol (20 ml) for 3 h. The solid precipitate was formed during reflux was collected, dried and recrystallized from dioxane as yellow crystals (0.47 g, 40%). m.p. 215-217 ºC. IR (KBr) 3435 (NH), 2924, 2853 (CH aliphatic), 1660, 1675 (2CO) and 1595 (C=N) cm^{-1}. ^1H NMR (DMSO-d_6): δ= 2.30 (s, 3H, CH_3 pyrazole), 3.70 (s, 2H, CH_2-S), 4.40 (s, 2H, S-CH_2), 7.30-8.00 (m, 10H, 2ArH) and 12.80 (s, 1H, NH). Anal. Calcd. for $C_{23}H_{18}N_4O_2S_2$(446.54): C; 61.86; H, 4.06; N, 12.55; O, 7.17; S, 14.36%. Found: C; 61.77; H, 4.15; N, 12.41; S, 14.45%.

Synthesis of 3-methyl-5-(((2-oxopropyl)thio)methyl)-1-phenyl-*1H*-pyrazolo[4',3':4,5]thieno[3,2-*d*]pyrimidin-7(*6H*)-one (10)

A mixture of compound (**7**) (1.49 g, 3.87 mmol), chloroacetone (0.47 ml, 3.87 mmol) and sodium acetate (0.7 g, 8.5 mmol), were refluxed in ethanol (20 ml) for 3 h then the mixture was allowed to cool. The solid product formed on cooling was collected and recrystalized from ethanol as a pale yellow crystals (1.34 g, 77 %). m.p. 178-180 ºC. IR: (KBr): 3420 (NH), 2920, 2850 (CH aliphatic), 1680, 1665 (2CO) and 1595 (C=N) cm^{-1}. ^1H NMR (DMSO-d_6): δ= 2.50 (s, 3H, CH_3 pyrazole), 2.60 (s, 3H, $COCH_3$), 3.70 (s, 2H, CH_2-S), 3.90 (s, 2H, S-CH_2), 7.30-7.80 (m, 5H, ArH) and 12.80 (s, 1H, NH). EI-MS: m/z 384 [M^+]. Anal. Calcd. for $C_{18}H_{16}N_4O_2S_2$: C; 56.23; H, 4.19; N, 14.57; O, 8.32; S, 16.68. Found: C; 56.18; H, 4.30; N, 14.41; S, 16.59.

Synthesis of 5-(3-amino-4,6-dimethylthieno[2,3-*b*]pyridine-2-yl)-3-methyl-1-phenyl-*1H*-pyrazolo[4',3':4,5]thieno[3,2-*d*]pyrimidin-7(*6H*)-one (11)

A mixture of the mercapto compound (**7**) (1.77 g, 3.87 mmol), 2-chloro-4,6-dimethylnicotinonitrile (0.64 g, 3.87 mmol) and sodium acetate (0.7 g, 8.5 mmol), were refluxed in ethanol (20 ml) for 3h and then allowed to cool. The solid product was collected and recrystalized from ethanol as yellowish white crystals (1.55 g, 63 %). m.p. 290-292 ºC. IR (KBr): 3415, 3400 (NH, NH_2), 3028 (CH aromatic), 2931 (CH aliphatic), 1678 (CO) and 1595 (C=N) cm^{-1}. ^1H NMR (DMSO-d_6): δ= 2.50 (s, 3H, CH_3 pyrazole), 3.30 (s, 3H, CH_3 pyridine), 4.00 (s, 3H, CH_3 pyridine), 6.10 (s, 2H, NH_2), 7.20-7.40 (m, 5H, ArH), 7.80 (s, 1H, CH pyridine) and 12.80 (s, 1H, NH). Anal. Calcd. for $C_{23}H_{18}N_6OS_2$: C; 60.24; H, 3.96; N, 18.33; O, 3.49; S, 13.98 . Found: C; 60.18; H, 4.10; N, 18.41; S, 13.85.

CONCLUSION

The aim of this work is to synthesize some new bi-functionally substituted thieno[2,3-*c*] pyrazole compounds which were subjected to react with different reagents to synthesize new heterocyclic rings fused or attached to thienopyrazole system namely: pyrimidinone and thien[2,3-*b*]pyridinyl compounds.

ACKNOWLEDGEMENTS

We thank Prof. Dr. Ahmed Abdo Geies, President of Assiut University and Professor of Organic Chemistry.

REFERENCES

[1]Daidone, G., Maggio, B., Raffa, D., Plescia, S., Schillaci, D., Raimondi, M.V., *Farmaco*, **2004,** *59*, 413. https://doi.org/10.1016/j.farmac.2004.01.016

[2]Ranatunge, R. R., Garvey, D. S., Janero, D. R., Letts, L. G., Martino, A. M., Murty, M. G., Richardson, S. K., Young, D. V., Zemetseva, I. S., *Bioorg. Med. Chem.*, **2004,** *12*, 1357. https://doi.org/10.1016/j.bmc.2004.01.012

[3]Bruno, S. S. O., Bondavalli, F., Ranise, A., Mosti, L., Menozzi, G., Fossa, P., Manetti, F., Morbidelli, L., Trincavelli, L., Martini C., Lucacchini, A., *Eur. J. Med. Chem*., **2004,** *39*, 153.https://doi.org/10.1016/j.ejmech.2003.11.007

[4]Urban, F. J., Anderson, B. G., Orrill, S. L., Daniels, P. J., *Org. Proc. Res. Dev*., **2001,** *5*, 575. https://doi.org/10.1021/op010222x

[5]Sawyer, J. S., Anderson, B. D., Beight, D. W., Campbell, R. M., Jones, M. L., Herron, D. K., Lampe, J. W., McCowan, J. R., McMillen, W. T., Mort, N., Parsons, S., Smith, E. C. R., Vieth, M., Weir, L. C., Yan, L., Zhang F., Yingling, J. M., *J. Med. Chem*., **2003,** *46*, 3954. https://doi.org/10.1021/jm0205705

[6]Bekhit, A. A., Fahmy, H. T. Y., Rostom, Sh. A. F., Baraka, A. M., *Eur. J. Med. Chem*., **2003,** *38*, 27.

[7]Baraldi, P. G., El-Kashef, H. S., Manfredini, S., de las Infantas, M. J. P., Romagnoli, R., Spalluto, G., *Synthesis*, **1998,** 1331. https://doi.org/10.1055/s-1998-6095

[8]Menozzi, G., Mosti, L., Schenone, P., Damico, M., Filippelli A., Rossi, F., *Farmaco*, **1992,** *47*, 1495.

[9]Matsuo, M., Tsuji, K., Konishi N., Nakamura, K., *Eur. Pat. Appl. EP*, **1991,** 418 845; Chem. Abstr., **1991,***115*, 71 593.

[10]Ong, H. H., Yasenchak, C. M., *Eur. Pat. Appl. EP*221 414; Chem. Abstr., **1987,** *107*, 198 314.

[11]Gewald, K., Rennert, S., Schindler, R., Schäfer, H., Prakt, J. *Chem*, **1995,** *337*, 472. https://doi.org/10.1002/prac.199533701101

[12]Briel, D., *Pharmazie*, **1998,** *53*, 227. https://doi.org/10.1016/s0168-1702(98)00009-4

[13]Sherif, S. M., Hussein, A. M., *Monatsh. Chem*., **1997,** *128*, 687. https://doi.org/10.1007/bf00807600

[14]Briel, D., *Pharmazie*, **1995,** *50*, 675. https://doi.org/10.1097/00006254-199509000-00022

[15]Brown K. J., Meth-Cohn, O., *Tetrahedron Lett.*, **1974,** *46*, 4069. https://doi.org/10.1016/s0040-4039(01)92086-6

[16]Wang, Z., Li, Z., Ren, J., Chen, H., *Heteroatom Chem*., **1999,** *10*, 303. https://doi.org/10.1002/(sici)1098-1071(1999)10:4%3C303::aid-hc7%3E3.0.co;2-h

[17]Ahluwalia, V. K., Dahiya, A., Bala, M., *Indian J. Chem*., **1996**, *35B*, 715.

[18]Bakhite, E. A., Geies, A. A., El-Kashef, H. S., *Phosphorus, Sulfur Silicon*, **2000,** *157*, 107. https://doi.org/10.1080/10426500008040516

[19]El Dean, A. M. K., Zaki, R. M., Abdulrazzaq, A. Y., *Russ. J. Bioorg. Chem.*, **2015**, *41*, 97. https://doi.org/10.1134/s1068162015010057

[20]Sayed, A. H., Zaki, R. M., El-Dean, A. M. K., Abdulrazzaq, A. Y., *Toxi. Rep*., **2015,** *2*, 1445. https://doi.org/10.1016/j.toxrep.2015.10.008

[21]Zaki, R. M., El-Dean, A. M. K., Abdulrazzaq, A. Y., *J. Chin. Chem. Soc*., **2015,** *62*, 112. https://doi.org/10.1002/jccs.201500292

[22]Wang, Z., Li, Z., Ren, J., Chen, H., *Heteroatom Chem.*, **1999,** *10*, 303. https://doi.org/10.1002/(sici)1098-1071(1999)10:4%3C303::aid-hc7%3E3.0.co;2-h

[13]Pawar, R. A., Patil, A. A., *Ind. J. Chem.*, **1994,** *33B*, 156.

[24]Rojahn, C. A., Fahr, K., *Ann. Chem.*, **1923,** *434*, 252. https://doi.org/10.1002/jlac.19234340114

[25]Kvitko, I. Y., Porai-Koshits, B. A., *Zh. Org. Khim.*, **1966,** *2*, 169. *Chem. Abstr.*,**1966,** *64(15)*, 867.

[26]Kishida, M., Hamaguchi, H., Akita, T., JP 63-267762, **1988**; *Chem. Abstr.*, **1989,** *111(57)*, 728. https://doi.org/10.1007/978-3-642-74784-7_379

[27]Imi, K., Masumoto, K., Murata, T., JP 63 05 01 038 [93 01, 038], **1993**; *Chem. Abstr*., **1993**, *118(284)*, 54.

Received: 05.12.2017.
Accepted: 20.01.2018.

EFFECT OF HYDROALCOHOLIC EXTRACT OF *CAPPARIS DECIDUA* (FORSSK.) EDGEW ON SERUM TESTOSTERONE AND SPERMATOGENESIS IN RATS

Prashant Kumar Dhakad,[a]* Pramod Kumar Sharma[a] and Sokindra Kumar[b]

Keywords: *Capparis decidua,* aphrodisiac, serum testosterone level, body weight, secondary sexual organ weight.

The effect of *Capparis decidua(Forssk.)Edgew* aqueous extract on the Wistar rat testes was investigated with a view to evaluating the pharmacological basis for the use of *Capparis decidua* hydroalcoholic extract as an aphrodisiac. Wistar rats were divided in the following experimental groups- control group (1 mL kg^{-1}), sildenafil citrate treated (5 mg kg^{-1}), *C. decidua* (100 mg kg^{-1}), *C. decidua* (200 mg kg^{-1}), per se group (only *C. decidua* 200 mg kg^{-1}). The hydroalcoholic extract of root, stem & leaves of *C. decidua* was studied for their effect on the body and secondary sexual organ weight, spermatogenesis, and serum testosterone level male rats. The animals were allowed free access to drinking solution during the 28 days period of exposure. At the end of the experimental period, rats were sacrificed, testis, epididymis, seminal vesicles and prostate glands were excised and weighed, and serum testosterone level was recorded. The testes underwent histological examination. Oral administration of the extract in Wistar rats showed significant dose-dependent influence on serum testosterone level (P<0.001) and spermatogenic effects in extract treated rats groups by increasing the weights of secondary sexual organs(P<0.001).

* Corresponding Author
Tel. No.: +91 8510860363
E-Mail: prashant.dhakad@galgotiasuniversity.edu.in
[a] Department of Pharmacy, Galgotias University, Greater Noida, India

INTRODUCTION

Propagation of one's race is the doctrine of every single living life form. Every living creature endeavour to accomplish this through the procedure of multiplication, which is the essential procedure that empowers animal groups to speak to itself in the accompanying age as its posterity.[1]

Variations from the norm in male regenerative frameworks like impotency, erectile dysfunction and the other way around are one of the principle issues that prompt sterility. An aphrodisiac is a substance that increments sexual intimacy.[2] It has been perceived for quite some time that specific antihypertensive drugs, centrally acting sympatholytic drugs, β-antagonists, antidepressants, antipsychotics, anticonvulsants, drugs with antimuscarinic effects and diuretics, adversely affect sexual working.[3] *Capparis decidua* (Forssk.)Edgew. (Kair) is a multipurpose perennial woody plant, belonging to caper family (Capparaceae), found largely in the hot dry region of different parts of India.[4]

Capparis decidua (Forssk.) Edgew is salt-tolerant and grows along saline hard planes in the Thar Desert of India. Mature plants form extensive root systems that penetrate deeply into the soil. Leaf stipules frame into spines to decrease transpiration. The stem bark is smooth, green when youthful and turns yellow or whitish dark as it develops. The roots, fruits, and various parts of these plants with potential therapeutic advantages have been used since long time. *C. decidua* contains constituents like phenolic compounds, alkaloids, flavonoids, terpenoids, steroids, vitamins, quarternary ammonium compounds and many more phytoconstituents that are responsible for its medicinal value.[5]

Previous studies suggested that the antimicrobial effects of *Capparis decidua* (Forssk.) Edgew may be due to presence of bioactive compounds, like flavonoids, phenolics, polyamine alkaloids, glucosinolates, and vitamins that decrease the growth of microbes.[6] Roots of this plant have been used as expectorant, carminative, sudorific, thermogenic, digestive, aphrodisiac, stimulant, antibacterial, anodyne, anthelmintic and in treating constipation, lumbago, odontalgia, amenorrhoea, arthritis, dyspepsia, and dysmenorrhoea. The root bark is known to be astringent, diaphoretic, alexeteric etc. Powder or infusion of root bark is used in a cough, dropsy, palsy, gout, rheumatism, asthma, intestinal worms and intermittent fever.

Nowadays people are swinging to herbal remedies to improve this infertility issue they are effectively agreeable to normal man. Research is done to discover the plant items that can be utilized to treat this sort of infertility problems.[7]

EXPERIMENTAL

Plant Materials

The complete plant of *Capparis decidua* was collected near fresh from Jaipur, Rajasthan, India. The plant was taxonomically identified and authenticated by Prof. Kailash Agrawal, Convener Herbarium committee, Department of Botany, University of Rajasthan, Jaipur. A voucher specimen was deposited at the herbarium of the Department of Botany, University of Rajasthan, Jaipur, Rajasthan, India. (R.No. RUBL 211645).

Experimental animals

Healthy Albino Wistar rats of both sexes weighing 150-250 g were obtained from Central Animal Facility AIIMS New Delhi. The experimental protocol was approved by Institutional Animal Ethics Committee CPCSEA No. -1149/PO/ERe/07/CPCSEA. Animals were housed under standard conditions of temperature (24±2 ˚C) and relative humidity (30-70 %) with 12:12 light: dark cycle. The animals were given standard pellet diet and water ad libitum.

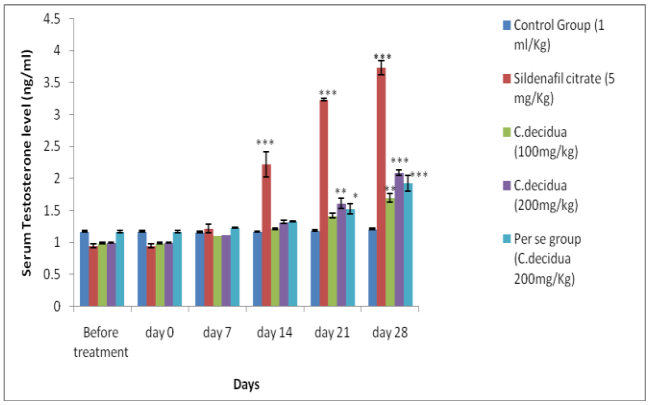

Figure 1. Effect of hydroalcoholic extract of *C. decidua* on serum testosterone level on male Wistar rats.

Preparation of test samples

The hydroalcoholic extract was dissolved in the distilled water and orally administered to the test groups. Sildenafil citrate was procured from the Cadila Pharmaceuticals Limited, Ahmadabad, Gujarat, India as a generous gift.

Experimental design

Adult male albino rats of Wistar strain were used for the experimentation. The animals were divided into 5 groups of 6 animals each and treated as follows. Group I: Control group (1 mL kg^{-1} distilled water p.o), Group 2: Sildenafil citrate treated (5 mg kg^{-1} p.o), Group 3: *C. decidua* (100 mg kg^{-1} p.o), Group 4: *C. decidua* (200 mg kg^{-1} p.o), Group 5: per se group (only *C. decidua* 200 mg kg^{-1} p.o). All the above treatments were given orally for 28 days. The serum testosterone level was determined before treatment, day 0, day 7, day 14, day 21 and 28th day. On the 29th day all the rats were sacrificed and the testis, epididymis, seminal vesicle, prostate were dissected out, surrounding blood vessels and tissues were removed and blotted free of blood and mucous. The tissues were weighed using electronic balance.

Histological studies

The testis and cauda epididymis from the opposite side was settled in Bouine's liquid, inserted in paraffin, sectioned at 5 µm thickness and stained in haematoxylin and eosin and prepared for histological investigations.[8]

Statistical analysis

All the values were reported as mean±S.E.M. Analysis of variance (ANOVA) was employed to analyze the data, while Tukey's multiple comparison tests were used to test for differences between individual treatments groups using Graph pad prism software version 5.0. $P<0.05$ was considered statistically significant.

RESULTS

A dose-dependent increase in serum testosterone concentration were observed on the 21st and 28th day of the study in *C. decidua* extract (100 mg kg^{-1}) ($P<0.01$), *C. decidua* extract (200 mg kg^{-1}) ($P<0.001$), per se group (only *C. decidua* extract 200 mg kg^{-1}) ($P<0.001$). While sildenafil citrate group showed an increase in serum testosterone level on 14th, 21st and 28th day of the study as compared to control group ($P<0.001$) (Figure 1).

The body weight has increased in all the experimental animal groups. This increase is 6.5 % in control rats whereas it is 32.3, 21.61, 25.20 and 14.54 %, respectively in the rats treated with Sildenafil citrate, *C. decidua* extract (100 mg kg^{-1}), *C. decidua* extract (200 mg kg^{-1}), per se group (only *C. decidua* extract 200 mg kg^{-1}). Sildenafil citrate group showed a 7.6 % increase in testis weight, a 6.94 % increase in seminal vesicle weight, an 8.91 % increase in weight of epididymides and a 9 % in prostate gland weight.

Table 1. Effect of hydroalcoholic extract of *C. decidua* on body weight and secondary sexual organ weight on male wistar rats.

Treatment groups	Body weight (g)		Weight of organs on 28th day (mg 100 g^{-1} of body weight)			
	Day 0	Day 28	Testes	Seminal vesicle	Epididymides	Prostate
Control Group (1 mL kg^{-1})	107.5	114.5±0.76	950.83±0.6	415±1.42	746.16±0.47	281.33±0.8
Sildenafil citrate (5 mg kg^{-1})	103.16	136.5±0.67***	1023.66±0.71***	443.83±1.08***	812.66±0.88***	306.66±0.49***
C. decidua (100 mg kg^{-1})	101	122.83±0.6***	1014.5±0.76***	434.33±1.28***	797.16±0.6***	296.83±0.6***
C. decidua (200 mg kg^{-1})	103.83	130±0.57***	1024.83±0.6***	449±1.53***	814.5±0.76***	316.5±0.76***
Per se group (*C. decidua* 200 mg kg^{-1})	103.16	118.16±0.94*	970.16±0.87***	419.83±0.94	762±0.96***	289±0.96***

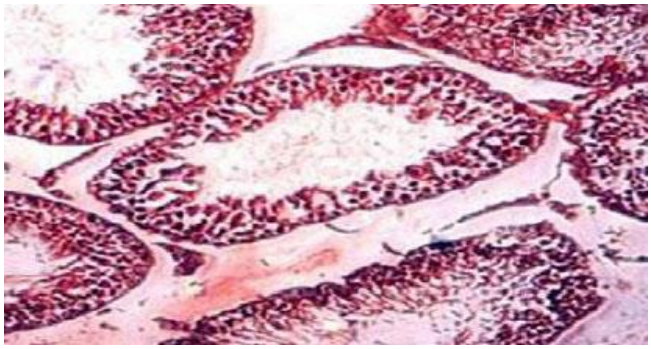

Figure 2. Control rat showing normal seminiferous tubules with normal spermatogenesis.

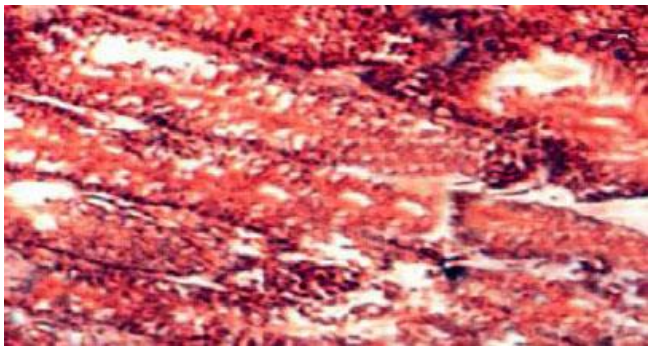

Figure 3. Sildenafil citrate treated rats showing increase in the size of seminiferous tubules, increase in the spermatogonia, spermatocytes and spermatids and spermatozoa.

The *C. decidua* extract (100 $mgkg^{-1}$) group showed an increment of 6.69 % in testis weight, a 4.65 % increase in seminal vesicle weight, a 6.83% increase in the weight of epididymides and a 5.50 % increase in prostate gland weight. Likewise, the *C. decidua* extract (200 $mgkg^{-1}$) group showed an elevation of 7.78 % in testis weight, an 8.19% increase in the weight of the seminal vesicle, a 9.15 % increase in the weight of the epididymides and a 12.50 % increase in prostate gland weight. Per se group (only *C. decidua* extract 200 $mgkg^{-1}$) showed an increment of 2.03 % in testis weight, a 1.16 % increase in seminal vesicle weight, a 2.12 % increase in the weight of epididymides and a 2.72 % increase in prostate gland weight after 28 days of treatment compared to the control group (Table 1).

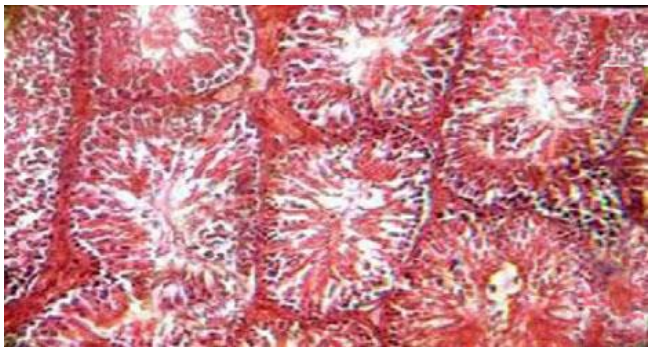

Figure 4. *C. decidua* (100 $mgkg^{-1}$) hydroalcoholic extract treated rat showing all types of spermatogenic elements and spermatozoa in the lumen.

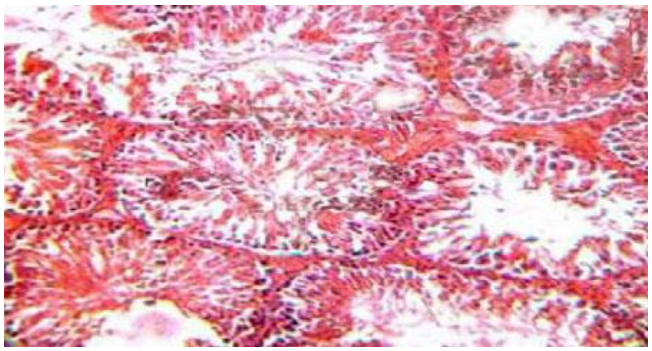

Figure 5. *C. decidua* (200 $mgkg^{-1}$) hydroalcoholic extract treated rat showing increased number of spermatogonia, spermatocytes and spermatids and more number of spermatozoa in lumen.

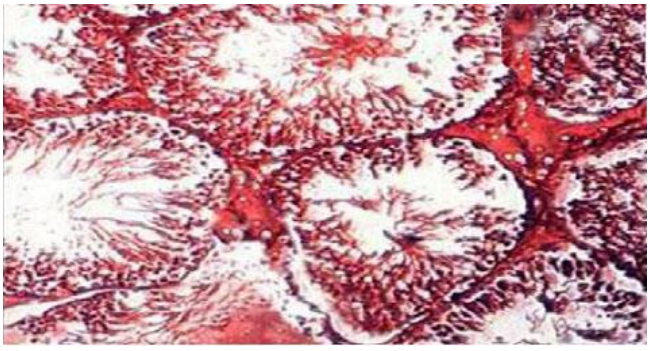

Figure 6. Per se group (200 $mgkg^{-1}$ of hydroalcoholic extract of *C. decidua*) showing moderate number of spermatogenic elements.

Histological examination demonstrated the control group with typical testicular structures, in confirmation with spermatogenesis. A noteworthy impact on spermatogenesis was noted following 28 days of treatment with the extract. The weight and size of the testis were found more in the plant extract treated groups. The germinal epithelium cells seemed, by all accounts, to be hyperactive. Substantial quantities of various cells at various phases of spermatogenesis were apparent. Sertoli cells were enlarged, highly processed, and rich in nutrients as appeared by very granulated cytoplasm. The expanding in the volume of the two cells and nuclei was strongly suggestive of steroid synthesis under the direct or indirect impact of the extract. The blood vessels of testis were slightly enlarged. Expanded spermatogenesis was obvious from the vast number of spermatozoa in the seminiferous tubules and was additionally appeared by the expansion in spermatogenic components compared with control group. (Figure 2-6).

DISCUSSIONS

In the present study administration of *C. decidua* extracts have stimulated the activity of testis and accessory organs. A significant ($P<0.001$) increase in testosterone level was found in the extract treated animals compared with control. It demonstrates that the extract has an impact at the endocrine level. Testosterone is the significant male gonadal hormone, and it is created by the interstitial Leydig cells in the testis. It is additionally the real factor for androgenicity.

A specific concentration of androgens is required for the initiation and maintenance of spermatogenesis and for the start and support of spermatogenesis and for the incitement of development and the working of the prostate and original vesicles. The expansion in testosterone level may improve androgen-dependent parameters such as mating behavior and the maintenance of spermatogenesis.[9-12]

Out of three extracts administered *C. decidua* (200 $mgkg^{-1}$) extract proved to be profoundly stimulant, *C. decidua* (100 $mgkg^{-1}$) extract is a medium stimulant and Per se group (*C. decidua* extract 200 $mgkg^{-1}$) is less stimulant in increasing the weight of testis and male reproductive accessory organs. There is likewise an advance in spermatogenesis as found in the expansion of spermatogenic components in the testis which might be because of the higher accessibility of pituitary follicle stimulating hormone (FSH), as FSH is known to invigorate the spermatogenesis. Both FSH and LH are important for meiosis and generation of spermatids. The possible increment in the number of spermatogonia, spermatocytes, and spermatids might be credited because of the expanded accessibility of FSH and LH in *C. decidua* extracts treated rats. The androgen synthesis in the testis is dependent on pituitary LH and FSH. The expanded weight in the accessory organ in treated rats demonstrates the extract may stimulate the FSH and LH release and testosterone production.[13,14]

Past phytochemical examines have demonstrated the *C. decidua*plant extract contains alkaloids, steroids, phenolic compounds, terpenoids, tannins, glycosides, flavonoids, and saponins. Saponins have been appeared to be responsible for endothelium-dependent nitric oxide release causing relaxation of the rat aorta. Nitric oxide is a noteworthy physiological boost for penile vasculature and trabecular smooth muscles, all necessary for penile erection.[15]

In this study, the investigation of different sexual parameters has approved the customary faith in the viability of the root, stem, and leaves of *C. decidua* for treating sexual dysfunctions. The outcomes additionally show the conceivable utilization of extract of *C. decidua* as an herbal alternative to the allopathic medicines that are gaining popularity for the treatment of sexual dysfunction.

Acknowledgements

We are very grateful to Prof. Kailash Agrawal & Dr. R. D Agarwal of Department of Botany, the University of Rajasthan for their appropriate and constructive suggestions. Authors are grateful to Dr. Amrish Kumar, Department of Pharmacy, School of Medical & Allied Sciences, for his unduly support.

References

[1]Patil, S. A., Sujaya, M., Patil, S. B., *Asian Pacific J. Reprod*., **2014**, *3(1)*, 23–29. https://doi.org/10.1155/2017/8204816

[2]Patel, D. K., Kumar, R., Laloo, D., Sairam, K., Hemalatha, S., *Asian Pac. J. Trop. Biomed*., **2012**, *2(3)*, S15681571. http://dx.doi.org/10.1016/S2221691(12)60454-7

[3]Ajiboye, T. O., Nurudeen, Q. O., Yakubu, M. T., *J. Basic Clin. Physiol. Pharmacol*., **2014**, *25(2)*, 241-248. DOI: 10.1515/jbcpp-2013-0061.

[4]Heywood, V. H., *Flowering Plants of the World*, Oxford University Press, Oxford, **1978**, 119.

[5]Ahmad, V. U., Ismail, N., Amber, A. U. R., *Phytochemistry*, **1989**, *28*, 2493–2495. https://doi.org/10.1016/S0031-9422(00)98012-9

[6]Kirtikar, K. R., Basu, B. D., *Indian Medicinal Plants*, Periodical Experts Book Agency, Delhi, India, **1933**, 2. ISBN 10: 817136053X.

[7]Dhakad, P. K., Sharma, P. K., Kumar, S., *Adv. Pharmacol. Pharm*., **2016**, *4(3)*, 27–39. DOI: 10.13189/app.2016.040302

[8]Gurr, E., *Staining animal tissues. In: Practical and theoretical*., Leonard Hill Limited, London, **1962**, 233. https://doi.org/10.5962/bhl.title.4476.

[9]Connel, G. M., Eik-Nes, K. B., *Steroids*, **1968**, *2*, 507-512. https://doi.org/10.1016/s0039-128x(68)80114-x

[10]Johnson, B.J., Ewing., *Science*, **1971**, *173*, 635-642. https://doi.org/10.1126/science.173.3997.635

[11]Holt, J. A., Kelch, R. P., Payne, A. H., *In vitro effect of rat LH and FSH and HCG on androgen (A) and estrogen (E) release from decapsulating rat testes.*, Proc. Annu. Meet Soc. Study Report, **1973**, *6*, 58-64.

[12]Dorrington, J. H., Armstrong, D. T., *Follicle stimulating hormone stimulates estradiol-17β synthesis in cultured sertoli cells.* Proc. Nat. Acad. Sci. USA, **1975**, *72*, 2677-2681.

[13]Hanyu, S., *Urol. Int*., **1988**, *43*, 219–224. DOI:10.1159/000281341.

[14]El-Sakka, A. I., Lue, T. F., *Sci. World J*., **2004**, *4*, 128–134. DOI 10.1100/tsw.2004.58.

[15]Thakur, M., Thompson, D., Connellan, P., Deseo, M., Morris, C., Dixit, V. K., *Andrologia*, **2011**, *43(4)*, 273–277. doi: 10.1111/j.1439-0272.2010.01068.

Received: 09.12.2017.
Accepted: 20.01.2018.

ADSORBENT FOR EFFICIENT REMOVAL OF MERCURY(II) FROM AQUEOUS SOLUTION

Saad S.M. Hassan,[a]* Ayman K. Kamel,[a] Nassar S. Awwad,[b,c] Awaad H. A. Aboterika[d] and Ibrahim S. Yahia[e,f]

Keywords: Removal, mercury, zinc oxide, sulfur, wastewater.

Decontamination of mercury from aqueous media remains a serious task for health and ecosystem protection. Removal of Hg(II) from the aqueous solution by ZnO:S has been investigated and elucidated. The effect of various parameters such as solution pH, adsorbent dose, contact time, initial adsorbate concentration has been studied and optimized. The optimized parameters for metal ion are pH value of 2.4, the equilibrium time was attained after 30 min, and the maximum removal percentage was achieved at an adsorbent loading weight of 0.08 g. It was found that the adsorption capacity of ZnO:S increased with increase in the initial mercury concentration. The equilibrium and kinetic data were found to be in good agreement with Freundlich isotherm model.

* Corresponding Authors
Fax: +20 2 26822991
E-Mail: saadsmhassan@yahoo.com (S.S.M. Hassan)
[a] Department of Chemistry, Faculty of Science, Ain Shams University, Cairo, Egypt
[b] Analytical Chemistry Department, Hot Labs Center, Atomic Energy Authority, Egypt
[c] Department of Chemistry, Faculty of Science, King Khalid University, P.O. Box 9004, Abha, Saudi Arabia
[d] Central laboratory, Faculty of Science, Ain Shams University, Cairo, Egypt
[e] Nano-Science & Semiconductors Labs, Department of Physics, Faculty of Education, Ain Shams University, Roxy, Cairo, Egypt
[f] Department of Physics, Faculty of Science, King Khalid University, P.O. Box 9004, Abha, Saudi Arabia.

INTRODUCTION

Mercury with unusual chemical and physical properties is universal pollutant. Even at very low concentration, mercury causes potential hazards due to its accumulation in food chain. A special characteristic of mercury is its strong absorption into biological tissues and slow elimination from them.[1] The major effects of mercury poisoning manifest as neurological and renal disturbances as it can easily pass the blood-brain barrier and affect the fetal brain. High concentrations of Hg(II) cause impairment of pulmonary function and kidney, chest pain and dyspnousea.[2,3] Numerous cases of mercury poisoning, or Minamata disease are reported in different countries around the world which resulted due to the consumption of fish and shellfish by human.[4]

Because of the above reasons, mercury must be removed to very low levels from wastewater generated in industries such as metal smelting and caustic-chlorine production in mercury cells, metal processing, plating and metal finishing.[5] Numerous physical and chemical separation processes, such as solvent extraction, ion-exchange, precipitation, membrane separation, reverse osmosis, coagulation and photoreduction,[6-9] have been applied for effective reduction of mercury concentrations from various aqueous solutions.

Among various technologies developed over the years for mercury removal, adsorption holds great promise due to the simplicity and relatively low-cost of adsorption technology as well as the effectiveness of adsorption method to purify water.[10]

Low-cost adsorbents already reported for the removal of Hg(II) include fly ash,[11] coal,[12-13-14] tree bark,[15] human hair,[16] fertilizer waste,[17] used tea leaves,[18] waste rubber,[19] rice-husk ash,[20] flax shive,[21] oil shale,[22] camel bone charcoal[23] and iron ore slime.[24]

The aim of this work is to assess the ability of ZnO:S to adsorb Hg(II) from aqueous solution. Effect of various parameters e.g. solution pH, contact time, initial Hg(II) concentration and solid/liquid ratio was studied for the optimization of removal process. Furthermore, Hg(II) adsorption isotherm and mechanism were measured and discussed.

EXPERIMENTAL

Materials

A stock Hg(II) nitrate (1000 mg L^{-1}) standard solution was supplied by Merck. A solution (10 mg L^{-1}) was prepared by dilution with deionized distilled water and used as adsorbate.

Adsorbent, i.e. ZnO nanoparticles was prepared by co-precipitation method. The starting materials were zinc acetate ($Zn(OAc)_2 \cdot 2H_2O$), thiourea and sodium hydroxide. To prepare sulphur doped zinc oxide (S:ZnO) with small percentage of sulphur, a 1 molar solution of zinc acetate was prepared in deionized water (Solution A). Similarly, 1 molar solution of thiourea was prepared in deionized water (Solution of B).

Then 50 mL of solution A and B are left on the magnetic stirrer/hotplate for 1 h at 60 °C and stirred at 800 rpm and then these solutions were mixed. Sodium hydroxide solution (4 mol) was added gradually to this mixture to increase the pH up to 10, this resulted in the formation of white-yellow precipitate. The precipitate was left on the magnetic stirrer/hotplate on the same condition for another 1 h, filtered and washed several times to remove any unwanted elements such as sodium and further organic materials by

deionized water/ethanol. The dry precipitate was left in a muffle furnace at 550 ºC for 2 h. After that, the furnace was slowly naturally cooled to the room temperature. A yellowish white precipitate was obtained.

Equipment

FTIR spectrometry was carried out with a Thermo-Nicolet model iS10. The surface micromorphology of materials was investigated using a scanning electron microscope (SEM) and element composition was analyzed using energy dispersive X-ray (EDX) by Joel Model LVSEM 6360 (Japan). An Orion digital pH/mV meter (Model SA 720) with a combination glass electrode (Orion 81-02) was used for all pH measurements. A Perkin-Elmer Flow Injection Mercury System (Model FIMS-100) was used for determination of mercury.

Sorption experiments

Batch sorption experiments were conducted by using 25 mL aliquots of a test solution containing 1.0 mg Hg(II). The solutions were adjusted to pH 1–7 and placed in 250 mL reagent bottles. A known quantity (0.01–0.10 g) of ZnO:S was added to each bottle and the pH was adjusted to 2.4 using 0.1 N of either nitric acid or sodium hydroxide solution. The solutions were agitated at a speed of 150 rpm for 5–60 min at 25 ± 1 °C in a shaking incubator. The zinc oxide:S was separated by filtration and mercury(II) content of the filtrate was determined using Flow Injection Mercury System (FIMS). The percentage removal (R, %) was calculated according to the following equation:

$$R = \frac{C_0 - C_e}{C_0} \times 100 \qquad (1)$$

where

R is the percent removal of mercury,

C_0 and C_e are the initial and final equilibrium mercury concentration respectively (mg L^{-1}).

Adsorption isotherms were obtained with different initial concentrations of Hg(II) while maintaining ZnO:S dosage at a constant level. In order to correct for any adsorption of mercury(II) on the container surface, control experiments were carried out in the absence of zinc oxide:S. These experiments indicated that no adsorption by the container walls was detected. In all experiments, the difference between the initial Hg(II) concentration (C_0) and the equilibrium concentration (C_e) was calculated and used to determine the adsorptive capacity (q_e) (mg g^{-1}) as follows:

$$q_e = \frac{V}{m}(C_0 - C_e) \qquad (2)$$

where

V is the total volume of mercury(II) solution (mL),

m is the mass of adsorbent used (g),

C_0, is the initial concentration of the mercury(II) solution (mg L^{-1}) and

C_e, is the residual mercury(II)concentration (mg L^{-1}).

The linear model, which describes the accumulation of solute by sorbent as directly proportional to the solution concentration is presented by the relation:

$$q_e = K_D C_e \qquad (3)$$

The constant of proportionality or distribution coefficient K_D is often referred to as the partition coefficient.

The Langmuir model represents one of the first theoretical treatments of non-linear sorption, and has been successfully applied to a wide range of systems that exhibit limiting or maximum sorption capacities. The model assumes uniform energies of adsorption onto the surface and no transmigration of the adsorbate in the plane of the surface.

The Langmuir isotherm is given by:

$$q_e = \frac{Q^0 b C_e}{1 + b C_e} \qquad (4)$$

where Q^0 and b are Langmuir constants related to adsorption capacity and energy of adsorption, respectively.[25]

Eqn. (4) is usually linearized by inversion to obtain the following form:

$$\frac{1}{q_e} = \frac{1}{Q^0} + \frac{1}{bQ^0}\frac{1}{C_e} \qquad (5)$$

Eqn. (5) is equally used to analyze batch equilibrium data by plotting $1/q_e$ versus $1/C_e$, which yields a linear plot if the data conform to the Langmuir isotherm. The essential characteristics of the Langmuir isotherm can also be expressed in terms of a dimensionless constant separation factor or equilibrium parameter (R_L), which is defined by Eqn. (6).[26]

$$R_L = \frac{1}{1 + b C_o} \qquad (6)$$

where C_0 is the initial solute concentration and b is the Langmuir's adsorption constant (L mg^{-1}).

The R_L value confirms the adsorption to be unfavourable ($R_L > 1$), linear ($R_L = 1$), favorable ($0 < R_L < 1$) or irreversible ($R_L = 0$).[27]

The Freundlich isotherm is the most widely used non-linear sorption model and is given by Eqn. (7).

$$q_e = K_F C_e^n \quad (7)$$

where K_F relates to sorption capacity and n to sorption intensity.

The logarithmic form of Eqn. (7) given below is usually used to fit data from batch equilibrium studies.

$$\log q_e = \log K_F + \frac{1}{n}\log C_e \quad (8)$$

RESULTS AND DISCUSSION

Effect of solid/liquid ratio

The experimental data presented in figure 1clearly show that under the present experimental conditions, the removal of mercury increases with increasing adsorbent dose. The removal of mercury increased from 80 % at 0.016 g L^{-1} adsorbent dose to more than 94.7 % at 0.08 g L^{-1} adsorbent dose. The observed mercury uptake increase is attributed to the increased adsorbent surface area available for contact with the Hg(II), which leads to increased number of surface-active groups. [28,29] The mercury uptake remains practically the same, ~95 %, at adsorbent dose > 0.08 g L.

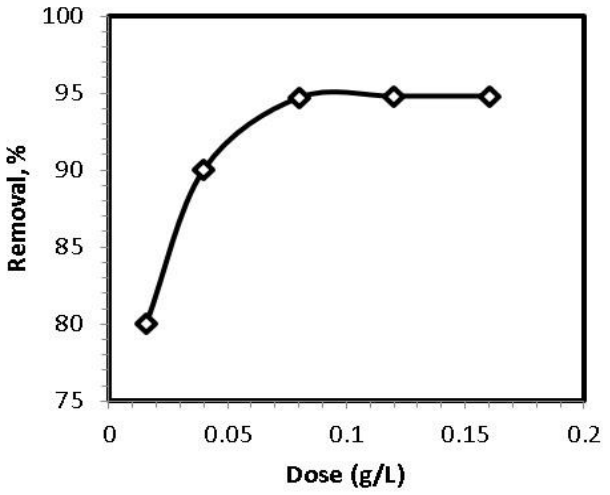

Figure 1. Effect of adsorbent dosage on the removal of Hg(II) by ZnO : S. Conditions: C_0 10 mg L^{-1}, time of contact, 30 min, pH 2.4 and temperature 25 °C.

Effect of contact time

Figure 2 shows that the uptake of Hg(II) increases with increasing contact time and that the adsorption process is saturated after approximately 30 min of contact time. The contact times at which the adsorption reaches equilibrium differs as revealed by saturation studies reported by other workers for the uptake of Hg(II)[30,31] and is related to the accessibility and the binding capacity of the sulphur.

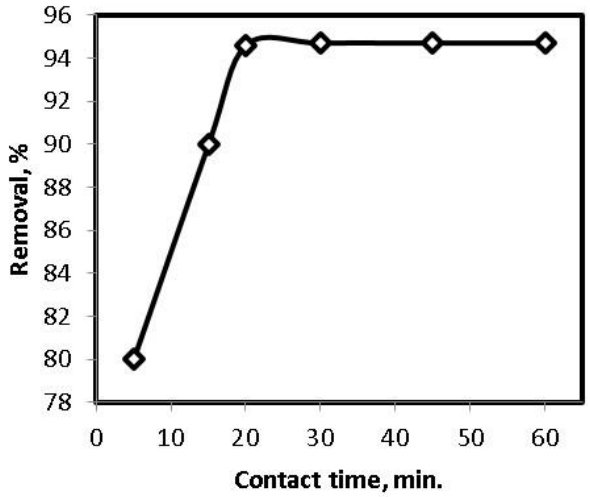

Figure 2. Effect of contact time on the removal of Hg(II) by ZnO:S. Conditions: C_0 10 mg L^{-1}, dose of ZnO:S 0.05 g, pH 2.4 and temperature 25 °C.

Effect of pH

To confirm the effect of pH on the adsorption of Hg to ZnO:S, a Hg adsorption experiment was performed while adjusting the initial pH of the Hg solution from pH 2 to 6 and maintaining this value for 30 min. A graph of the pH effect is shown in Fig. 3.

The uptake of Hg(II) as a function of hydrogen ion concentration was determined in the pH range of 2-6. At pH values below 2.4, hydrogen ions are likely to compete with mercuric ions and to note that at pH > 6, mercury precipitates.[32] The maximum adsorption was observed at pH 2.4, in general the results indicated that the adsorption is highly pH dependent. Similar results have been reported in previous studies.[23,33,34]

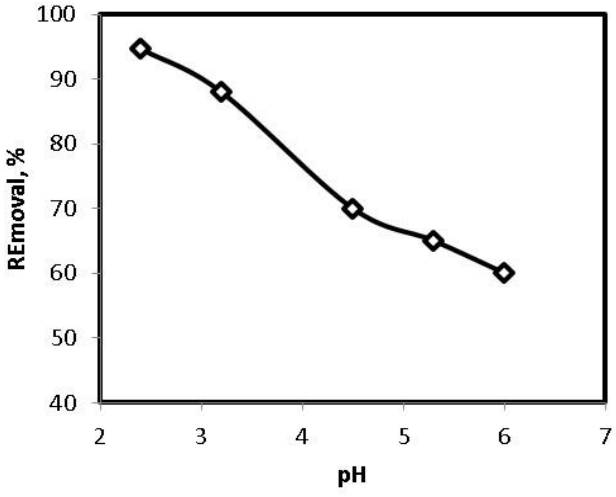

Figure 3. Effect of pH on the removal of Hg(II) by ZnO:S. Conditions: C_0 10 mg L^{-1}, dose of ZnO:S 0.05 g, contact time 30 min. and temperature 25°C.

Adsorption isotherms

Adsorption data usually discussed and explained by adsorption isotherms, such as the linear, Langmuir and Freundlich isotherms. These isotherms relate metal uptake per unit weight of the adsorbent q_e to the equilibrium adsorbate concentration in the bulk fluid phase C_e.

Eqns. (3), (5) and (7) are usually used for the analysis of equilibrium batch experiment data assuming linear, Langmuir and Freundlich isotherms, respectively.

Figures 4, 5 and 6 present the linear, Langmuir and Freundlich isotherm plots of mercury adsorption on the ZnO:S. The equilibrium data were fitted very well to all three sorption isotherms. These plots were used to calculate the isotherm parameters given in Table 1 for mercury. The data obtained represent a favorable adsorption in the case of adsorption of Hg(II) ions (R_L = 0.999). The shape of isotherm is given by the value of R_L as given in Table 1. The ongoing adsorption process is favourable.

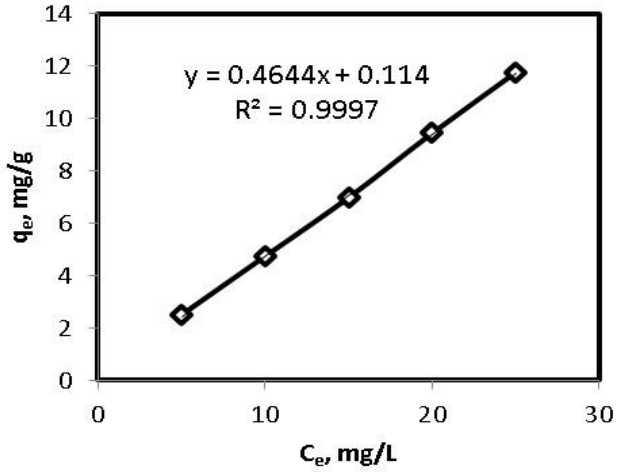

Figure 4. Linear isotherm plot for the adsorption of mercury on ZnO:S.

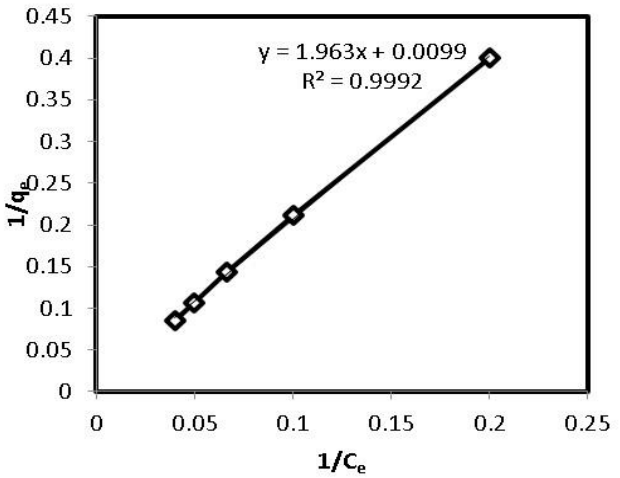

Figure 5. Langmuir isotherm plot for the adsorption of mercury on ZnO:S.

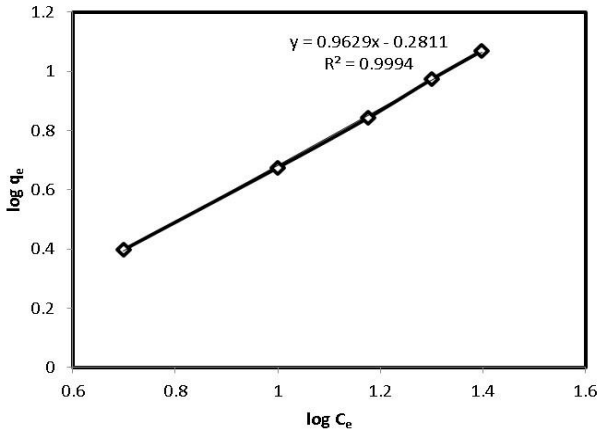

Figure 6. Freundlich isotherm plot for the adsorption of mercury on ZnO:S.

Table 1. Summary of isotherm parameters for the adsorption of mercury on ZnO:S.

Linear	Frendlich's			Langmuir		
K_D, L g^{-1}	K_F	n	R^2	Q^0, ,mg g^{-1}	b, L g^{-1}	R^2
0.470	0.535	1.045	0.9994	101.01	5.043	0.9992

Removal of Hg(II) from wastewater

In order to survey the capability of the prepared adsorbents for removal of Hg(II) from actual wastewater, some batch experiments were conducted on chloralkali wastewater. Mercury concentration in the chloralkali wastewater is in the range of 2-30 mg L^{-1}. The ZnO:S is a good adsorbent with high capability for adsorption of mercury ions (94%) from wastewater.

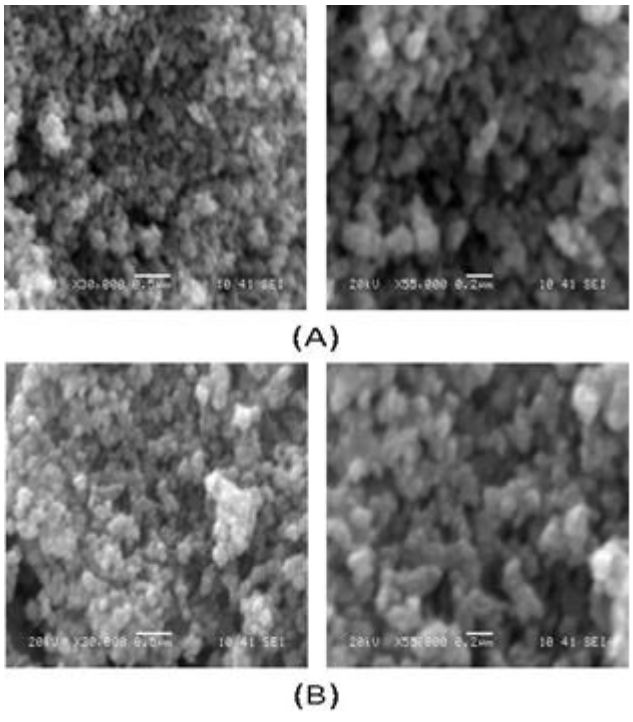

Figure 7. Electron microscopy scanning of the ZnO:S. (A) before (X = 10,000 and Bar = 1 μm) and (B) after contact with mercury solution. (X = 2500 and Bar = 10 μm).

Verification of adsorption

A scanning electron microscopic (SEM) investigation expose changes in the morphology of ZnO:S before and after impregnation in Hg(II) solutions (Fig.7a,b). The uptake of Hg(II) is demonstrated by the change of the morphology of adsorbent's surface.

Energy dispersive X-ray analysis (EDX analysis) was carried out for ZnO:S before and after impregnation in Hg(II) solutions and results obtained are depicted in Figure 8. Figure 8b shows an EDX analysis which confirms the presence of mercury in the ZnO:S adsorbent.

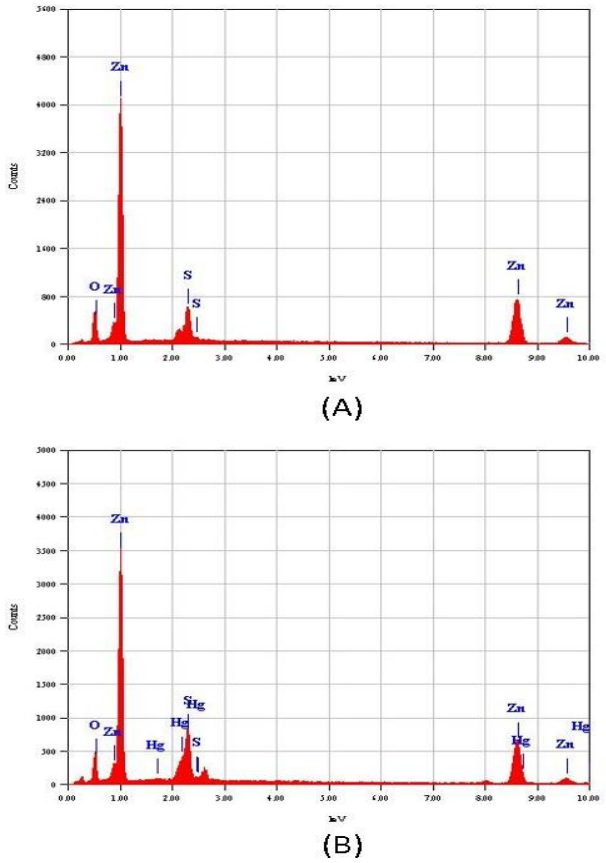

Figure 8. EDX analysis of ZnO:S (A) before, and (B) after contact with mercury.

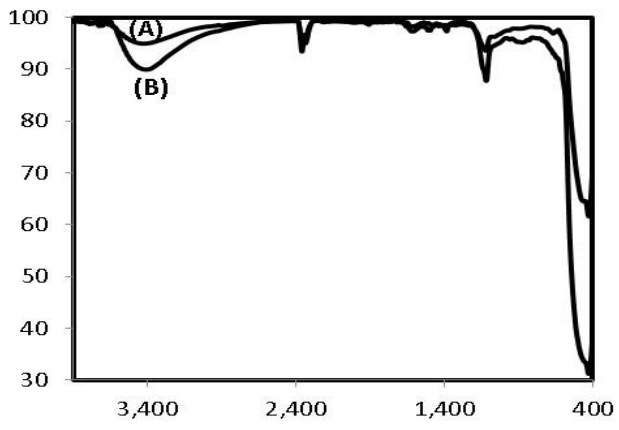

Figure 9. IR spectra of ZnO:S (A) before and (B) after contact with mercury.

The FTIR spectrum of ZnO:S after exposure to Hg(II) nitrate shows a new characteristic band at 1380 cm^{-1} due to nitrate group beside peaks at 1630 cm^{-1} is due to the bending of water molecule. The peak in the range of 400-500 cm^{-1} is due to the presence of ZnO bond. The FTIR spectrum of ZnO:S indicates significant changes after exposure to Hg(II) which indicate that binding processes have taken place on the surface of adsorbent (Figure 9).

A comparison of the adsorption capacity (Q_0) of ZnO:S with different adsorbents previously used for Hg(II) removal from wastewater effluents indicates remarkable capacity of the proposed sorbent (Table 2).

Table 2. Adsorption capacities for different adsorbents used for Hg removal from wastewater.

Adsorbent	Adsorption capacity, Q^0 (mg g^{-1})	Ref.
Bone charcoal	28.33	23
Activated carbon derived from waste coconut buttons	78.89	35
Sago waste carbon	55.60	36
Dates nut carbon	1.16	37
Chemically modified banana stem	132.25	38
Palm shell	83.33	39
Bamboo leaf powder	27.11	40
Peel biomass of *Pachiraaquatica Aubl.*	0.71	41
exfoliated graphene oxide-L-cystine	79.36	42
Graphene Oxide-Carbon Composite	68.80	43
Carbon Aerogel	45.62	44
Graphene oxide foam	35.00	45
Thiol-functionalized graphene oxide	107.52	46
Poly(glycidyl methacrylate)	56.18	47
ZnO:S	101.01	This work

CONCLUSIONS

Zinc oxide doped with sulphur has been used for removal of Hg(II) from wastewater effluents. The present work showed that ZnO:S follows the adsorption isotherm models tested, Freundlich and Langmuir. However, the Freundlich isotherm is the best-fit isotherm. The Langmuir adsorption capacity is 101.01 mg of Hg(II) per gram of the adsorbent. Removal of 10 mg L^{-1} of Hg(II) was achieved by 0.08 g of ZnO:S at pH 2.4.

REFERENCES

[1]MadhavaRao, M., Kumar R., PadalaVenkateswarlu, D. H. K., Seshaiah, K., *J. Environ. Manage*, **2009**, *90*, 634. DOI: 10.1016/j.jenvman.2007.12.019.

[2]Berglund, F., Bertin, M., *Chemical Fallout*, Thomas Publishers, Springfield, **1969**.

[3]Krishnamoorthi, C. R., Vishwanthan, P., *Toxic metal in the Indian Environment*, Tata McGraw-Hill Publishing Co. Ltd, New Delhi **1991**.

[4]Hodgson, E., *A Textbook of Modern Toxicology*, Wiley & Sons, **2004**, 41.

[5]Peters, R. W., Ku, Y., *AIChE Symp.*, **1985**, *81*, 9.

[6]Chiarle, S., Ratto, M., Rovatti, M., *Water Res.*, **2000**, *34*, 2971. DOI: https://doi.org/10.1016/S0043-1354(00)00044-0.

[7]Patterson, J. W., Passono, R., *Metals Speciation-Separation and Recovery*, Lewis Publisher, New York, **1990**.

[8]Larson, K. A., *Ind. Eng. Chem. Res.*, **1992**, *31*, 2714. DOI: 10.1021/ie00012a013

[9]Skubal, L. R., Meshkov, N. K., *J. Photoch. Photobiol A: Chem.*, **2002**, *148*, 211. DOI: 10.1016/S1010-6030(02)00079-5

[10]Atwood, D. A., Zaman, M. K., *Struct. Bonding*, **2006**, *120*, 163-182.

[11]Sen, A. K., De, A. K., *Water Res.*, **1987**, *21*, 885. DOI: https://doi.org/10.1016/S0043-1354(87)80003-9

[12]Pandey, M. P., Chaudhuri, M., *Water Res.*, **1982**, *16* 1113. DOI: https://doi.org/10.1016/0043-1354(82)90127-0

[13]Karthikeyan, J., Chaudhuri, M., **1986**, *20*, 449. DOI: https://doi.org/10.1016/0043-1354(86)90192-2

[14]Cullen, G. V., Siviour, N. G., *Water Res.*, **1982**, *16*, 1357. DOI: https://doi.org/10.1016/0043-1354(82)90214-7

[15]Deshkar, A. M., Bokade, S. S., Dara, S. S., *Water Res.*, **1990**, *24*, 1011–1016. DOI: 10.1016/0043-1354(90)90123-N

[16]Tan, T. C., Chia, C. K., Teo, C. K., *Water Res.*, **1985**, *19*, 157. DOI: https://doi.org/10.1016/0043-1354(85)90193-9

[17]Srivastava, S. K., R. Tyagi, N. Pant, *Water Res*., **1985**, *23*, 1161. DOI: https://doi.org/10.1016/0043-1354(89)90160-7

[18]Singh, D. K., Tiwari, D. P., Saksena, D. N., *Indian J. Environ. Health*, **1993,** *35*, 169.

[19]Rowley, A. G., Husband, F. M., Cunningham, A. B., *Water Res.*, **1981**, *18*, 981. DOI: https://doi.org/10.1016/0043-1354(84)90248-3

[20]Tiwari, D. P., Singh, D. K., Saksena, D. N., *J. Environ. Eng*., **1995**, 479. DOI: https://doi.org/10.1061

[21]Cox, M., El-Shafey, E., Pichugin, A. A., Appleton, Q., *J. Chem. Technol. Biotechnol*., **2000**, *75*, 427. DOI: 10.1002/(SICI)1097-4660(199911)74:11<1019::AID-JCTB152>3.0.CO;2-N

[22]Daifullah, A. A. M., Awwad, N. S., *Al-Azhar Bull. Sci*., - *Proc. 5th Int. Sci. Conf.*, **2003**, 57.

[23]Hassan, S. S. M., Awwad, N. S., Aboterika, A. *J. Hazard. Mater*., **2008**, *154*, 992–997. DOI: 10.1016/j.jhazmat.2007.11.003

[24]Sarkar, S., Sarkar, S., Biswas, P., *J. Environ. Chem. Eng.*, **2017**, *5*, 38. DOI: https://doi.org/10.1016/j.jece.2016.11.015

[25]Langmuir, I., *J. Am. Chem. Soc*., **1918**, *40*, 1361. DOI: 10.1021/ja02242a004.

[26]Zare, F., Ghaedi, M., Daneshfar, *Chem. Eng. J*., **2015**, *273*, 296. DOI: https://doi.org/10.1016/j.cej.2015.03.002

[27]Alzaydien, A. S., *Am. J. Environ. Sci.*, **2009**, *5*, 197. DOI: 10.3844/ajessp.2009.197.208

[28]Akar, T., Kaynak, Z., Ulusoy, S., Yuvaci, D., Ozsari, G., Akar, S. T., *J. Hazard. Mater*., **2009**, *163*, 1134. DOI: https://doi.org/10.1016/j.cej.2008.07.027

[29]Shao, W., Chen, L., Lu, L., Luo, F., *Desalination*, **2011**, *265*, 177–183. DOI: https://doi.org/10.1016/j.desal.2010.07.049

[30]Mishra, S. L., Tiwari, D., Prasad, S. K., Dubey, R. S., Mishra, M., *J. Radioanal. Nucl. Chem.*, **2007,** *24*, 257. DOI: 10.1007/s10967-007-1108-y

[31]Wu, X. W., Ma, H. W., Li, J. H., Zhang, J., Li, Z. H., *J. Colloid Interface Sci.*, **2007**, *315*, 555. DOI: https://doi.org/10.1016/j.jcis.2007.06.074

[32]Deshicar, A. M., Bokade, S. S., Dara, S. S., *Water Res.*, **1990**, *24*, 1011. DOI: https://doi.org/10.1016/0043-1354(90)90123-N

[33]Srivastava, S. K., Tyagi, R., Pant, N., *Water Res.*, 1989, *23*, 1161. DOI: https://doi.org/10.1016/0043-1354(89)90160-7

[34]Dawlet, A., Talip, D., Yu Mi, H., MaLiKeZhaTi, *Procedia Environ. Sci*, **2013**, *18*, 800-808. DOI: 10.1016/j.proenv.2013.04.108

[35]Anirudhan, T. S., Screkumari, S. S., *J. Environ. Sci.*, **2011,** *23(12)*, 1989. DOI : https://doi.org/10.1016/S1001-0742(10)60515-3

[36]Kadirvelu, K., Kavipriya, M., Karthika, C., Vennilamani, N., Pattabhi, S., *Carbon*, **2004**, *42(4)*, 745. DOI : https://doi.org/10.1016/j.carbon.2003.12.089.

[37]Kannan, N., Malar, S. J. S., *Indian J. Chem. Technol.*, 2005, *12*, 522.

[38]Manohar, D. M., Noeline, B. F., Thayyath, S. A., *Sep. Sci. Technol.*, **2014**, *49*, 1259. DOI: http://dx.doi.org/10.1080/01496395.2013.876046

[39]Ismaiel, A.A., Aroua, M.K., Yusoff, R., *Chem. Eng. J.*, **2013**, *225*, 306. DOI : http://dx.doi.org/10.1080/01496395.2013.876046

[40]Mondal, D. K., Nandi, B. K., Purkait, M. K., *J. Environ. Chem. Eng.*, **2013,** *1*, 891. DOI : https://doi.org/10.1016/j.jece.2013.07.034

[41]Santana, A.J., dos Santos, W.N.L., Silva, L.O. B., das Virgens, C.F., *Environ. Monit. Assess*., **2016**, 188. DOI: 10.1007/s10661-016-5266-7

[42]Kumar, S.K., Jiang, A.S.J., *RSC Adv.*, **2015**, *5*, 6294. DOI: 10.1039/C4RA12564A

[43]Esfandiyari, T., Nasirizadeh, N., Dehghani, M., Ehrampoosh, M.H., *Chin. J. Chem. Eng*., Available online 20 March 2017, In Press, Corrected Proof.

[44]Meena, A.K., Mishra, G. K., Rai, P. K., Rajagopal, C., Nagar, P. N., *J. Hazard. Mat.*, **2005**, *122*, 161. DOI: https://doi.org/10.1016/j.jhazmat.2005.03.024

[45]Henriques, B., Gonçalves, G., Emami, N., Pereira, E., Vila, M., Marques, P.A.A.P., *J. Hazard. Mater.*, **2016**, *301*, 453. DOI: https://doi.org/10.1016/j.jhazmat.2015.09.028

[46]Kumar, A.S. K., Jiang, S. J., Tseng, W. L., *J. Environ. Chem. Eng.*, **2016**, *4*, 2052. DOI: https://doi.org/10.1016/j.jece.2016.03.034

[47]Kim, H. H., Lee, T. G., *J. Ind. Eng. Chem.*, **2017**, *47*, 446. DOI: https://doi.org/10.1016/j.jiec.2016.12.019

Received: 09.12.2017.
Accepted: 20.01.2018.

ECOLOGICAL HUMAN IMPRINT IN EGYPT: PROSPECTIVE ANALYSIS AND VIEWS FROMECOLOGICAL SUSTAINABILITY AND MODELING

Safwat H. Shakir Hanna[a]*and Magdy T. Khalil[b]

Keywords: Ecological human imprint, ecological sustainability, modelling.

The Ecological Human Imprint (E_{HI}) is a measuring tool to assess the carrying capacity of an area with regard to the use of the planet's natural resources. Additionally, it will be acting as a feedback to policies and strategies utilized in measuring the sustainable development. It will measure the ability of policies that can be implemented to reduce environmental impact. The new index (E_{HI}) is an important measure for calculating the human demands and impacts on environment. In this respect, the E_{HI} is a function of all the parameters that interact between the power of ecosystem productivity, human interactions and activities on a particular ecosystem or the demand from that ecosystem. The present paper is covering and analysing the ecosystems' productivity and the human demand from the ecosystems. It includes comprehensive analyses in measuring the possibility of capabilities of the Egyptian ecosystems to provide goods and services to its population. Additionally, we have discussed the models that can be used in measuring the sustainability of ecosystems and, in particular, the natural resources of Egypt. Further, a comprehensive model called E_{HI} and national resources changes of Egypt (E_{HI}-NR-EG) has been formulated. This describes the status of the ecosystems' productivity and assesses the impact of change of any parameter that affects the current status of natural resources and their availability to human population within the Egyptian boundaries. In addition, attempts have been made to provide some answers to issues which arises due to the impact of human activities on natural resources

* Corresponding Authors
E-Mail: safwat_shakir@yahoo.com
[a] Chemical Engineering Department, College of Engineering, Prairie View A&M University, The Texas A&M University System, Prairie View, TX 77446, USA.
[b] Faculty of Science, Ain Shams University, Egypt.

INTRODUCTION

Egypt population density is 98,092,423 people as on Wednesday, October 18, 2017, based on the latest United Nations estimates (http://www.worldometers.info/world-population/egypt-population) with an annual average of population growth rate of 1.87-2.72 % percent. Further, the population density in Egypt is 98 km^{-2}. In this respect, 38.8 **%** of the population is urban (37,826,341 people in 2017). This has an increasing impact on the natural resources to meet the demands from the human population. Egypt occupies 100.1 million hectares, out of which 67,000 hectares are covered by forest, 3.5 million by cropland and 20,000 by grazing land, with 1.3 million hectares supporting its built infrastructure. Bordering the Mediterranean and the Red Sea, Egypt has 5.0 million hectares of continental shelf and 0.6 million hectares of inland water (Egyptian Census Bureau). In this respect, the natural resources have not increased as the increased trends of human population. Therefore, if the natural resources that provide goods and services for the survival of Egypt's human population are not increased or developed to sustain the development, then what will happen? It is an important question that the Egyptian government, Non-Governmental Organization (NGO), scientists, researchers and Egyptian people should answer to secure the continuation of sustainable development in the country.

In Egypt, human population and demands for food production have increased to the degree that the Nile lands cannot support and provide the essential crops. These are issues being studied by the Government to find solutions. If one third of the Nile Delta is to be inundated by waters of the Mediterranean, Egypt may not be able to produce much of the crops that are already in dire shortage.[1] Further, as the result of the increasing population, the Egyptian sustainable development will be impossible.

MATERIALS AND METHODS

Data Collection

Data are collected from different series available on public domain website of the World Bank,[2,3] United Nation Environmental Program (UNEP),[4] United Nation Development Program (UNDP),[5] United Nation Food and Agriculture Organization (FAO),[6] (FOASTAT),[7] (UNFPA, 2001),[8] WWF reports, 2002,[9,10,11,12] 2004,[13] 2006,[14] 2008,[15] 2010[16] and 2012,[17] and WRI 1960-2005,[18,19] and series WRI 2000-2001.[20] The data were analyzed using the regression, correlation, and statistical methodologies using Sigma Plot Software (Version 8, Version 11.2), 2D software of SPSSSCIENCE, 2002, (2009-2010),[20] STELLA software 2006 and 2010[21,22] and SAS, 2011 a,b.[23,24]

Construction of a simulation model with STELLA software

The simulated model was constructed using several parameters such as human population, annual increase in population, biological capacity of ecosystems, water resources, and demands from nature. The data was converted to global hectare. The model was used to predict the ecological human imprint of demand from the existing resources and the ecological capacities of ecosystems that will support the sustainable development for the up-coming one hundred years. This model was applied to Egypt as Ecological Human Imprint (E_{HI}) and national resources

changes of Egypt (E_{HI}-NR-EG). In this respect we have used the Stella Software to create an executable program using the two or fourth order Runge–Kutta integration method. The model was used to predict the changes in ecological footprint demands and footprint capacities according to several parameters such as the human population change including the fertility changes, factors impacted on population growth, cropped lands, grazing lands, fisheries, build-up lands, vegetative lands, water resources, etc. The model has the capacity to predict for the next year, next decade, next twenty-five years, next fifty-years and for the next hundred year. The model takes into considerations the relaxed assumptions, moderate assumptions, conservative assumptions and very conservative assumptions of changing data parameters. The model hypothesis is presented in the Figure 1.

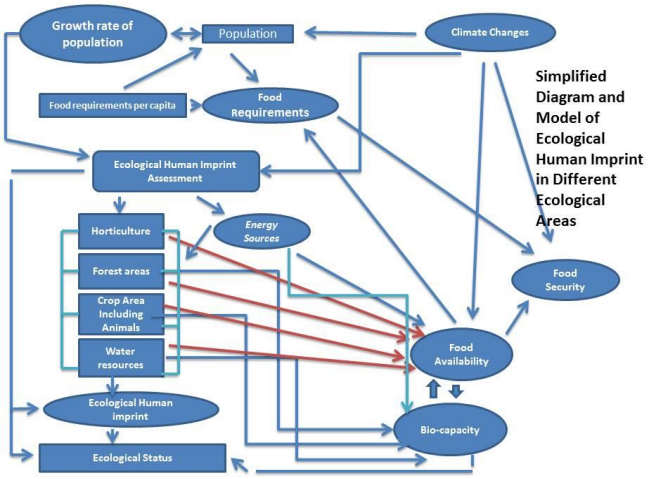

Figure 1. Simplified diagram for the E_{HI} model in Egypt.

RESULTS AND DISCUSSION

The According to recent United Nations estimates, global population is increasing by approximately 80 million — the size of Germany — each year (Vital Sign, 2012, UNDP 2013).[5] Additionally, the Egyptian population is increasing by average of two millions/per year since 1960. For example in year 2017, the human population of Egypt has increased by 2,062,826 people, with a growth rate of 2.18 %. This is an alarming rate for the Egypt and it is difficult to sustain its development with its limited resources.

Data in Tables 1-7 and Figure 2 indicate that the (E_{HI}) of Egypt is increasing with an increase in the human population. This means that the demands on the natural resources of Egypt is increasing and this is putting high pressure on the natural resources that are not available and this will lead to import many of the natural resources from other countries. This is seen in Figure 3. It illustrates the availability of the biological capacity in Egypt and shows the decline in the availability of bio-capacity per capita. The bio-capacity measures the capacity for supplying goods and services to the country from the available natural resources. The decline of global hectare per capita is about 0.14 hectare per capita when the human population had reached around 80 million people. This means that the basic needs from the natural resources are not met and the extreme difficulties are arising continuously. Further Figure 4 indicates that the relationship between deficit in biological capacity and human population of Egypt and shows the declining the biological capacity of Egypt lands for producing the biological capacities to support the goods, products and services in Egypt.

According the simulation model of (E_{HI}-NR-EG), the model have several senarios according to the increase of human populatuion from relaxed assumption, moderate assumption and conservative assumption of growth of human population of Egypt as the following rate: therefore, the rate of relaxed asumption is about 1.7 %, moderate assumption of 1. 2 % and conservatiove rate of growth of 1.0 %. This will lead us to emphasize the magintude of the problem of increasing the human popualtion.

The simulation model has indicated the following major points in relation to the natural resources and biological capacity of the ecosystems. In this respect the model Figure 5 shows that the human population at growth rate is 2.1%, Egyptian biological capacity and Egyptian biological demands from the Earth as calculated by the E_{HI}-NR-EG, the graph shows that demands is increasing and at the same time the population will grow to 186.97 million people in 2050 and the biological capacity will decrease indicating in the maintenance index as covering 15% of the Egyptian population. However when human population growth rate is 1.5%, the Egyptian biological demands from the Earth will increase and at the same time the population will grow to 109 million people in 2050 and the biological capacity will decrease indicating that the maintenance index is covering 16 % of the Egyptian population (Figure 6). In addition, when human population growth rate is 1.0 %, the Egyptian biological demands from the Earth will increase and at the same time the population will grow to 70.5 million people in 2050 and the biological capacity will decrease indicating that the maintenance index is covering 17 % of the Egyptian population. In this respect, with decreasing the human population growth rate, the model is giving improvement within the natural resources allowing support of Egyptian people (Figure 7).

From the above analysis, we can come to the most important scientific analysis for explaining the challenges that the Egyptian government will face in the near future to accommodate all the human beings who are living on its natural resources. Shakir Hanna et. al[25] indicated that with increasing human imprint on global scale can be of consideration. In this respect, the Egyptian government has to consider vigorous family planning and reduction of the family production of kids. The high fertility rate can impose costly burdens on Egypt's economy and sustainability. This will overload the natural resources for increasing demands from the overload of population. This will allow the country to borrow money to support its people. In other words, increasing human population cause the declining ability of the country to support its citizens. Accordingly, with fewer children, families will have more disposable income to save or invest. This constitutes a "demographic bonus," which may help to spur economic growth, create jobs, and in turn reduce unemployment. In 1995, the unemployment rates were 31.5 and 11.8 percent among secondary school and University graduates respectively.[26] This will lead the declining the poverty for the people of Egypt.

Table 1. List of variables and parameters that are used in the study of Egyptian Ecological Human Imprint.

Variable	Interpretation	Unit used in the model
GBC	Global Biological Capacity of the Egyptian lands	In million hectares that generate the biological capacity of the lands of Egypt
GBD	Global Biological Demand from the Egyptian lands	In million hectares that consumed from biological capacity by human beings living on the land.
E_{HI}	Ecological Human Imprint Index	Calculated by Information Theories and Technological Advances Factor as positive and negative impacts and converted to Global Million hectares
GDC	Global Deficit Capacity	In million hectares
Egp	Egyptian Population	In million people

Table 2. Egyptian Population in million, Egyptian Global Biological Capacity (GBC), Egyptian Global Biological Demand (GBD) and Maintenance Index of the Egypt Earth up to Year 2010. 1.7 % Growth Rate of Human Population, Surface area = 1 million sq. km

Year	Population	GBD	GBC	CBC-GBD	GBC/GBD
1961	28.80	0.09	0.01	-0.08	0.22
1970	35.45	0.11	0.02	-0.09	0.16
1980	43.64	0.12	0.02	-0.10	0.16
1990	53.72	0.14	0.02	-0.12	0.14
2000	66.13	0.17	0.02	-0.14	0.11
2010	81.41	0.20	0.03	-0.17	0.15

Table 3. Predicted Values Calculated for Egyptian Population, GBC, GBD and Maintenance Index of the Egyptian Earth from Year 2010-2050 assuming 1.7 % Growth Rate of Human Population.

Year	Population	GBD	GBC	CBC-GBD	GBC/GBD
2010	81.41	0.20	0.03	-0.17	0.15
2020	100.22	0.23	0.03	-0.20	0.13
2030	123.37	0.28	0.04	-0.24	0.142
2040	151.86	0.34	0.05	-0.29	0.147
2050	186.94	0.41	0.06	-0.35	0.146

Table 4. Egyptian Population, GBC, GBD and Maintenance Index of the Egypt Earth up to Year 2010, assuming 1.5 % Growth Rate of Human Population.

Year	Population	GBD	GBC	CBC-GBD	GBC/GBD
1961	28.80	0.09	0.01	-0.08	0.22
1970	33.42	0.10	0.02	-0.08	0.16
1980	33.79	0.11	0.02	-0.09	0.16
1990	45.02	0.12	0.02	-0.10	0.14
2000	52.34	0.14	0.02	-0.12	0.11
2010	60.62	0.15	0.02	-0.13	0.15

Table 5. Predicted Values Calculated for Egyptian Population, GBC, GBD and Maintenance Index of the Egyptian Earth from Year 2010-2050 assuming 1.5 % Growth Rate of Human Population.

Year	Population	GBD	GBC	CBC-GBD	GBC/GBD
2010	60.63	0.15	0.02	-0.13	0.15
2020	70.31	0.17	0.03	-0.15	0.17
2030	81.66	0.20	0.03	-0.17	0.15
2040	94.77	0.22	0.03	-0.19	0.14
2050	109.99	0.25	0.04	-0.22	0.16

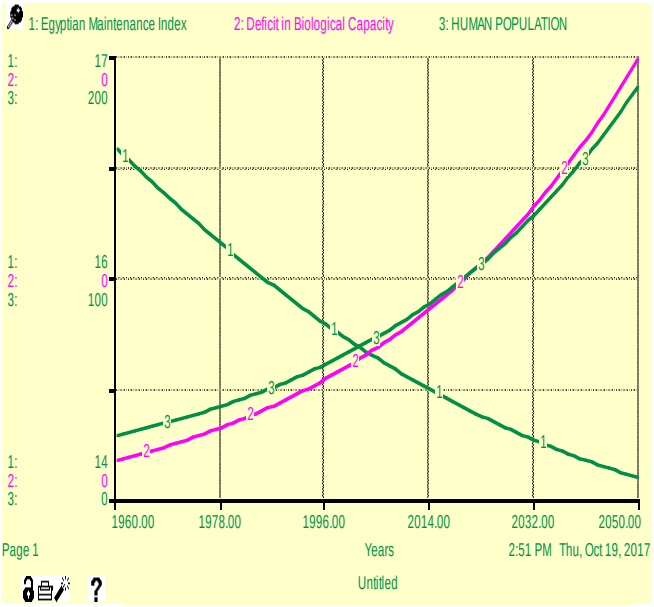

Figure 5. Simulation model for Egyptian human population and Egyptian maintenance index (EMI %) and deficit in GBC assuming a 2.1 % annual growth rate.

Table 6. Egyptian Population, GBC, GBD and Maintenance Index of the Egypt Earth up to Year 2010, assuming 1 % Growth Rate of Human Population.

Year	Population	GBD	GBC	CBC-GBD	GBC/GBD
1961	28.80	0.09	0.01	-0.08	0.22
1970	31.61	0.10	0.02	-0.08	0.20
1980	35.14	0.10	0.02	-0.09	0.22
1990	38.82	0.11	0.02	-0.09	0.18
2000	42.88	0.12	0.02	-0.10	0.16
2010	47.37	0.13	0.02	-0.11	0.15

Table 7. Predicted Values Calculated for Egyptian Population, GBC, GBD and Maintenance Index of the Egyptian Earth from Year 2010-2050 assuming 1 % Growth Rate of Human Population.

Year	Population	GBD	GBC	CBC-GBD	GBC/GBD
2010	47.37	0.13	0.02	-0.11	0.15
2020	52.37	0.14	0.02	-0.12	0.14
2030	57.71	0.15	0.02	-0.13	0.13
2040	63.84	0.16	0.02	-0.14	0.13
2050	70.50	0.17	0.03	-0.15	0.17

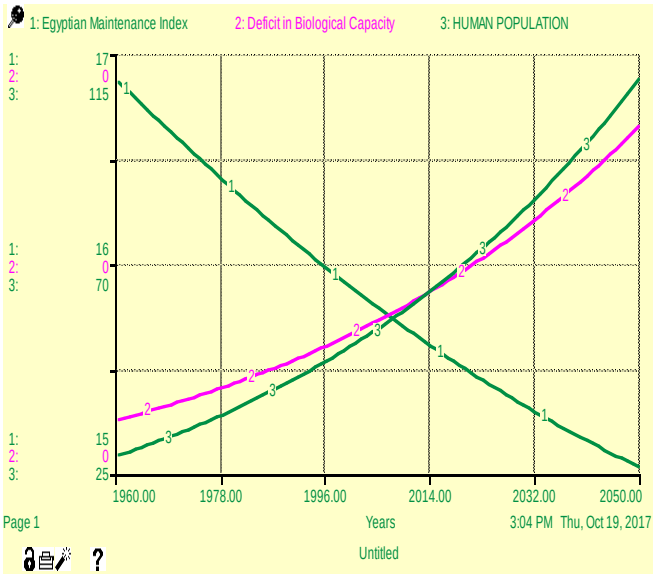

Figure 6. Simulation model for Egyptian human population and Egyptian maintenance index (EMI %) and deficit in GBC assuming a 1.5 % annual growth rate.

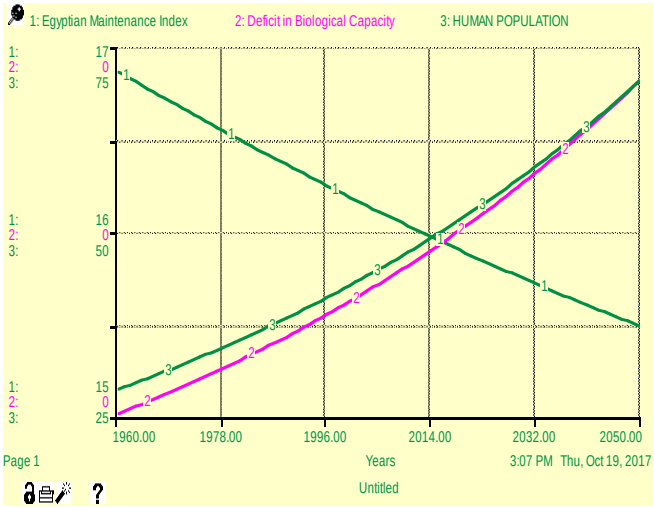

Figure 7. Simulation model for Egyptian human population and Egyptian maintenance index (EMI %) and deficit in GBC assuming a 1 % annual growth rate.

CONCLUSIONS

It is important to in force the family planning in Egypt because the (E_{HI}) of the Egyptian society is increasing and in consequence the increase demands from natural resources to produce the goods and services. From the data that series we studied there is a concern when it comes to the production of food requiring for all people of Egypt to support their lives. According to Us Department of Agriculture (USDA), the required average number of calories that are needed to support every human being is 2000 Calories per day. This is translated to the production of 2000X365X 98 million people in the country will turn to 7.154 calories per year. [13] The question is from where we can get all these calories to feed the whole population for Egypt in a one year? In general some people are not receiving these calories and many people are in malnutrition and in a very high poverty and the country cannot support all the people.

REFERENCES

[1]Agrawala, S.; Moehner, A.; El Raey, M.; Conway, D.; van Aalst, M.; Hagenstad, M. and Smith, J., *Development and climate change in Egypt: focus on coastal resources and the Nile*. Com/env/epoc/dcd/dac(**2004**)1/final

[2]WorldBank,.1960-2012. *Data Series and Research*. The World Bank Organization. http://data.worldbank.org/topic/ agriculture-and-rural-development.

[3]WorldBank, 1960-2008. *Data Series and Research*. The World Bank worldbank.org/topic/ agriculture-and rural-development.

[4]UNEP. *A Planet in Ecological Debt*, Arendal Maps and Graphics Library: UNEP **2009**. http://maps.grida.no/go/graphic/a-planet-in-ecological-debt,

[5]UNDP. *The Rise of the South: Human Progress in a Diverse World. Human Development Report*. The United Nations Development Programme. Gilmore Printing Services Inc., Canada, **2013**, 216 pp.

[6]FAOSTAT *FAO Statistical Database- Data Series* 1960-2008 Food and Agriculture Organization, UN, www.fao.org, Rome, Italy.

[7]FAOSTAT *Data Series.Food and Agriculture Organization*,UN, www.fao.org, Rome, Italy, **2008**.

[8]UNFPA. The State of World Population. **2001**.

[9]WWF, *The Global Conservation Organization*, Living planet report/ footprint, **2002**.

[10]WWF. *Living Planet Report*, World Wide Fund for Nature.(WWF),http://www.panda.org/livingplanet.,Geneva, Switzerland, **2002**.

[11]WWF, *The Global Conservation Organization*, living planet report/ footprint, **2002**.

[12]WWF, *Living Planet Report* Edited by Jenkins M., Jakubowska J., Gaillard V., Groombridge B., M.WackernagelMonfreda, C., Deumling D., Gurarie E., Friedman S., Linares A.C., Sánchez M.A.V., Falfán I.S.L., Loh, J. Randers., S.J. and C. Monfreda, *World Wildlife Fund* (WWF), www.panda.org,, International. Avenue du Mont-Blanc, CH-1196 Gland, Switzerland. 2002

[13]WWF, *Living Planet Report*, World-Wide Fund for Nature International (WWF), Global Footprint Network, UNEP World Conservation Monitoring Centre.WWF, Gland, Switzerland.http://www.panda.org/livingplanet, **2004**.

[14]WWF, *Living Planet Report*, World Wide Fund (WWF) for Nature, Gland, Switzerland http:// www.panda.org/livingplanet, **2006**.

[15]WWF, *Living Planet Report*, Edited by Humphrey S., Chapagain A., Bourne G., Mott R., Oglethorpe J., Gonzales A., Atkin M., Loh J., Collen B., McRae L., Carranza T.T., Pamplin F.A., Amin R., Baillie J.E.M., Goldfinger S., Wackernagel M., Stechbart M., Rizk S., Reed A., Kitzes J., Peller A., Niazi S., Ewing B., Galli A., Wada Y., Moran D., Williams R., Backer W.D., Hoekstra A.Y. and Mekonnen, M., 2008 World Wide Fund (WWF), www.panda.org,, International Avenue du Mont-Blanc 1196 Gland, Switzerland, **2008**.

[16]WWF, *Living Planet Report*. World Wide Fund for Nature, Gland, Switzerland, **2010**.

[17]WWF, *Living Planet Report*, Biodiversity, biocapacity and better choices.Editor in chief: *Monique Grooten.*, Lead editors: *Rosamunde Almond and Richard McLellan.* Editorial team: *Nigel Dudley, Emma Duncan, NatasjaOerlemans and Sue Stolton*, **2012**.

[18]WRI, World Resources Institute.. *Earth Trends Environmental Information*, World Resource Institute (WRI). World Resource Institute: WRI http://Earthtrends.wri.org/. **1960-2005**

[19]WRI, World Resources Institute .2000-2001. *People and Ecosystems: The Fraying Web of Life*. WorldResources Institute (WRI), Washington DC, USA, **2000**.

[20]SIGMAPLOT Version 13. https://systatsoftware .com /products/ sigmaplot/

[21]STELLA Isee System. *Technical Document for the iThink and STELLA Software*. **2006**. Available at: http://www.iseesystems.com..

[22]STELLA. *Stella®, High Performance System,* Inc., USA. 2010. Available at: http://www.hps-inc.com/ stellavpsr.htm.

[23]SAS Institute Inc. *SAS/STAT Product Documentation*. SAS Institute Inc., Cary, NC. **2011**., URL http://support.sas.com/documentation/onlinedoc/stat/.

[24]SAS Institute Inc. *SAS/STAT User's Guide* {Procedures. SAS Institute Inc., Cary, NC.) **2011**., URL http://support.sas.com/documentation/onlinedoc/stat/indexproc.html#stat93.

[25]Shakir Hanna, S. H. Harris, K. T., Osborne-Lee, I. W., Cesaretti, G. P, Misso, R. and Andreopoulou, Z. S. Global Ecological Human Imprint, SustainableDevelopment and Environment: Assessmentand Impacts. *Eur. J. Sustain. Dev.*, **2014**, *3(3)*, 1-24. DOI 10.14207/ejsd.2014.v3n3p1

[26]Institute of National Planning, Egypt Human Development Report. **1996**

Received: 20.11.2017.
Accepted: 20.01.2018.

PROBABILITY DISTRIBUTIONS ASSESSMENT FOR MODELING GAS CONCENTRATION IN CAMPO GRANDE, MS, BRAZIL.

Amaury de Souza,[a] Zaccheus Olaofe,[b] Shiva Prashanth Kumar Kodicherla,[c] Priscilla Ikefuti,[d] Luciana Nobrega[e] and Ismail Sabbah[f]

Keywords: Statistical analysis; distribution of probability; performance indicators; air pollutants.

The predominant air pollutants in urban cities are (NO_x = (NO + NO_2), O_3 and (OX = (O_3 + NO_2). This research focused on pollutant variables that cause damage to human health as well as to the environment. Thus, seven statistical models {Weibull (W), Gamma (G), Log-normal (L), Frechet (Fr), Burr (Bur), Rayleigh (R) and Rician (Ri)} were chosen to fit the observations of the air pollutants. An average hourly data from one year to 2015 were considered. In addition, performance indicators {Mean Absolute Error (MAE), Root Mean Square Error (RMSE), Mean Absolute Percentage Error (MAPE)} were applied, to determine the quality criteria for adjustment of the frequency distributions. The best distribution that adapts to the observations of the variables was the RICIAN distribution, the log-normal distribution for COD. The probabilities of the concentration of exceedances were calculated,(predicted) from the cumulative density function (cdf) obtained from the best fit distributions.

*Corresponding Authors
E-Mail: amaury.de@uol.com.br
[a] Federal University of Mato Grosso do Sul, C.P. 549, 79070-900 Campo Grande, MS – Brazil
[b] University of Cape Town: Rondebosch, Western cape, South Africa.
[c] Department of Civil Engineering, Room No. EB 577, Engineering Building (EB), Xi'an Jiaotong-Liverpool University (XJTLU), Suzhou Industrial Park, Suzhou, P. R. China.
[d] University of São Paulo; Department of Physical Geograpy, São Paulo- SP- Brazil
[e] Universidade Federal da Paraiba, Depto de Engenharia dos Materiais, João Pessoa, PB, Brasil
[f] Department of o Natural Sciences, College of Health Sciences, the Public Authority for Applied Education and Training, Kuwait

INTRODUCTION

Air pollution in urban areas causes adverse effects on the human health and the environment. In addition, cities face increasing urban pollution and it has negative effects on the rapid population growth. Recent studies have also proven over time that industrialization and the use of motor vehicles are the two main contributors to urban air pollutions.

One of the main problems caused by air pollution in the urban areas is the presence of photochemical oxidizers. Among these pollutants, ozone (O_3) and nitrogen dioxide (NO_2) are particularly important since they are susceptible to provoking adverse effects on the human health (OMS, 2000). The formation of ozone at ground level depends on the intensity of the solar radiation, the absolute concentration of NOx and the VOCs (Volatile Organic Compounds), and the ratio between NOx and VOCs.[1]

The ozone concentration increases with the growing intensities of solar radiation and the air temperature. The concentration of photochemical oxidizers may be reduced throughout the control of their precursors, which are nitrogen oxides NO_x (NO and NO_2) and VOCs.[2-8]

In Campo Grande, some studies and climate monitoring campaigns have been carried out,[2,9-17] for studying the atmospheric dispersion modelling to explore the results of climate change.

In literature, probability distributions have been used to adjust the concentrations of air pollutants, including the: Weibull distribution,[18] Lognormal distribution,[19] Gamma distribution,[20] distribution of Rayleigh,[21] distribution of Gumbel[22] and Frechet's distribution.[23] Using a variety of performance indicators, such as the: mean absolute error (MAE), root mean square error (RMSE), concordance index (d_2), bias normalized absolute error (NAE), prediction accuracy) and the coefficient of determination (R_2).

The objectives of this study are to adjust the probability distributions for the concentration of three air pollutants (NO_x, O_3 and OX) using seven statistical models.

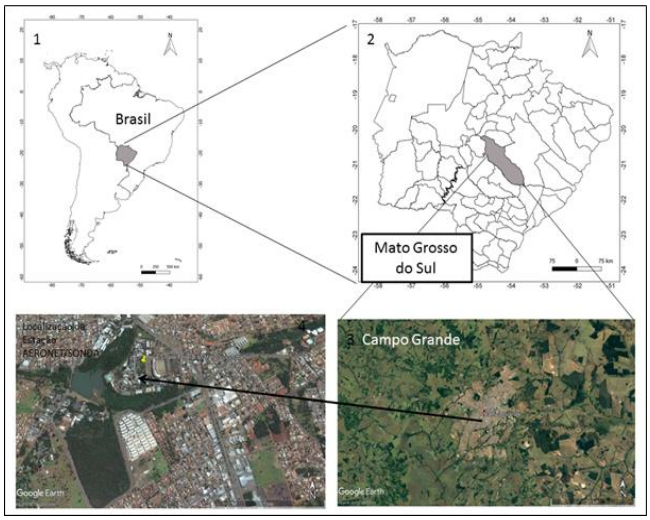

Figure 1. Location of the Municipality of Campo Grande in the State of Mato Grosso do Sul, and the continuous air monitoring station located on the campus of the Federal University of Mato Grosso do Sul, Campo Grande, MS.

MATERIALS AND METHODS

Studied and observational data

Campo Grande is the capital city of South Mato Grosso (MS) state, located in the southern of Brazil Midwest region, sited in the center of the state. Geographically, the city is near to the Brazilian border with Paraguay and Bolivia. It is located at 20°26'34'' South and 54°38'47'' West longitude. Figure 1 shows the location of Campo Grande, capital of the state of Mato Grosso Sul (MS). It occupies a total area of 8,096.051 km² or 3,126 mi², representing 2.26 % of the total state area, within 860,000 inhabitants (2016) and a corresponding HDI of 0.78. The urban area is approximately 154.45 km² or 60 mi², where tropical climate and dry seasons predominate, with two clearly defined seasons: warm and humid in the summer, and less rainy and mild temperatures in winter months.

During the months of the winter, the temperature can drop considerably, arriving on certain occasions to the thermal sensation of 0 ºC or 32 ºF with occasional and light freezing. The year average precipitation is usually at 1,534 mm, with small up or down variations. The main pollution problems in the city are attributed to the: traffic of vehicles, raise of building activities, the presence of dumping grounds, use of small power generators running on oil to supply power to the electric grid, and finally, to the induced fire outbreak used to clean up local terrains.

Ensemble of observational data

The air quality and meteorological variables are monitored by an automatic station operated at the Institute of Physics of the Federal University of South Mato Grosso (UFMS). This met station is located inside the university campus, about 8 km or 5 miles to the west of downtown. The main sources of pollution in that area are the building activities; therefore, there are no significant precursor sources of ozone identified close to the region. The ozone levels of Campo Grande area are stored in a regular database since 2004.

The equipment of measurements was installed at the top of a tower from where air samples are extracted throug vertical pipes that are placed approximately 2 meters above the ground level.

The three considered pollutants, NO_x (NO + NO_2), OX (O_3 + NO_2) and O_3, were measured continuously for a one–year period (2015).

The equipment used for measurements include a nitrogen oxide analyzer (AC31M–using chemiluminescence method), an ozone analyzer (O341M–LCD/UV Photometry). All equipment was made by Environnement S.A.

Modelling of the climatological datasets

The statistical models (Weibul, Rayleigh, Gamma, Lognormal, Frechet, Burr and Rician) used for fitting of the observed datasets (NOx, O_X and O_3) are defined as follow:

Weibull (W) PDF

The Weibull probability density function (pdf) of a 2-parameter distribution is given as the derivative of a cumulative distribution function (cdf) expressed in Eqn. (1)

$$f_w(k,C) = \frac{k}{C}\left(\frac{v}{C}\right)^{k-1} exp\left[-\left(\frac{v}{C}\right)^{k}\right] \quad (1)$$

The Weibull cumulative distribution function (cdf) is given by Eqn. (2)

$$F_w(k,C) = 1 - exp\left[-\left(\frac{v}{C}\right)^{k}\right] \quad (2)$$

where

k and *C* are the shape and scale parameters of the Weibull distributions derived from the time series of the climatological datasets;

v is the time series observations from each variable/dataset.

Meanwhile, the shape parameter "*k*" is obtained from the maximum likelihood estimator (MLE) as expressed:

$$k = \left(\frac{\sum_{i=1}^{N} \ln\left(v_i\right) v_i^{k}}{\sum_{i=1}^{N} \ln v_i^{k}} - \frac{\sum_{i=1}^{N} \ln(v_i)}{N} \right)^{-1} \quad (3)$$

Once the *k* values are calculated, the scale parameter values are obtained from Eqn. (4)

$$C = \left(\frac{\sum_{i=1}^{N} v_i^{k}}{N} \right)^{\frac{1}{k}} \quad (4)$$

where *N* is the number of time series dataset points. Meanwhile, Eq. (3) is apply to each climate observations and solve iteratively with an initial guess of 2 (*k*=2) until *k* values converge after several iterations.

Rayleigh (R)P DF

Substituting k=2 into Eqs (1) and (2), the Rayleigh pdf of a continuous distribution $f_r(v,k,C)$, is given as:

$$f_r(k,C) = \frac{2v}{C^2} exp\left[-\left(\frac{v}{C}\right)^2\right] \quad (5)$$

The Rayleigh cumulative distribution function (cdf) is given:

$$F_r(k,C) = 1 - exp\left[-\left(\frac{v}{C}\right)^2\right] \quad (6)$$

Gamma (G) PDF

The pdf of a gamma distribution is defined by Olaofe and Folly:[24]

$$f_g(k,C) = \frac{v^{k-1}}{C^k \Gamma(k)} exp\left[-\left(\frac{v}{C}\right)\right] \quad (7)$$

where f_g and $\Gamma(k)$ are the pdf of gamma distribution and the gamma function of (k), respectively. k and C are the shape and scale parameters of the Gamma distribution derived from the time series observations.

The cumulative density function (cdf) of a Gamma distribution is defined as

$$F_g(k,C) = \frac{1}{C^k \Gamma(k)} \int_0^v t^{k-1} exp\left(-\left(\frac{t}{C}\right)\right) dt \quad (8)$$

where F_g is the cumulative density function of a gamma distribution.

Lognormal (L) PDF

Lognormal was used to fit the ozone concentration data. The location parameter of the lognormal distribution is estimated from the expression:

$$\mu = \ln \frac{\left(\bar{v}\right)^2}{\sqrt{\left[\sigma + \left(\bar{v}\right)^2\right]}} \quad (9)$$

where σ is the variance of the observed dataset and μ is the lognormal scale (sigma) parameter

The scale parameter of the lognormal distribution is estimated as

$$\varphi = \sqrt{\ln\left(1 + \frac{\sigma}{\left(\bar{v}\right)^2}\right)} \quad (10)$$

where φ is the μ (location) parameter.

The probability density function and the cumulative distribution function of a lognormal pdf are defined below

$$f_l(\mu,\varphi) = \frac{1}{v\varphi\sqrt{2\pi}} \exp\left(-\frac{\ln(v-\mu)^2}{2\varphi^2}\right) \quad (11a)$$

$$F_l(v,\varphi) = 1 - \text{erfc}\left(\frac{(\ln v - \mu)^2}{2\varphi^2}\right) \quad (11b)$$

where φ , μ, f_l, F_l and erfc$(\ln v\text{-}\mu)^2/2\varphi^2$ are the location parameter, scale (sigma) parameter, lognormal pdf and cdf, and error function of $(\ln v\text{-}\mu)^2/2\varphi^2$, respectively.

In another literature,[25] the lognormal distribution with probability density function was given by Lu:

$$f(x) = \frac{1}{x\lambda\sqrt{2\pi}} \exp\left[-\frac{1}{2}\left(\frac{\ln x\sigma}{\lambda}\right)^2\right] \quad (12a)$$

The cumulative density function form for normal distribution is

$$f(x) = \frac{1}{2\pi} \int_{-\infty}^{\frac{\ln x - \sigma}{\alpha}} e^{\frac{-x^2}{2}} dt \quad (12b)$$

σ is obtained by solution below

$$\sigma = \frac{1}{n}\sum_{i=1}^{n} \ln(x_i) \quad (12c)$$

and α by using solution below

$$\lambda = \sqrt{\frac{1}{n}}\left[\ln(x_i) - \sigma\right] \quad (12d)$$

Frechet (F) PDF

The density function of the generalized extreme value (GEV) distribution with shape ($k \neq 0$), location (μ) and the scale (δ) parameters are given:[26]

$$f_f(k,\mu,\delta) = \left(\frac{1}{\delta}\right)\exp\left(-\left(1+k\frac{\nu-\mu}{\delta}\right)^{-\frac{1}{k}}\right)\left(1+k\frac{\nu-\mu}{\delta}\right)^{-1-\frac{1}{k}} \quad (13)$$

where f_f is the probability density function of a Frechet (GEV) distribution

Rician (Ri) PDF

The density function of a Rician distribution is given as:[27]

$$f_n(s,\delta) = I_0\left(\frac{\nu s}{\delta^2}\right)\frac{\nu}{\delta^2}\exp\left(-\frac{(\nu^2+s^2)}{2\delta^2}\right) \quad (14)$$

where

$s \geq 0$ and $\delta = 0$ are non-centrality and scale parameters, respectively;

I_0 is the zero-order modified Bessel function of the first kind.

The two parameters of the Rician distribution are estimated as:

$$s = \frac{1}{N}\prod_{i=1}^{N}\nu_i\frac{I_1(z)}{I_0(z)} \quad (15)$$

$$\delta = \sqrt{0.5\left(\frac{1}{N}\prod_{i=1}^{N}\nu_i^2 - s^2\right)} \quad (16)$$

where $I_1(z)$ is the first-order modified Bessel function of the first kind and $z = \nu_i s/\delta^2$. A good numerical optimization algorithm with a starting value is needed to solve Eqn. (15).

Burr (B) PDF

The density function (pdf) of the Burr distribution is given by the expression:

$$f_{bur}(s,\delta) = I0\left(\frac{\nu s}{\delta^2}\right)\frac{\nu}{\delta^2}\exp\left(-\frac{\nu^2+s^2}{2\delta^2}\right) \quad (17)$$

Accuracy Test

The accuracy results are essential for determining the effectiveness of the statistical models. Thus, accuracy check is carried out by comparing the observed climate distribution with predicted/modeled distributions. The observed data is the values from the monitoring systems whereas the modeled datasets are obtained from the fitted distributions.[26] The various tests for determining the goodness-of-fit of the models (pdfs) are expressed below:

Mean Absolute Error (MAE)

The mean absolute error is used for testing the predicted distribution of observed climatological variables (NO_x, OX and O_3) against the observed distribution. It is often defined as the mean of the absolute errors derived from the observed and predicted values. The mathematical equation is defined as:

$$\mathrm{MAE} = \frac{\sum_{i=1}^{N}|y_i - x_i|}{N} \quad (18)$$

where

x_i is the observed values of the air pollutants;

ν is the predicted/modeled values from Weibull, Rayleigh, and Gamma, Lognormal models etc.

Root Mean Square Error (RMSE)

It is used for comparison of the predicted from the observed values. The root means square error for the best fit statistical model is given as:

$$\mathrm{RMSE} = \left(\frac{\sum_{i=1}^{N}|y_i - x_i|}{N}\right)^{1/2} \quad (19)$$

Mean Absolute Percentage Error (MAPE)

The mean absolute percentage error is calculated as:

$$\mathrm{MAPE} = \left(\frac{1}{N}\sum_{i=1}^{N}(y_i - x_i)\times 100\right) \quad (20)$$

RESULTS AND DISCUSSIONS

The description statistics of average values of air pollutants for the sampling period (2015) was being shown in Table 1. The annual mean values of the gases (NO, NO_2, NO_x, OX and O_3) was higher than the median, indicating a high concentration recorded for the studied period. Most of the data is concentrated to the left of PDF charts with few high values. There was an increase in mean, median, roughness and persuasion values, indicating a growing problem of air pollution in Campo Grande.

Table 1. Descriptive analysis of pollutants for the sampling period (2015).

Variable	Count	Mean	St.Dev	Coef.Var	Minimum	Median	Maximum	Skewness	Kurtosis
NO (ppb)	8776	7.069	11.583	163.87	0.000	3.700	165.000	5.11	38.11
NO_2 (ppb)	8776	5.6624	5.6530	99.84	0.0000	4.1000	60.2000	2.41	9.63
NO_x (ppb)	8776	12.721	13.708	107.76	0.000	8.800	165.000	3.39	18.25
OX (ppb)	8776	21.766	10.826	49.74	2.000	20.200	95.400	1.04	2.23
O_3 (ppb)	8776	16.109	9.832	61.03	1.000	15.100	79.700	1.00	1.99

Source: UFMS-Institute of Physics

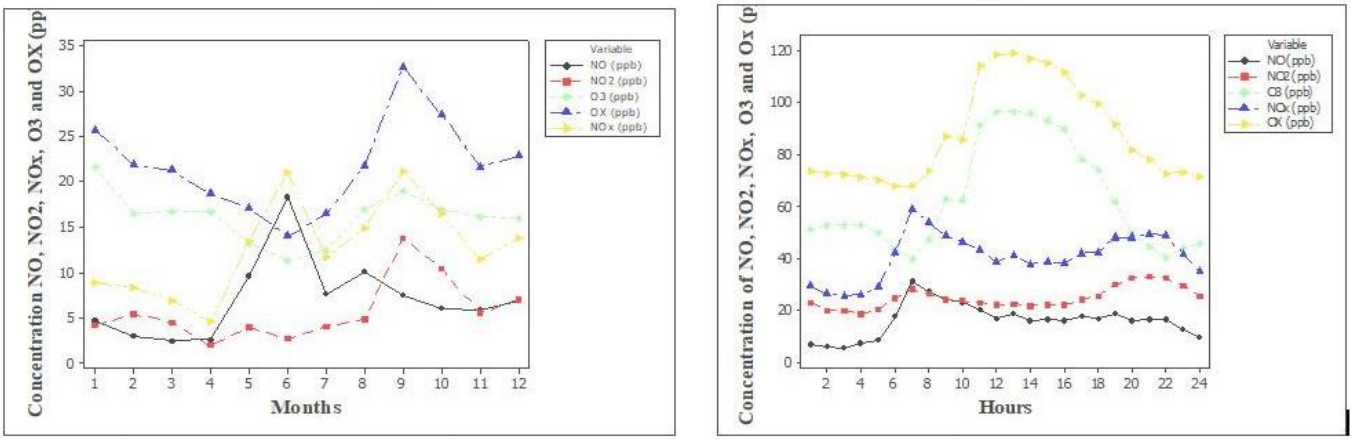

Figure 2. Average of measured values for a daily period of NO, NO_2, NO_x, O_3 and O_x concentrations. The interval between measurements equals 1 hour.

Hourly variation of O_3, NO, NO_2, O_X and NO_x concentrations

The average per diem variation observed for the NO, NO_2, NO_x, OX and O_3 concentrations are presented in Fig 2. Generally, the daily cycle of the ozone concentration reaches its peak at middle day and presents smaller concentrations during the night. The ozone concentration slowly increases after the first rays of the sunshine, getting to its maximum value during the daylight period, and after which it starts to decrease slowly until the next morning.

Figure 2 shows a displacement of about 2 hours in the morning between the NO and NO_2 peaks. In the morning, NO_2 is produced by oxidation of NO,[2] because NO can be converted to NO_2 in the presence of peroxy radicals, but at night, NO and NO_2 concentrations have a slight increase caused by increased in vehicular traffic during the rush hour (6:00 p.m.) and the influence of night boundary layer stability. At this time NO_2 reached its peaks at 6:00 p.m.

Figure 2 shows an increase in O_3 concentrations during the day, starting at 8:00 p.m. and peaking at 2 p.m. NO is converted to NO_2 by reaction with O_3, but during the daytime, NO_2 is converted back to NO as a result of photolysis, which leads to O_3 regeneration.[8] O_3 concentration in urban atmospheres peaked during the daytime from at 14:00 - 15:00, when there is a maximum in solar radiation intensities and air temperature. This increase is by photolysis of NO_2 and by the increase in the height of the boundary layer during the daytime that can result in the O_3 mixture due to thermal stratification and convective heat transfer to the surface of the air at higher altitudes. After reaching the maximum concentration at 14:00-15:00 hr., the concentration of O_3 decreases due to a decrease of the photochemical activity.

Higher OX concentrations occurred in the afternoon, thus revealing an influence of the photochemical processes.[5,8] Also, OX decreases due to the absence of solar radiation at night. This lack of radiation hinders the formation of NO_2 and O_3 by photolytic reactions, as well as the reactions of NO_2 with NO_3, and of NO2 with O_3.[28]

While O_3 and a large percentage of NO_2 concentrations are the secondary contaminants, NO is a primary contaminant, formed through a complex set of chemical reactions. At 07:00 a.m, the sunlight begins to induce a series of photochemical reactions. NO is converted in NO_2 through a reaction with O_3. During the shining hours, NO_2 is converted again into NO because of photolysis, which induces the regeneration of O_3.

Another factor influencing the atmospheric air pollutant concentrations is the height of the mixture layer over the city. In a shiny day, the pollutants are diluted when the mixture layer increases during the day and stays limited to the inside of NPBL during the night. Emitted pollutants, like NO, are kept underneath (such an inversion), and it can cause an increase of hourly average concentration of NO_x overnight.

Chemistry of O_3, NO and NO_2

The basic chemistry that led to the production and destruction of ozone has been detailed elsewhere.[28]

$$NO_2 + h\nu \longrightarrow NO + O \quad (21)$$

$$O + O_2 \longrightarrow O_3 + M \quad (22)$$

$$O_3 + NO \quad NO_2 + O_2 \quad (23)$$

M represents a molecule absorbing the excess of vibrational energy and thus stabilizing the O_3 molecule that has been formed, normally it is N_2 or O_2; hν represents the photon energy, with a 424 nm wavelength; and O is an active monoatomic molecule of oxygen.

The plots of the pdfs and cdfs for three air pollutant variables (NO, O_3, OX) in Campo Grande are presented in Fig 3. The plots show that for: *NO* - the functions (W, R, and G), fit well in the range of 0 to 30 ppb ; For the functions (L, Ri, NP), they overestimate in the range of 0 to 3, underestimate in the range of 3 to 12 and overestimate in the range of 12 to 30 ppb. The functions that fit the NO concentration best are Rayleigh and Rician. (please confirm again W, R, G, L, Ri, NP. Also, I don't know what NP stands for)

O_3- the functions (W, R and G) underestimates the concentrations of 0 to 18 ppb and overestimate in the range of 18 to 35 ppb, while the R function overestimates in the range of 13 to 18 ppb . For the other functions (L, Ri, NP) overestimated in the range of 0 to 12 ppb, underestimated in the range of 12 to 17 ppb; for Ri underestimated in the range of 12 to 17 ppb and underestimated in the range of 17 to 25 ppb; For the functions (Fr, Bur) they fit well in the 0 to 23 ppb range, with the exception of Bur that underestimates in the range of 17 to 25 ppb and the range of 25 to 35 the overestimate functions. For ozone the best function that fits is the Rician;

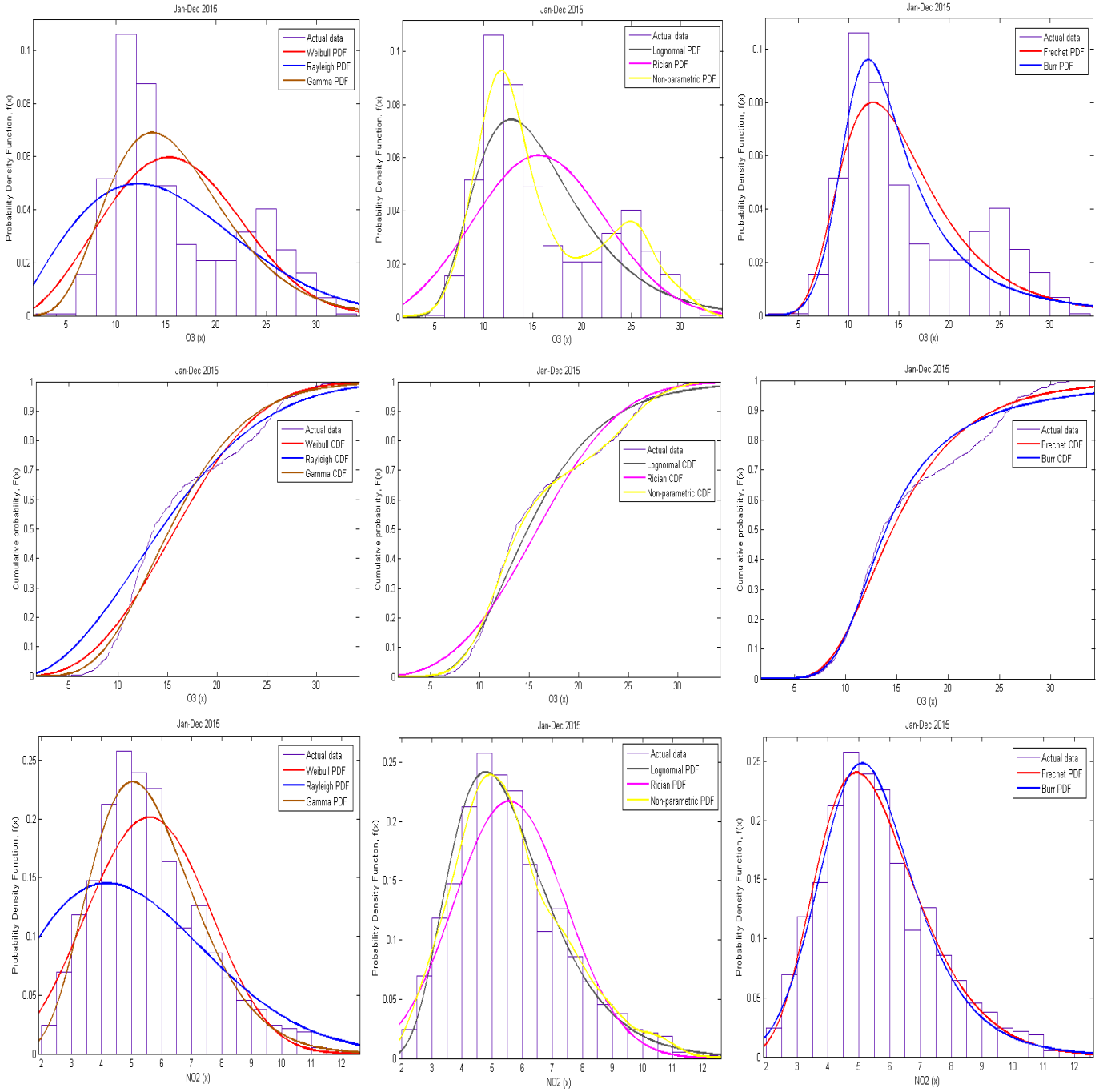

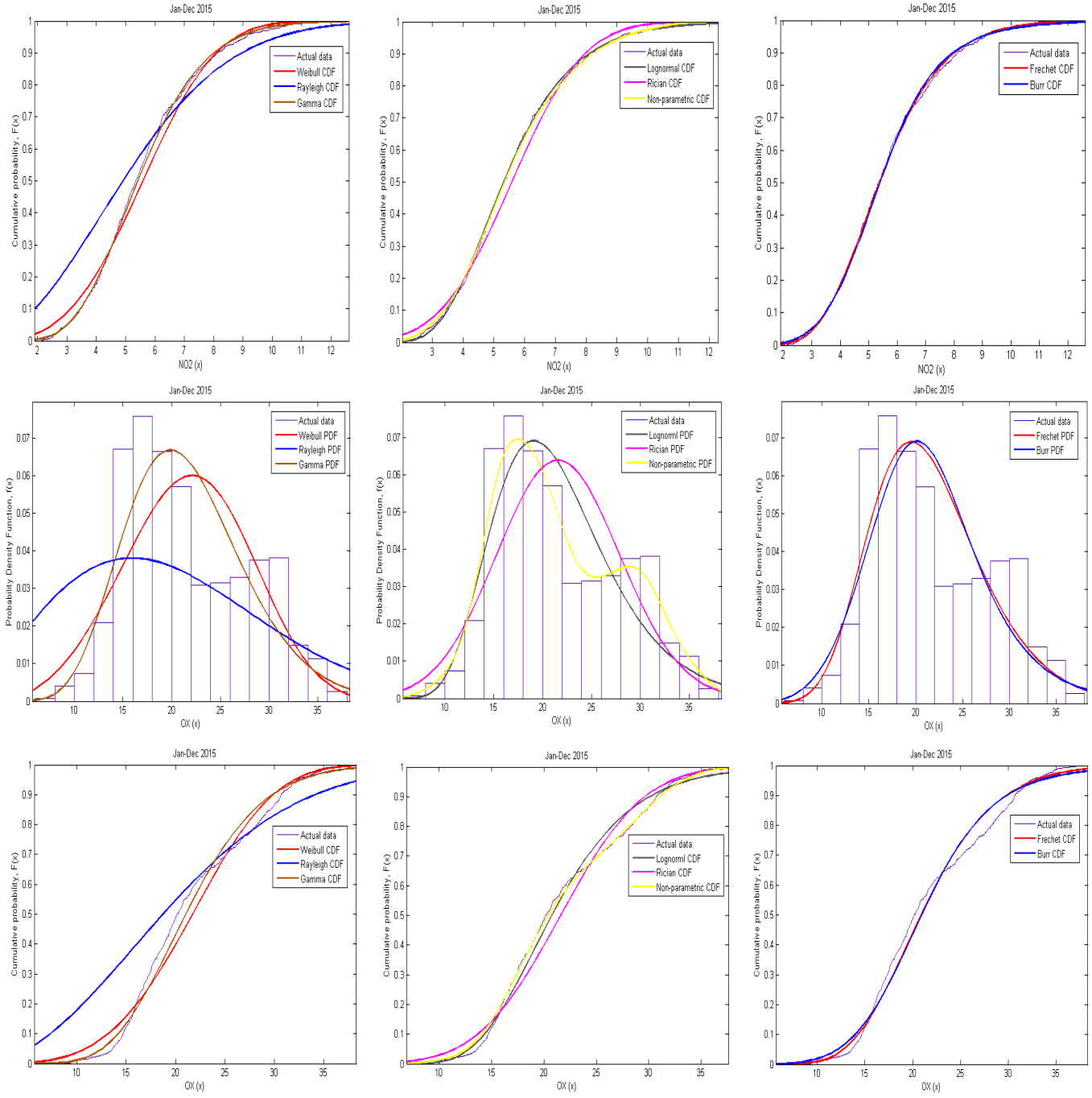

Figure 3. – Plots of the pdfs and cdfs for three air pollutant variables (NO, O_3, OX) in Campo Grande.

OX- for the functions (W, R, G) underestimates the concentrations of 0 to 25 ppb and overestimate in the range of 25 to 40 ppb; For the functions (L, RI, NP) overestimated in the range of 0 to 15 ppb, underestimated in the range of 15 to 28 for Ri and overestimated for L and NP in the range of 15 to 23 ppb, in the range of 28 to 40 overestimate To Ri and underestimated for L and NP. The best function that fits for OX is Rician. In order to compare the quality of several pdfs to sample variable concentration data, several statistics were used in related studies for analysis of O_3, NO and OX. The most used are coefficient of determination, Chi-square (χ^2) test results, Kolmogorov-Smirnov test (KS) and square root mean square error (RMSE). In most studies, a visual evaluation of overlapping adjusted pdfs To the histograms of the data is also performed The RMSE are applied in theoretical cumulative probabilities against empirical or theoretical cumulative probabilities of the concentrations of the observed variables. These statistics are also calculated with variable data in the form of frequency histograms.

In addition to the analysis performed on the distributions of the variables, some authors also evaluated the adequacy of pdfs to adjust the concentration distributions obtained by the sample variables or to predict the concentrations. In this case, the pdfs are first adjusted to the data of the variables. Then, the theoretical distributions of concentration density are derived from the pdfs adjusted for the variables. Finally, the fit quality measurements are calculated using the theoretical density distributions and the distribution estimated from the NO, O_3, OX variables of the sample.

Figure 3 shows seven PDFs, namely Weibull (W), gamma (G), log-normal (L), Frechet (Fr), Burr (Bur), Rayleigh (R) and Rician (Ri) Of the variables studied in the data set.

Graphically, it can be seen that the Rician PDF produces the best fit. Rayleigh and gamma distributions correspond to the histogram to a lesser extent and provide the poorest adjustments. It can be seen from the figures that these variables present different forms of histograms. The parameter values obtained for these distributions and the assembly precision based on the performance index criteria presented in Table 2. It can be seen that both statistical indicators gave similar results in all cases. The Weibull (W), Rician (Ri), log-normal (L) functions provide the smallest adjustment error for the data sets. This is also verified in Figure 3. Statistical tests show that the Rician distribution is the best choice for the data set. However, the Weibull PDF also provides fairly accurate results for the variables. Rayleigh PDF gives a very poor performance and is a poor fit. The performance of these three PDFs to evaluate the concentrations of the variables were also analyzed and the results are summarized in Table 2.

The Rayleigh PDF produced the maximum error between the PDFs and produced significant errors in the evaluation of the concentrations of the variables. Overall, Weibull, Rician, and lognormal PDFs resulted in fewer errors, and among the three functions, while Rician was ranked number 1 based on performance index criteria. It can be said that the evaluation of these distribution functions based on the quality of the adjustment criteria alone is not enough. These criteria should be used to identify appropriate distributions before a detailed analysis is made. As these PDFs installed can be used for different applications by the industries, public managers in decision-making, the performance of these PDFs for specific applications, such as prediction of the concentration of pollutants, should also be evaluated. The results show that there are an underestimation and overestimation of the concentration density of the pollutants in general, depending on the concentration range. The percentage errors mainly show that this underestimation and overestimation of the concentrations of these pollutants, which may be due to the heating effect and the atmosphere.

The distributions gamma has also been used to fit the probability density functions of daily air pollutant concentration.[29] The pollutants studied have a different statistical distribution, due to the different diffusion characteristics of the individual pollutant in the air and to the interaction of diffusion characteristics and local geography, climatic conditions in Campo Grande. The distributions gamma has also been used to fit the probability density functions of daily air pollutant concentration.[29]

The current study showed that the pollutants studied O_3, OX and NO had different statistical distribution. The difference might be due to the different diffusion characteristics of individual pollutant in the air, and the interaction of diffusion characteristics and local geography, weather conditions in Campo Grande. The underlying mechanisms need to be further explored.

The current analysis shows that the statistical distributions of better performance of several air pollutants in Campo Grande are different. For example, Nan-Hung Hsieh and Chung-Min Liao claimed that the probability distributions for all air pollutants in Taiwan were approximate to be a lognormal distribution.[30] In addition, Neustadter[31] revealed that the total suspended particulate is obviously logically distributed, whereas sulfur dioxide and nitrogen dioxide are rationally estimated by lognormal distributions. However, Oguntunde[32] showed that the Gamma pdf is the best distribution model for the carbon monoxide concentration modelling in Lagos State, Nigeria. Hai-Dong Kan and Bing-Heng Chen indicated that the best fit distributions for PM10 concentrations in Shanghai were lognormal.[33]

In Malaysia, Noor et al.[26] found that the best distribution fits the PM10 observations in Nilai was the Gamma distribution while the log-normal distribution is more appropriate in Shah Alam. Razali et al. referred to lognormal distribution as the best distribution that fitted to the carbon monoxide data in Bangi, Malaysia.[34] Accordingly, there is no common distribution of air pollutants and it differs from the studied region and time. It is important to carry out a comparative analysis in order to find out which distribution better fits the air pollutants in a particular location in order to provide a better estimate of the air quality at that location.

Table 2 presents the results tests for fitting for different distributions to the air pollutants data. The preferable results were highlighted by italicizing and bold. We found that out of the distributions considered, the Rician and Gamma distribution significantly fits with most of the air pollutants data in Campo Grande which are NO, O_3 and OX, while O_3 is fitted well with Weibull distribution.

Performance Indicators

The values of the performance indicators for the variables concentration in Campo Grande were tabulated in Table 2. A small value of the MAE indicates that the distribution of the Rician fits well the sampled data of the variables (O_3 and OX), while the best fit that is appropriated is the function of Rayleigh. The smaller MSE and RMSE values indicate that the physician's distribution best fits the variables data while the lower COD value indicates that the Rician distribution fits the variable data

CONCLUSION

Based on the statistical characteristics of the concentrated air variables studied in Campo Grande, result findings indicate that the mean of the concentrations of the variables for the monitoring data sets was higher than the values of the medians showing that all observations are positively inclined to the right, with few extreme concentrations. The Weibull (W), gamma (G), log-normal (L), Frechet (Fr), Burr (Bur), Rayleigh (R) and Rician (Ri) distributions have been analyzed with the selected datasets.

Table 2. Performance indicators for variables concentration in Campo Grande.

MAE

Datasets	*Weib*	*Rayl*	*Gam*	*Logn*	*Rician*	*Frechet*	*Burr*
NO	0.0121	**0.0100**	0.0185	0.0665	0.0118	0.0224	0.0217
O_3	0.0025	0.0167	0.0088	0.0422	**0.0015**	0.0237	0.0083
OX	0.0024	0.0152	0.0057	0.0437	**0.0003**	0.0247	0.0275

MSE

Datasets	*Weib*	*Rayl*	*Gam*	*Logn*	*Rician*	*Frechet*	*Burr*
NO	0.00021	0.00014	0.00048	0.000997	**0.0001422**	0.00069	0.00064
O_3	0.00001	0.00040	0.00010	0.00023	**0.0000031**	0.00079	0.00011
OX	0.00001	0.00033	0.00004	9.49E-05	**0.0000001**	0.00094	0.00108

RMSE

Datasets	*Weib*	*Rayl*	*Gam*	*Logn*	*Rician*	*Frechet*	*Burr*
NO	0.0143	0.0119	0.0220	0.031571	**0.0119**	0.0263	0.0252
O_3	0.0029	0.0201	0.0101	0.015156	**0.0018**	0.0281	0.0107
OX	0.0028	0.0182	0.0065	0.009742	**0.00032**	0.0306	0.0328

COD

Datasets	*Weib*	*Rayl*	*Gam*	*Logn*	*Rician*	*Frechet*	*Burr*
NO	0.8662	0.9305	0.8117	0.658254	**0.9306**	0.8046	0.8278
O_3	0.9854	0.4589	0.9173	0.847021	**0.9945**	0.7032	0.8540
OX	0.9958	0.6093	0.9465	0.890939	**0.9998**	0.2916	-0.1592

MAPE

Datasets	*Weib*	*Rayl*	*Gam*	*Logn*	*Rician*	*Frechet*	*Burr*
NO	6.6708	8.0654	6.7749	-3.2820	**8.0636**	4.8187	5.7405
O_3	3.1229	-67.4508	4.5800	-45.0314	**1.6711**	-22.5415	-1.2100
OX	-0.5213	-37.8984	1.7815	-1.6104	**0.3108**	-32.7144	82.4431

Performance indicators were also applied, which were mean absolute error (MAE), root mean square error (RMSE), the mean absolute percentage error (MAPE) to determine the quality criteria for the adjustment of the distributions.

The best distribution that adapts to the observations of the variables was the Rician, Weibull and the lognormal distribution. The pdf and cdf graphs obtained in this research can be used to predict the probabilities of exceedances.

The importance of statistical analysis in the field of atmospheric pollution for environmental engineering is shown in this research as it's useful for to adjustment of the data sets of pollutants with the best statistical model, in turn, to successfully estimate the exceedances of pollutants.

However, this work can still be improved with the application of other types of distributions and to adjust the monitoring data of the time series of air pollution.

REFERENCES

[1]Nevers, N. D., *Air Pollution Control Engineering*, 2nd ed. McGraw-Hill Companies, Inc., New York, **2000**, 571–573.

[2]de Souza, A., Aristone, F., Kumar, U., Kovač-Andrić, E., Arsić, M., Ikefuti, P. and Sabbah, I. Analysis of the Correlations Between NO, NO_2 and O_3 Concentrations in Campo Grande – Ms, Brazil., *Eur. Chem. Bull.*, **2017**, *6(7)*, 284-291. DOI:10.17628/ecb.2017.6.284-291

[3]Agudelo-Castaeda, D. M., Teixeira, E. C., Rolim, S. B. A., Pereira, F. N., & Wiegand, F. Measurement of particle number and related pollutant concentrations in an urban area in South Brazil. Atm. Environ., **2013**, *70*, 254-262. https://doi.org/10.1016/j.atmosenv.2013.01.029

[4]Kurtenbach, R., Kleffmann, J., Niedojadlo, A., Wiesen, P., Primary NO_2 emissions and their impact on air quality in traffic environments in Germany. *Env. Sci. Eur*., **2012,** 24, 21. https://doi.org/10.1186/2190-4715-24-21

[5]Notario, A., Bravo, I., Adame, J. A., Diaz–de–Mera, Y., Aranda, A., Rodriguez, A., Rodriguez, D., Analysis of NO, NO_2, NO_x, O_3 and oxidant ($OX=O_3+NO_2$) levels measured in a metropolitan area in the southwest of Iberian Peninsula. *Atm. Res*., **2012,** *104*, 217–226. https://doi.org/10.1016/j.atmosres.2011.10.008

[6]Mazzeo, N. A., Venegas, L. E. and Choren, H. Analysis of NO, NO_2, O_3 and NO_x Concentrations Measured at a Green Area of Buenos Aires City during Wintertime. Atm. Environ., **2005**, *39*, 3055–3068. https://doi.org/10.1016/j.atmosenv.2005.01.029

[7]Ghazali N. A, Yahaya A. S., Nasir, M. Y. and Mokhtar M. I. Z., Predicting Ozone Concentrations Levels Using Probability Distributions. ARPN Journal of Engineering and Applied Sciences. vol. 9, N. 11 november, 2014.

[8]de Souza, A.; Kovač, E., Matasovi, B., Markovi, B., Assessment of Ozone Variations and Meteorological Influences in West Center of Brazil, from 2004 to 2010. *Water, Air and Soil Pollution*, **2016**, *227*, 313.; Han, S.; Bian, H., Feng, Y., Liu, A., Li, X., Zeng, F., Zhang, X., Analysis of the Relationship between O_3, NO and NO_2 in Tianjin, China. *Aerosol Air Qual. Res.*, **2011**, *11*, 128–139. https://doi.org/10.4209/aaqr.2010.07.0055

[9]de Souza, A., Aristone, F., Arsic, M., Kumar, U., Souza, A., Evaluation of Variations in Ground-Level Ozone (O_3) Concentrations. *Ozone-Sci. Eng.*, **2017**, *39*, in press.

[10]de Souza, A.; Aristone, F.; Pavao, H. G., Santos, D. A. S., Kovač, E. Pires, J. C.; Ikefuti, P., Meteorological Impact Factors on the Modeling of Ozone Concentrations Using Analysis of Temporal Series and Multivariate Statistic Methods. *Holos (Natal. Online)*, **2017**, *5*, 2-16.

[11]de Souza, A., Kovač, E., Matasovi, B., Markovi, B., Assessment of Ozone Variations and Meteorological Influences in West Center of Brazil, from 2004 to 2010. *Water, Air Soil Pollut*., **2016**, *227*, 313. https://doi.org/10.1007/s11270-016-3002-0

[12]de Souza, A., Aristone, F., Sabbah, I., Modeling the Surface Ozone Concentration in Campo Grande (MS)-Brazil Using Neural Networks. Natural Science, **2015**, *7*, 171-178. https://doi.org/10.4236/ns.2015.74020

[13]de Souza, A., Aristone, F., Modeling of Surface and Weather Effects Ozone Concentration Using Neural Networks in West Center of Brazil. *J. Climatol. Weather Forecast.*, **2015**, *3*, 1-4-4.

[14]de Souza, A., Aristone, F., Pavão, H. G., Fernandes, W. A., Development of a Short-Term Ozone Prediction Tool in Campo Grande-MS-Brazil Area Based on Meteorological Variables. *Open J. Air Pollut.*, **2014**, *3*, 42-51. https://doi.org/10.4236/ojap.2014.32005

[15]de Souza, A., Aristone, F., Silva, G. B. M., Fernandes, W. A., Temporal Variation of the Concentration of Carbon Monoxide in the Center West of Brazil. *Atm. Climate Sci.*, **2014**, *4*, 563-568, https://doi.org/10.4236/acs.2014.44051

[16]de Souza, A., Fernandes, W. A., Surface ozone measurements and meteorological influences in the urban atmosphere of Campo Grande. *Acta Sci. Technol*., **2013,** *36*, 141-146. https://doi.org/10.4025/actascitechnol.v36i1.18379

[17]Pires, J. C. M., Souza, A., Pavão, H. G., Martins, F. G., Variation of surface ozone in Campo Grande, Brazil: meteorological effect analysis and prediction. *Environ. Sci. Pollut. Res. Int.*, **2014**, *21*, 10550-10559. https://doi.org/10.1007/s11356-014-2977-6

[18]Wang, X. and Mauzerall, D. L., Characterizing Distributions of Surface Ozone and its Impact on Grain Production in China, Japan and South Korea: 1990 and 2020, *Atm. Environ*., **2004**, *38(74)*, 4383-4402. https://doi.org/10.1016/j.atmosenv.2004.03.067

[19]Hadley, A. and Toumi, R. Assessing Changes to the Probability Distribution of Sulphur Dioxide in the UK Using Lognormal Model. *Atm. Environ*., **2002**, *37(24)*, 455-467.

[20]Singh, P., Simultaneous Confidence Intervals for the Successive Ratios of Scale Parameters, *J. Stat. Plan. Infer.*, **2004**, *36(3)*, 1007-1019.

[21]Celik, A. N., A Statistical Analysis of Wind Power Density Based on The Weibull and Rayleigh Models at The Southern Region of Turkey. *Renew. Energy*, **2003**, *29*, 593-604. https://doi.org/10.1016/j.renene.2003.07.002

[22]Phien, H. N., A Computer Assisted Learning Package for Flood Frequency Analysis With the Gumbel Distribution, Adv. Eng. Software, **1989**, *11*, 206-212. https://doi.org/10.1016/0141-1195(89)90051-X

[23]Caleyo, F., Velázquez, J. C. Valor, A. and Hallen, J. M. Probability distribution of pitting corrosion depth and rate in underground pipelines: A Monte Carlo study. *Corr. Sci.*, **2009**, *51*, 1925-1934. https://doi.org/10.1016/j.corsci.2009.05.019

[24]Olaofe, Z. O. and Folly, K. A., Statistical analysis of wind resources at Darling for energy production; International J. Renew. Energy Res., **2012**, *2(2)*, 250-251.

[25]Lu, H. C. Estimating the Emission source reduction of PM10 in central Taiwan, *Chemosphere*, **2003**, *54*, 805-814. https://doi.org/10.1016/j.chemosphere.2003.10.012

[26]Noor, N. M., Tan, C. Y., Ramli, N. A., Yahaya, A. S., Yusof, N. F. F. M., Assessment of various probability distributions to model Pm 10 concentration for industrialized area in peninsula Malaysia: A case study in Shah Alam and Nilai. *Aust. J. Basic Appl. Sci*., **2011**, *5(12)*, 2796-2811.

[27]Olaofe Z. O., Assessment of the offshore wind speed distributions at selected stations in the South-West Coast, Nigeria; *Int. J. Renew. Energy Res*., **2017**, *7(2)*, 565-577.

[28]Jenkin, M. E. and Clemitshaw, K. C., Ozone and other secondary photochemical pollutants: chemical processes governing their formation in the planetary boundary layer, *Atm. Environ.*, **2000**, *34*, 2499–2527, https://doi.org/10.1016/S1352-2310(99)00478-1

[29]Rumburg, B., Alldredge, R. and Claiborn, C. Statistical distributions of particulate matter and the error associated with sampling frequency. *Atm. Environ.*, **2001**, *35*, 2907-2920. https://doi.org/10.1016/S1352-2310(00)00554-9

[30]Kan, H. D. and Chen, B. H., Statistical Distributions of Ambient Air Pollutants in Shanghai, China, *Biomed., Environ. Sci*., **2004**, *17*, 366-372.

[31]Neustadter, H. E., Sidik, S. M. and Burr, J. C. Jr., "Statistical Summary and Trend Evaluation of Air Quality Data for Cleveland, Ohio, in 1967-1971: Total Suspended Particulate, Nitrogen Dioxide, and Sulphur Dioxide," NASA TN D-6935, **1972**.

[32]Oguntunde, P., Odetunmibi O. and Adejumo A., A Study of Probability Models in Monitoring Environmental Pollution in Nigeria, *J. Probability Statistics*; **2014**, Article ID 864965, 6 pages, http://dx.doi.org/10.1155/2014/864965.

[33]Hsieh N.-H. and Liao, C.-M., Fluctuations in air pollution give risk warning signals of asthma hospitalization. *Atm. Environ*., **2013**, *75*, 206-216. https://doi.org/10.1016/j.atmosenv.2013.04.043

[34]Razali, A. M., Desvina, A. P. Sapuan, M. S. Zaharim, A., Distributional Fit of Carbon Monoxide Data. *Advances in Environment, Computational Chemistry and Bioscience*, **2012**, 147-152, ISBN: 978-1-61804-147-0

Received: 22.11.2018.
Accepted: 22.01.2018.